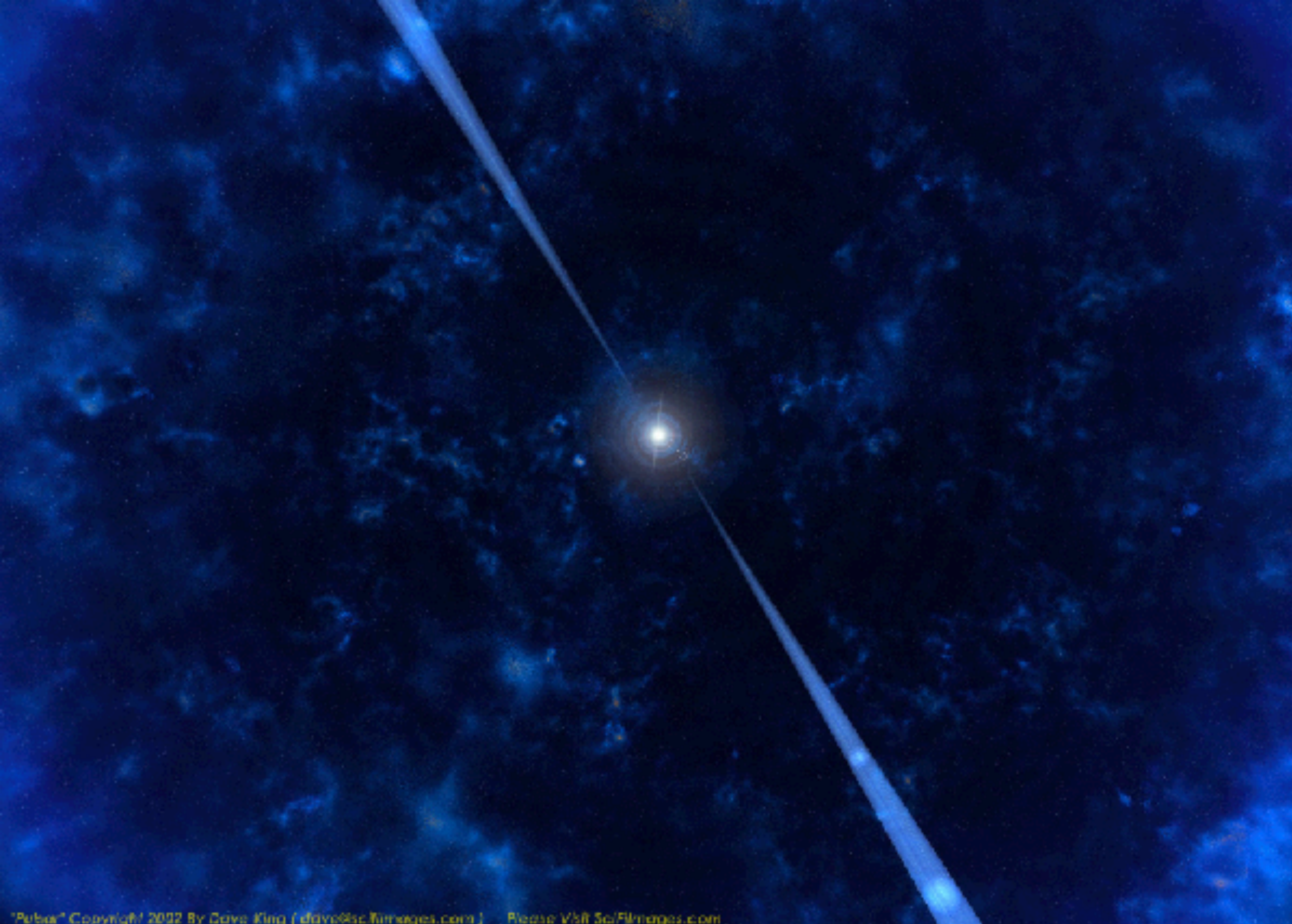

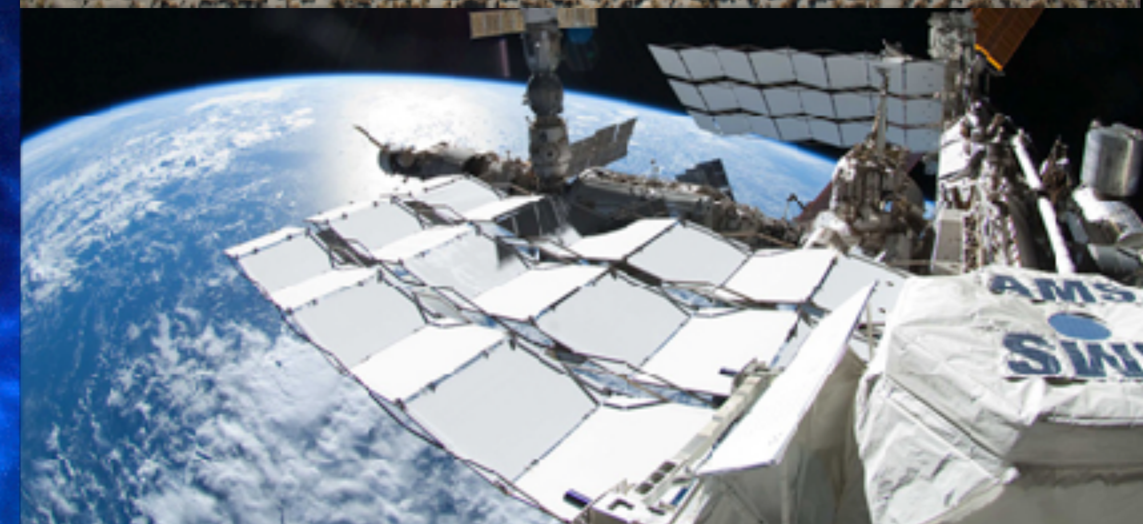

TIM LINDEN

HAWC SHEDS LIGHT ON MILKY WAY PULSARS

University of Maryland JSI Seminar

May 11, 2017

THE OHIO STATE UNIVERSITY

CENTER FOR COSMOLOGY AND ASTROPARTICLE PHYSICS

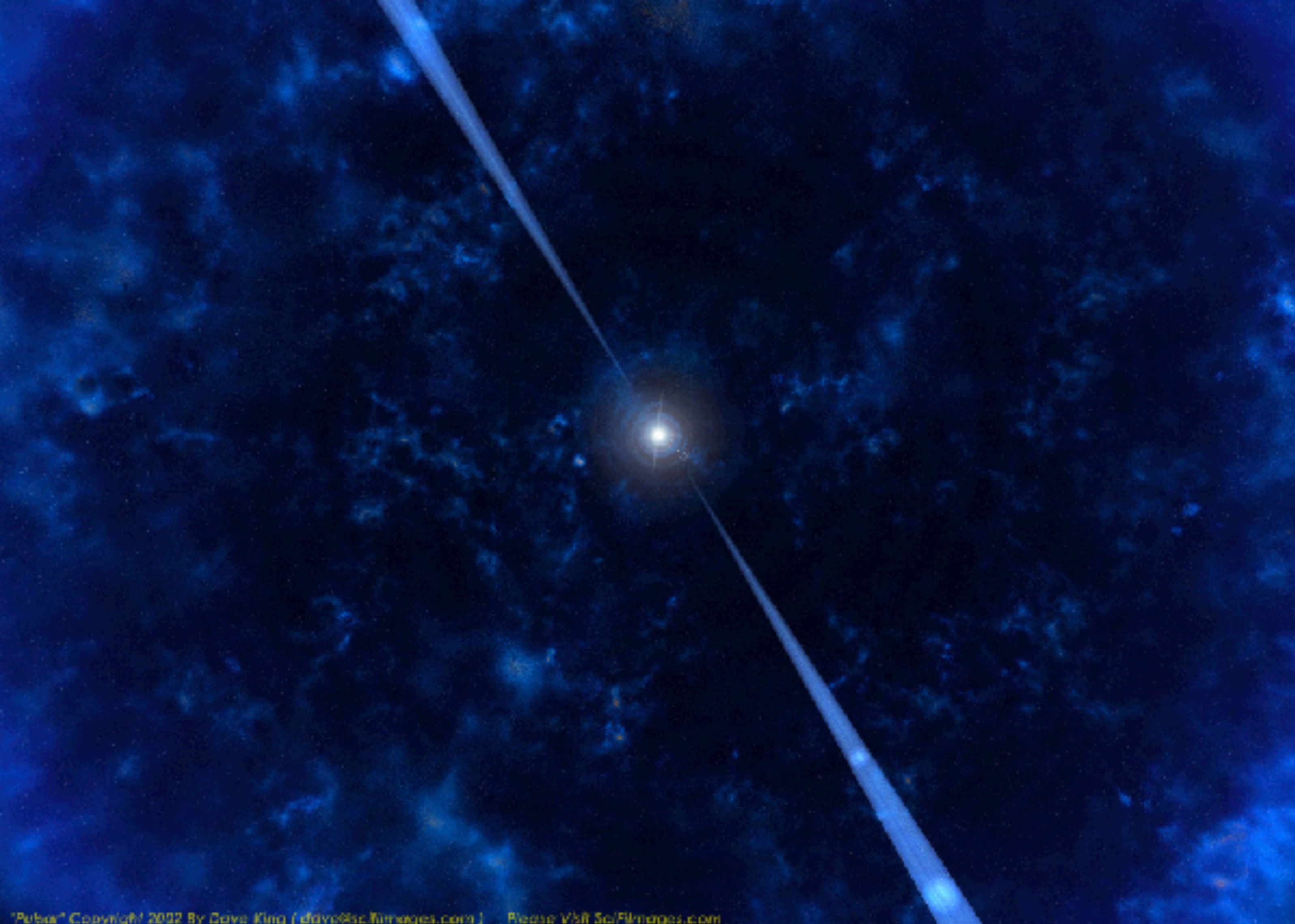


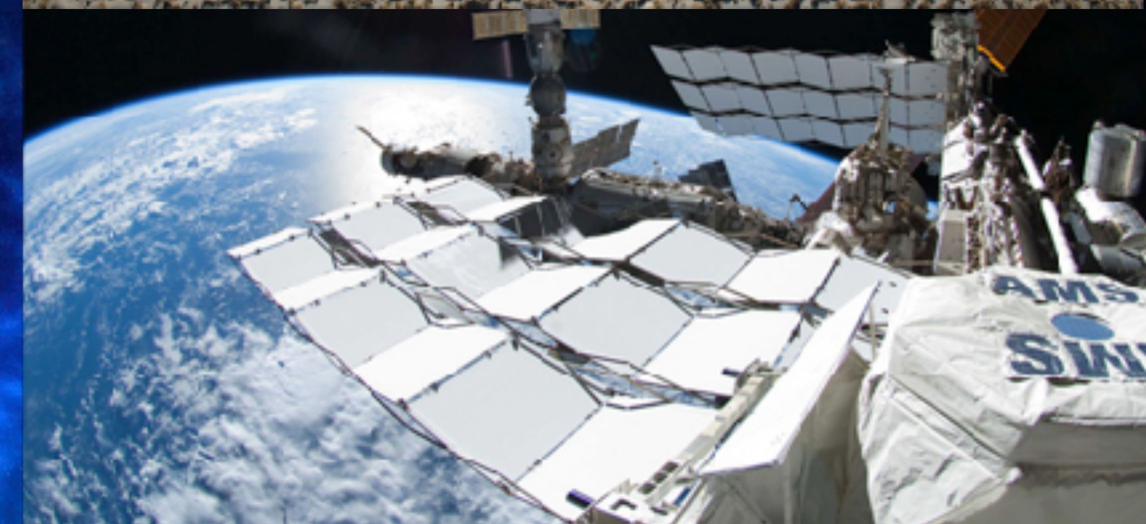

TIM LINDEN

HAWC SHEDS LIGHT ON MILKY WAY PULSARS

WITH: KATIE AUCHETTL, JOSEPH BRAMANTE, ILIAS CHOLIS, KE FANG, DAN HOOPER, SHIRLEY LI

- **The kinetic energy of the rotating neutron star is the <u>ultimate power source</u> of all pulsar, PWN, and halo emission.**

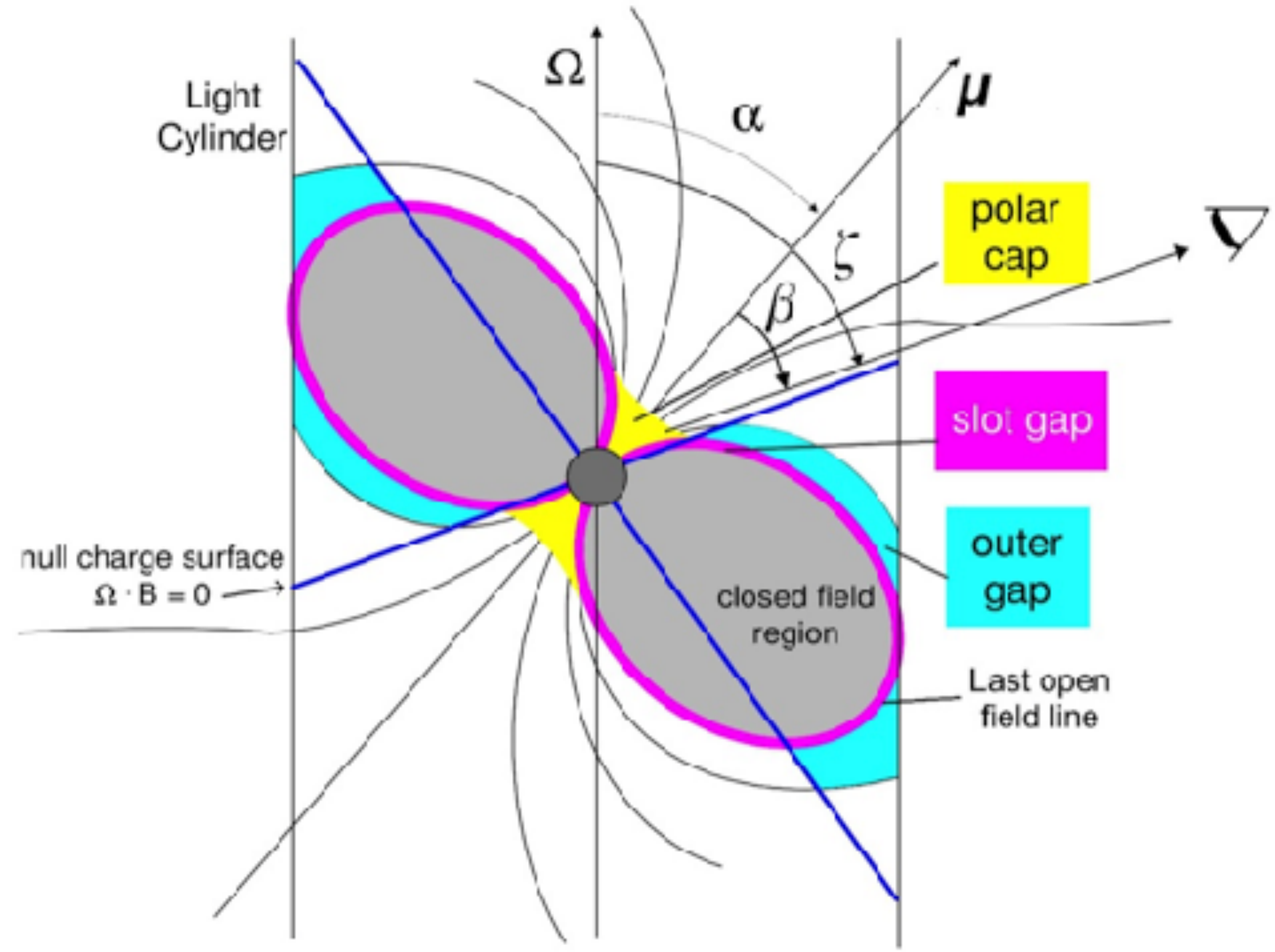

- **Additionally, a substantial radio, gamma ray and e^+e^- flux is produced locally at the pulsar position.**

- **The e^+e^- spectrum depends sensitively on the geometry of the acceleration region.**

- The energy scale is set by competition between particle acceleration and synchrotron energy losses.

- As an example, slot gap models predict e^+e^- energies as high as 10 TeV.

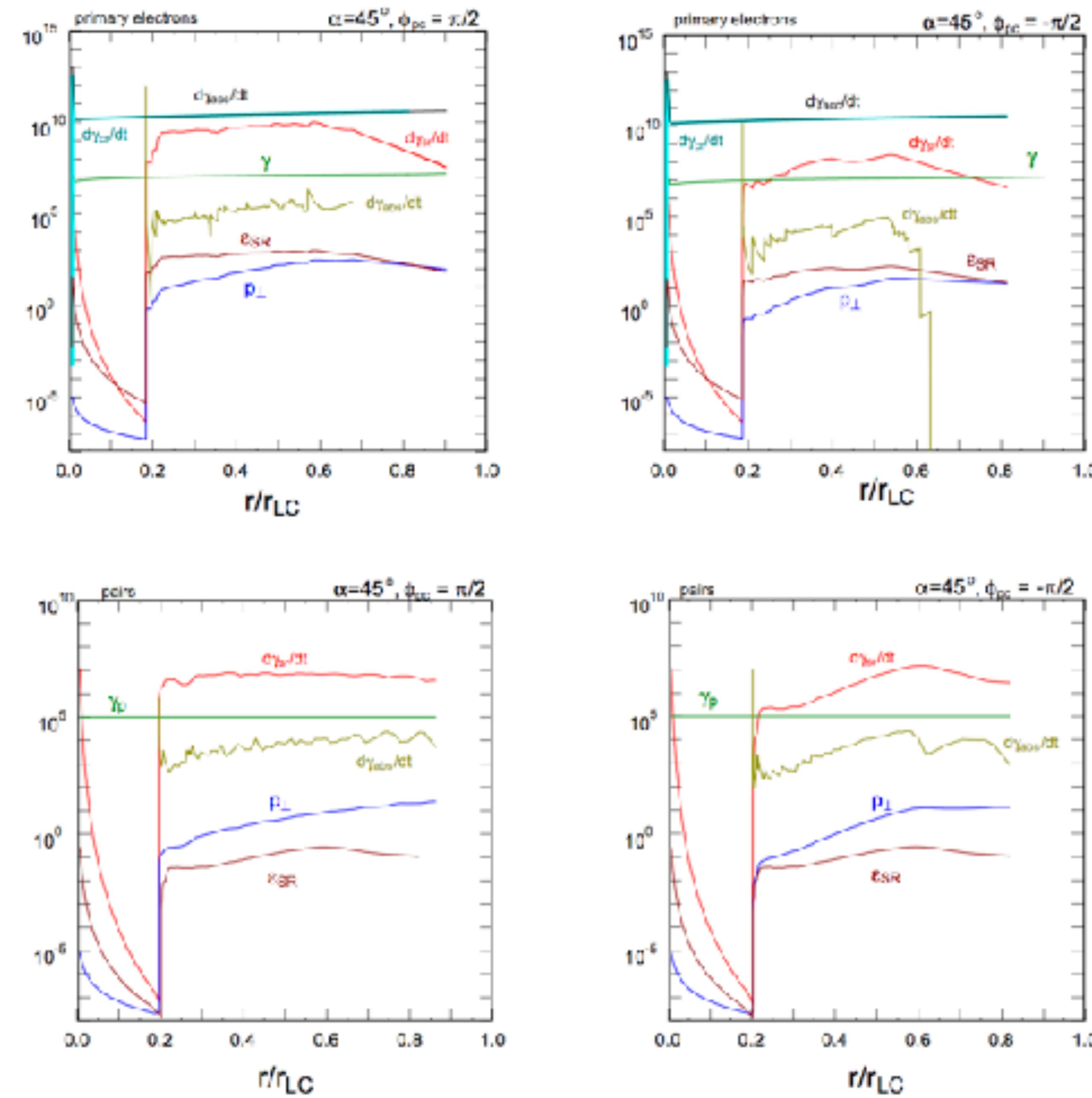

- The spectrum and intensity of these electrons are of critical importance for models of MSPs and pulsars without associated PWN.

- Electrons are reaccelerated by the pulsar wind nebula.
- Synchrotron Spectrum Demands:
  - Voltage > 30 PeV
  - Electron Energy > 1 PeV.

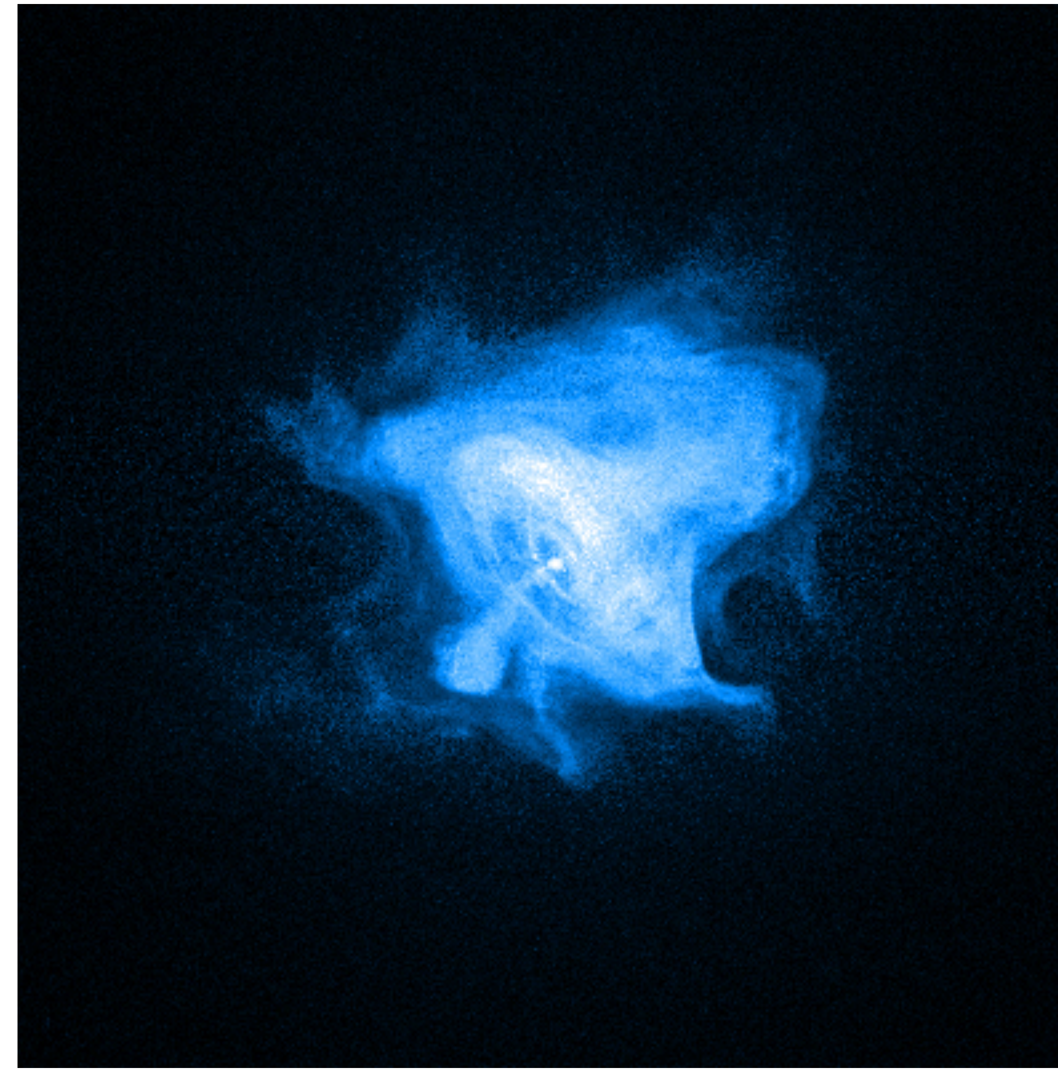

Blandford & Ostriker (1978)
Hoshino et al. (1992)
Coroniti (1990)
Sironi & Spitkovsky (2011)

- First-order Fermi Acceleration, magnetic reconnection, shock driven reconnection, etc. are all possible (but problematic) models.

- **Fortunately, we can remain agnostic as to the physical mechanism which produces the TeV electron spectrum near pulsars.**

- **Following observations, we will assume that a power-law electron spectrum with an exponential cutoff exists immediately surrounding the termination shock of the pulsar wind nebula.**

1611.03496
astro-ph/0202232

- The boundary of the pulsar wind nebula occurs at the termination shock, where the relativistic wind is stopped by the dense ISM.

- The radius of the termination shock can be calculated as:

$$R_{\rm PWN} \simeq 1.5 \left(\frac{\dot{E}}{10^{35}\,{\rm erg/s}}\right)^{1/2} \times \left(\frac{n_{\rm gas}}{1\,{\rm cm}^{-3}}\right)^{-1/2} \left(\frac{v}{100\,{\rm km/s}}\right)^{-3/2} {\rm pc}$$

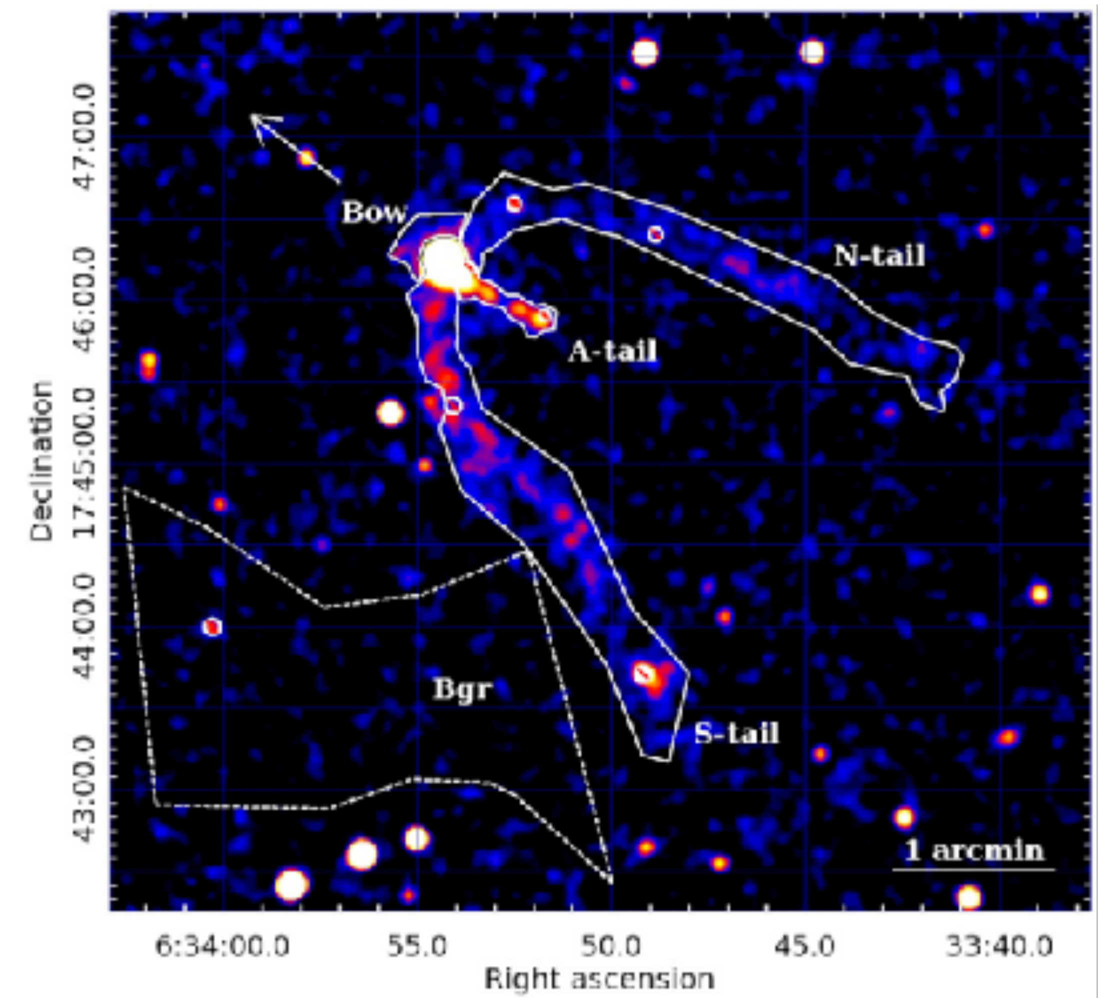

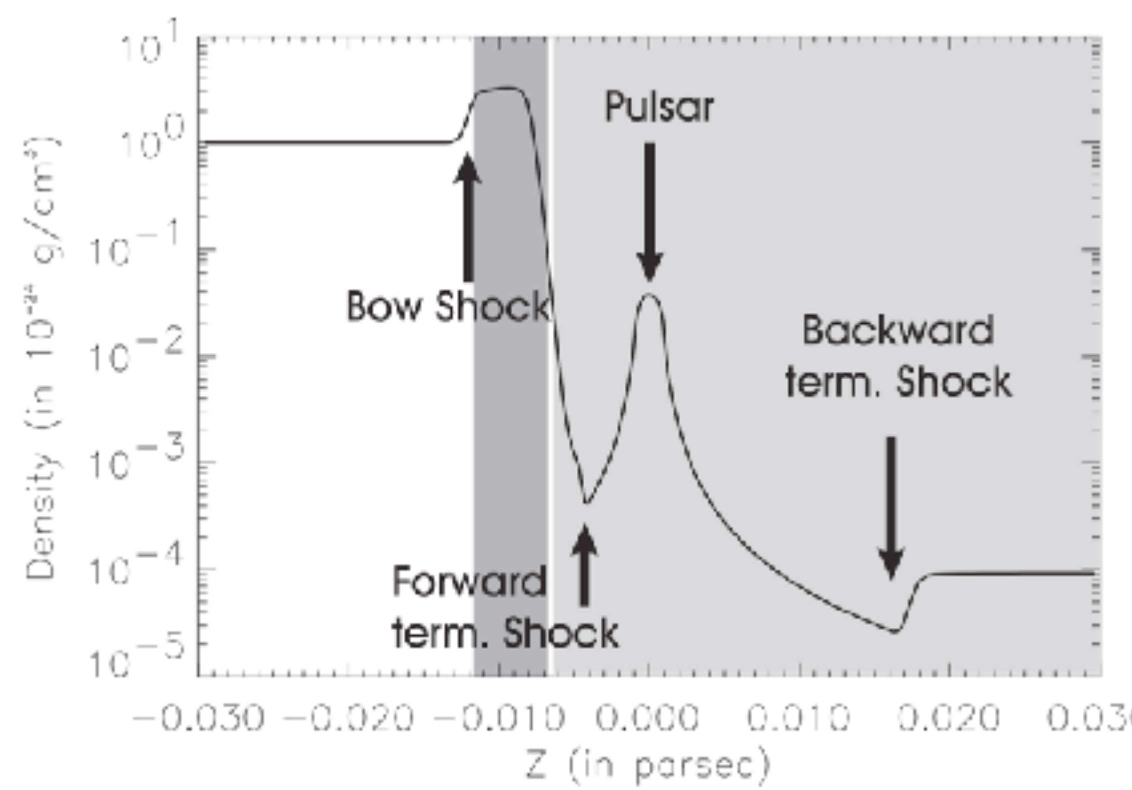

- The cooling inside PWN is significant.
- The spectrum of the PWN changes as a function of:
  - age
  - distance from pulsar

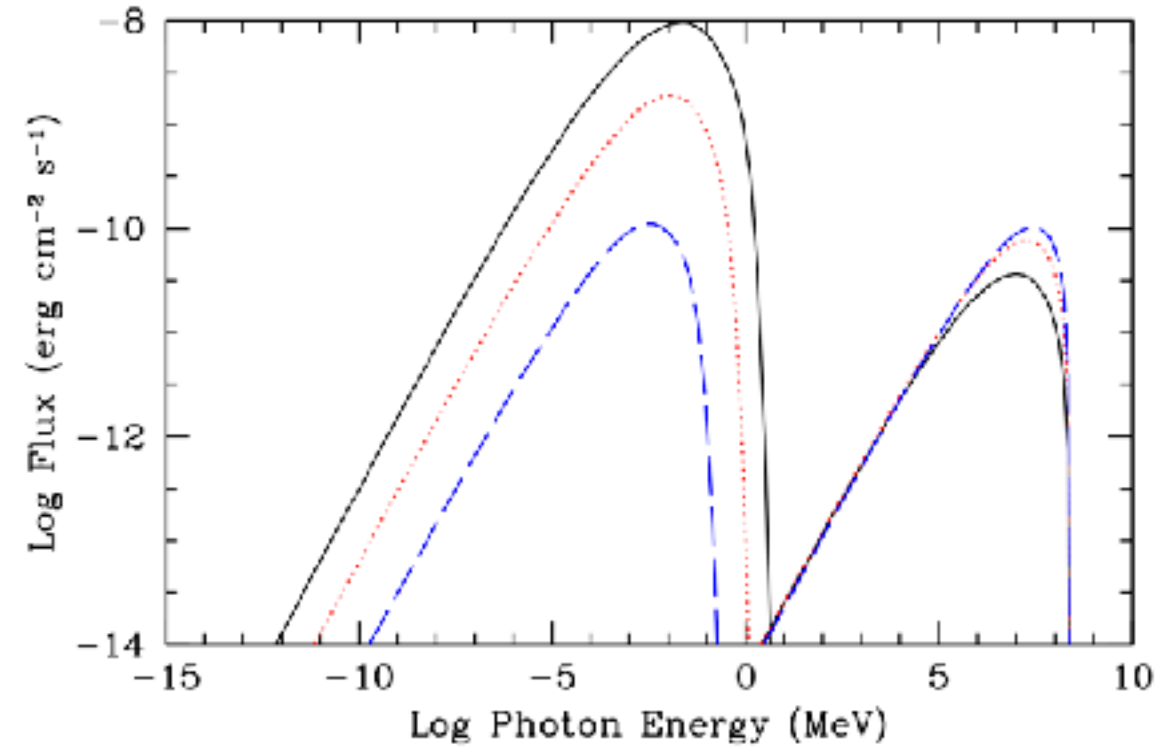

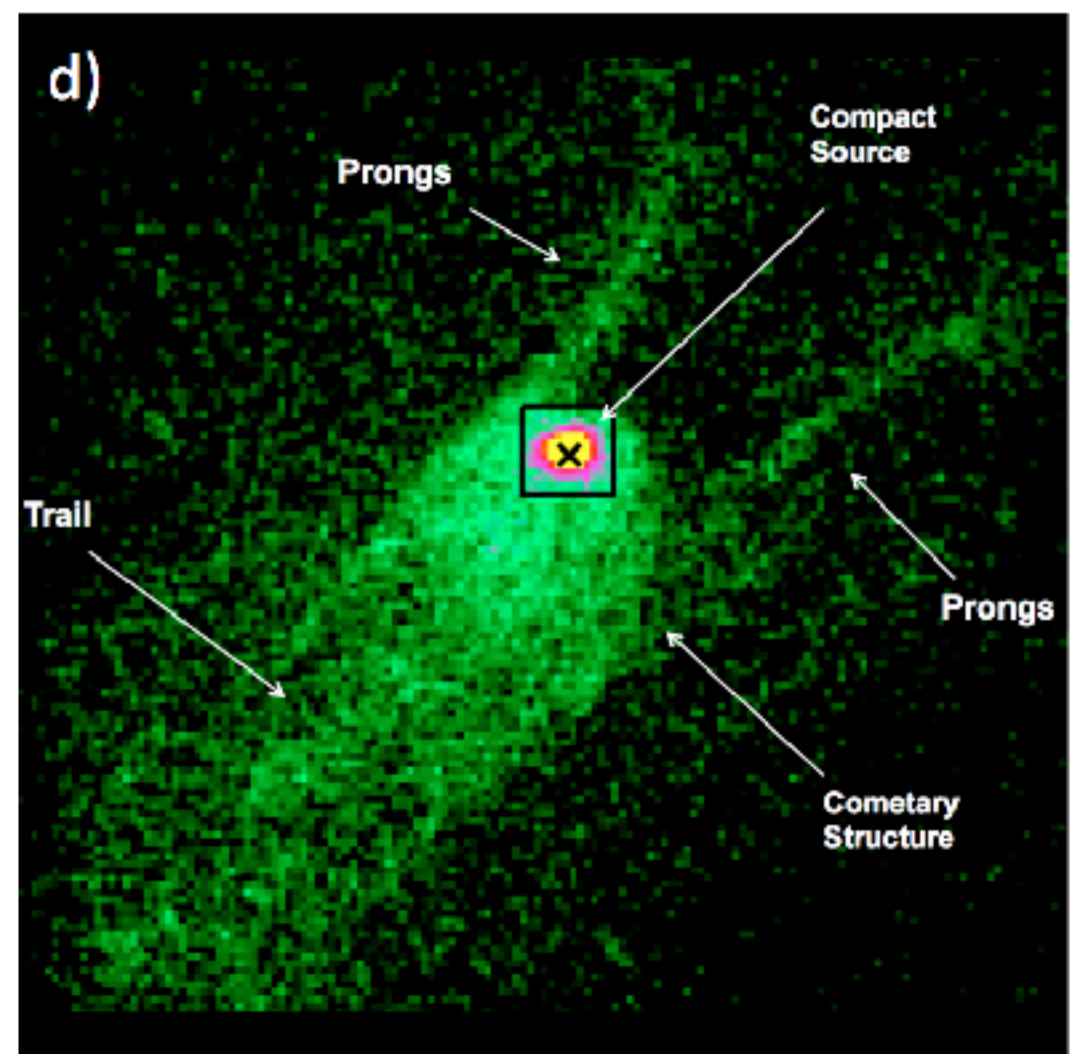

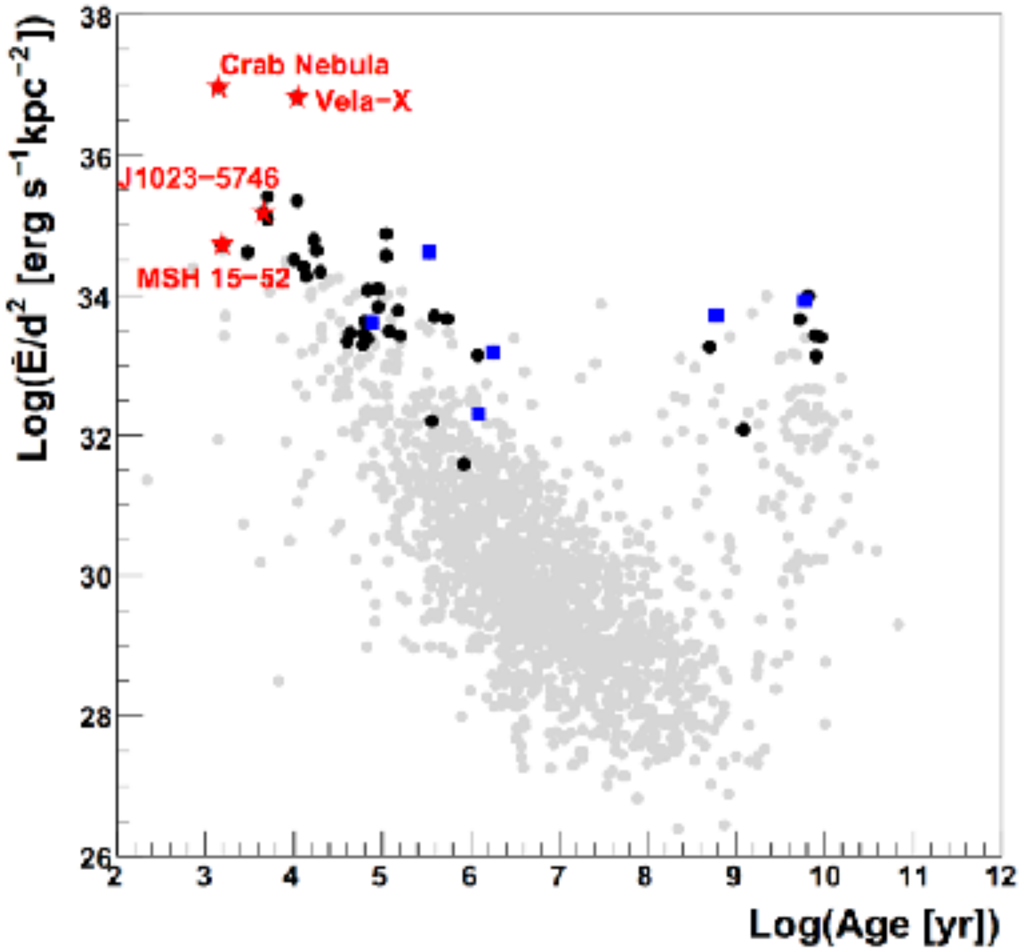

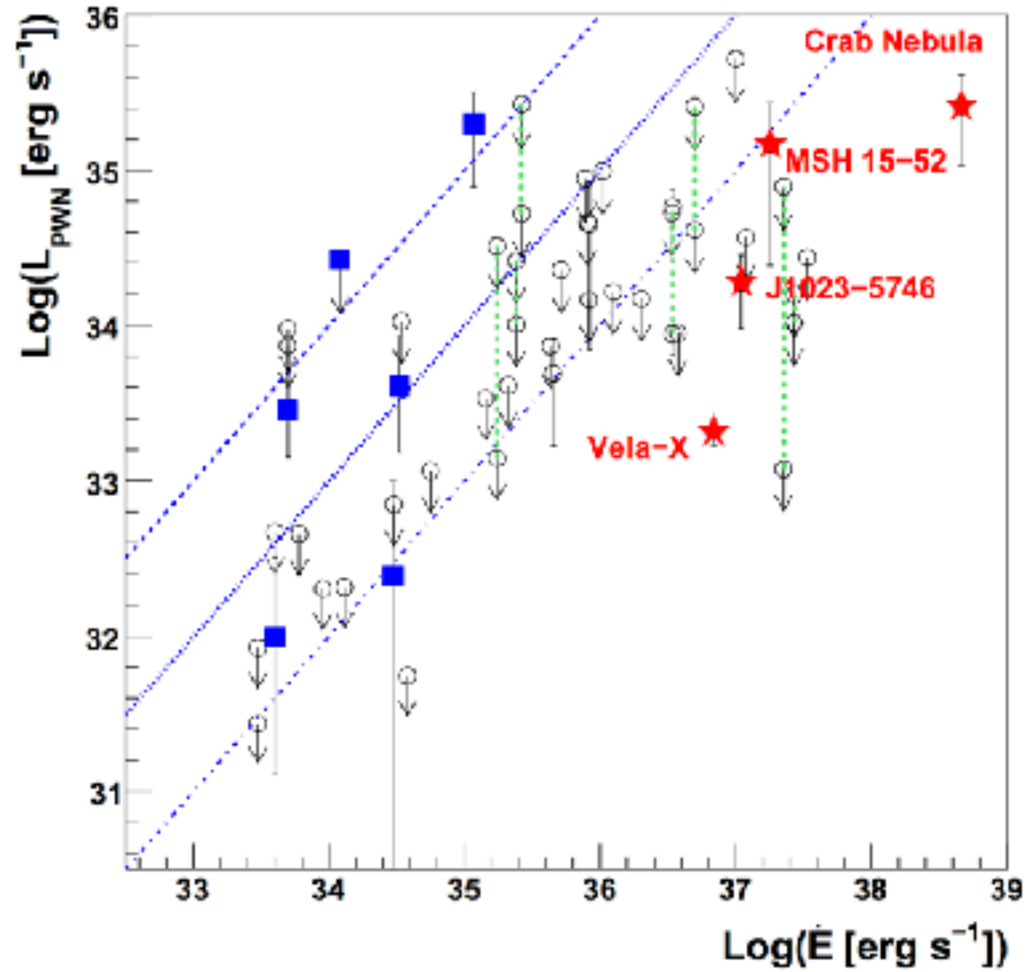

- Fermi-LAT observations have discovered TeV PWN around several systems:
- Indicative of the TeV electron origin of these sources.
- Very hard spectrum of sources make GeV observations difficult.

Table 1 HGPS sources considered as firmly identified pulsar wind nebulae in this paper.

HGPS name	ATNF name	Canonical name	$\lg \dot{E}$	τ_c (kyr)	d (kpc)	PSR offset (pc)	Γ	$R_{\rm PWN}$ (pc)	$L_{1-10\,\rm TeV}$ (10^{33} erg s^{-1})
J1813−178[1]	J1813−1749		37.75	5.60	4.70	< 2	2.07 ± 0.05	4.0 ± 0.3	19.0 ± 1.5
J1833−105	J1833−1034	G21.5−0.9[2]	37.53	4.85	4.10	< 2	2.42 ± 0.19	< 4	2.6 ± 0.5
J1514−591	B1509−58	MSH 15−52[3]	37.23	1.56	4.40	< 4	2.26 ± 0.03	11.1 ± 2.0	52.1 ± 1.8
J1930+188	J1930+1852	G54.1+0.3[4]	37.08	2.89	7.00	< 10	2.6 ± 0.3	< 9	5.5 ± 1.8
J1420−607	J1420−6048	Kookaburra (K2)[5]	37.00	13.0	5.61	5.1 ± 1.2	2.20 ± 0.05	7.9 ± 0.6	44 ± 3
J1849−000	J1849−0001	IGR J18490−0000[6]	36.99	42.9	7.00	< 10	1.97 ± 0.09	11.0 ± 1.9	12 ± 2
J1846−029	J1846−0258	Kes 75[2]	36.91	0.728	5.80	< 2	2.41 ± 0.09	< 3	6.0 ± 0.7
J0835−455	B0833−45	Vela X[7]	36.84	11.3	0.280	2.37 ± 0.18	1.89 ± 0.03	2.9 ± 0.3	$0.83 \pm 0.11^{*}$
J1837−069[8]	J1838−0655		36.74	22.7	6.60	17 ± 3	2.54 ± 0.04	41 ± 4	204 ± 8
J1418−609	J1418−6058	Kookaburra (Rabbit)[5]	36.69	10.3	5.00	7.3 ± 1.5	2.26 ± 0.05	9.4 ± 0.9	31 ± 3
J1356−645[9]	J1357−6429		36.49	7.31	2.50	5.5 ± 1.4	2.20 ± 0.08	10.1 ± 0.9	14.7 ± 1.4
J1825−137[10]	B1823−13		36.45	21.4	3.93	33 ± 6	2.38 ± 0.03	32 ± 2	116 ± 4
J1119−614	J1119−6127	G292.2−0.5[11]	36.36	1.61	8.40	< 11	2.64 ± 0.12	14 ± 2	23 ± 4
J1303−631[12]	J1301−6305		36.23	11.0	6.65	20.5 ± 1.8	2.33 ± 0.02	20.6 ± 1.7	96 ± 5

- **H.E.S.S. observations indicate a significant population of TeV sources coincident with pulsar wind nebulae.**

Table 4 Candidate pulsar wind nebulae from the pre-selection.

HGPS name	ATNF name	$\lg \dot{E}$	τ_c (kyr)	d (kpc)	PSR offset (pc)	Γ	$R_{\rm PWN}$ (pc)	$L_{1-10\,\rm TeV}$ ($10^{33}\,\rm erg\,s^{-1}$)
J1616−508 (1)	J1617−5055	37.20	8.13	6.82	< 26	2.34 ± 0.06	28 ± 4	162 ± 9
J1023−575	J1023−5746	37.04	4.60	8.00	< 9	2.36 ± 0.05	23.2 ± 1.2	67 ± 5
J1809−193 (1)	J1811−1925	36.81	23.3	5.00	29 ± 7	2.38 ± 0.07	35 ± 4	53 ± 3
J1857+026	J1856+0245	36.66	20.6	9.01	21 ± 6	2.57 ± 0.06	41 ± 9	118 ± 13
J1640−465	J1640−4631 (1)	36.64	3.35	12.8	< 20	2.55 ± 0.04	25 ± 8	210 ± 12
J1641−462	J1640−4631 (2)	36.64	3.35	12.8	50 ± 5	2.50 ± 0.11	< 14	17 ± 4
J1708−443	B1706−44	36.53	17.5	2.60	17 ± 3	2.17 ± 0.08	12.7 ± 1.4	6.6 ± 0.9
J1908+063	J1907+0602	36.45	19.5	3.21	21 ± 3	2.26 ± 0.06	27.2 ± 1.5	28 ± 2
J1018−589A	J1016−5857 (1)	36.41	21.0	8.00	47.5 ± 1.6	2.24 ± 0.13	< 4	8.1 ± 1.4
J1018−589B	J1016−5857 (2)	36.41	21.0	8.00	25 ± 7	2.20 ± 0.09	21 ± 4	23 ± 5
J1804−216	B1800−21	36.34	15.8	4.40	18 ± 5	2.69 ± 0.04	19 ± 3	42.5 ± 2.0
J1809−193 (2)	J1809−1917	36.26	51.3	3.55	< 17	2.38 ± 0.07	25 ± 3	26.9 ± 1.5
J1616−508 (2)	B1610−50	36.20	7.42	7.94	60 ± 7	2.34 ± 0.06	32 ± 5	220 ± 12
J1718−385	J1718−3825	36.11	89.5	3.60	5.4 ± 1.6	1.77 ± 0.06	7.2 ± 0.9	4.6 ± 0.8
J1026−582	J1028−5819	35.92	90.0	2.33	9 ± 2	1.81 ± 0.10	5.3 ± 1.6	1.7 ± 0.5
J1832−085	B1830−08 (1)	35.76	147	4.50	23.3 ± 1.5	2.38 ± 0.14	< 4	1.7 ± 0.4
J1834−087	B1830−08 (2)	35.76	147	4.50	32.3 ± 1.9	2.61 ± 0.07	17 ± 3	25.8 ± 2.0
J1858+020	J1857+0143	35.65	71.0	5.75	38 ± 3	2.39 ± 0.12	7.9 ± 1.6	7.1 ± 1.5
J1745−303	B1742−30 (1)	33.93	546	0.200	1.42 ± 0.15	2.57 ± 0.06	0.62 ± 0.07	0.014 ± 0.003
J1746−308	B1742−30 (2)	33.93	546	0.200	< 1.1	3.3 ± 0.2	0.56 ± 0.12	0.009 ± 0.003

- **H.E.S.S. observations indicate a significant population of TeV sources coincident with pulsar wind nebulae.**

1702.08280

- Intriguingly, H.E.S.S. finds that many of these sources are significantly larger than the putative PWN size.

- This is particularly true for older, low-energy systems.

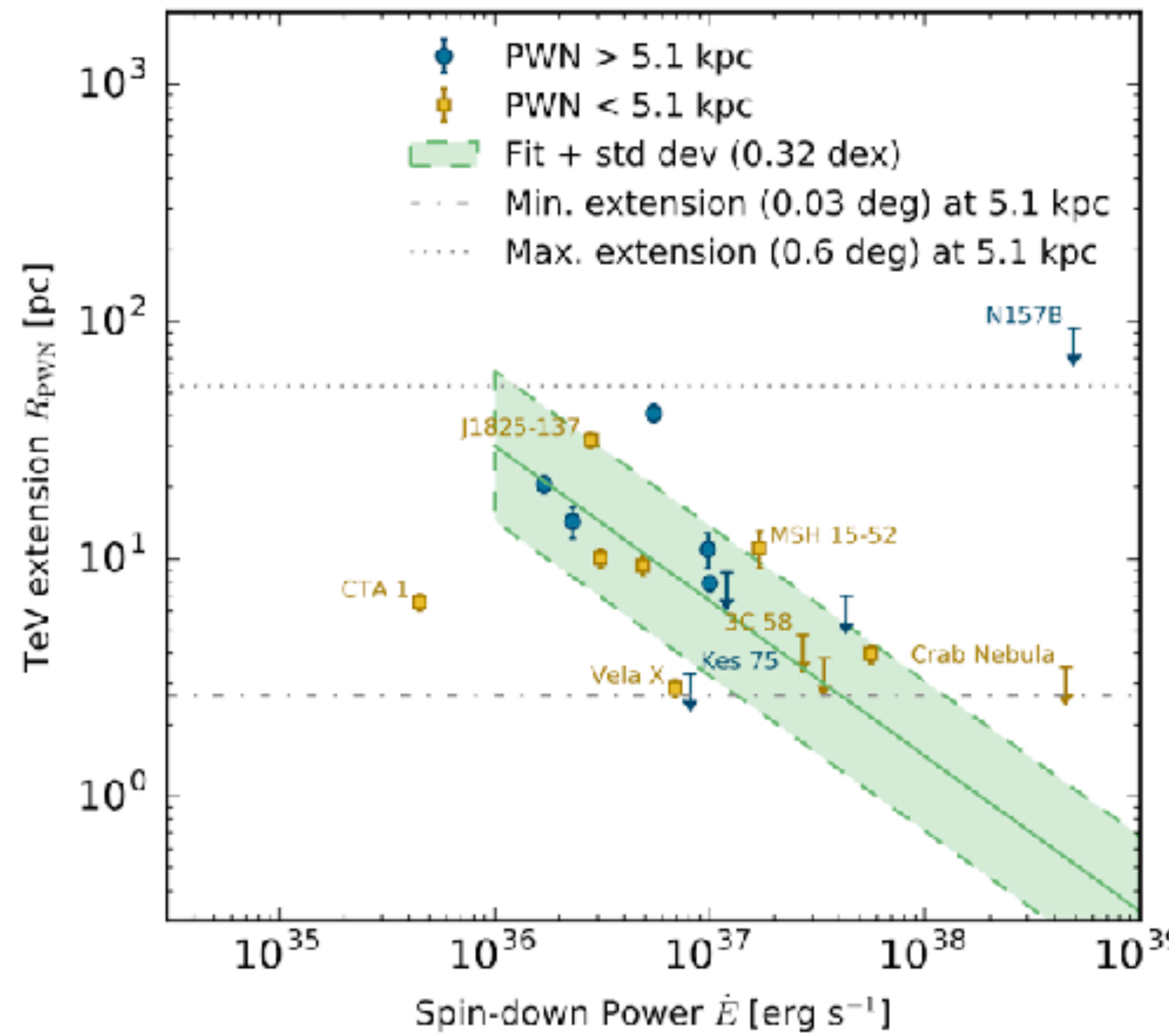

- Constraints on the exact energy dependence are relatively poor.

MILAGRO OBSERVATIONS OF EXTENDED EMISSION FROM GEMINGA

- Milagro finds emission surrounding the Geminga pulsar with a FWHM of $2.6^{+0.7}_{-0.9}$ °
- This corresponds to a 5-10 pc extent assuming a Geminga distance of 250^{+230}_{-80} pc
- Note the large uncertainty on the Geminga distance.

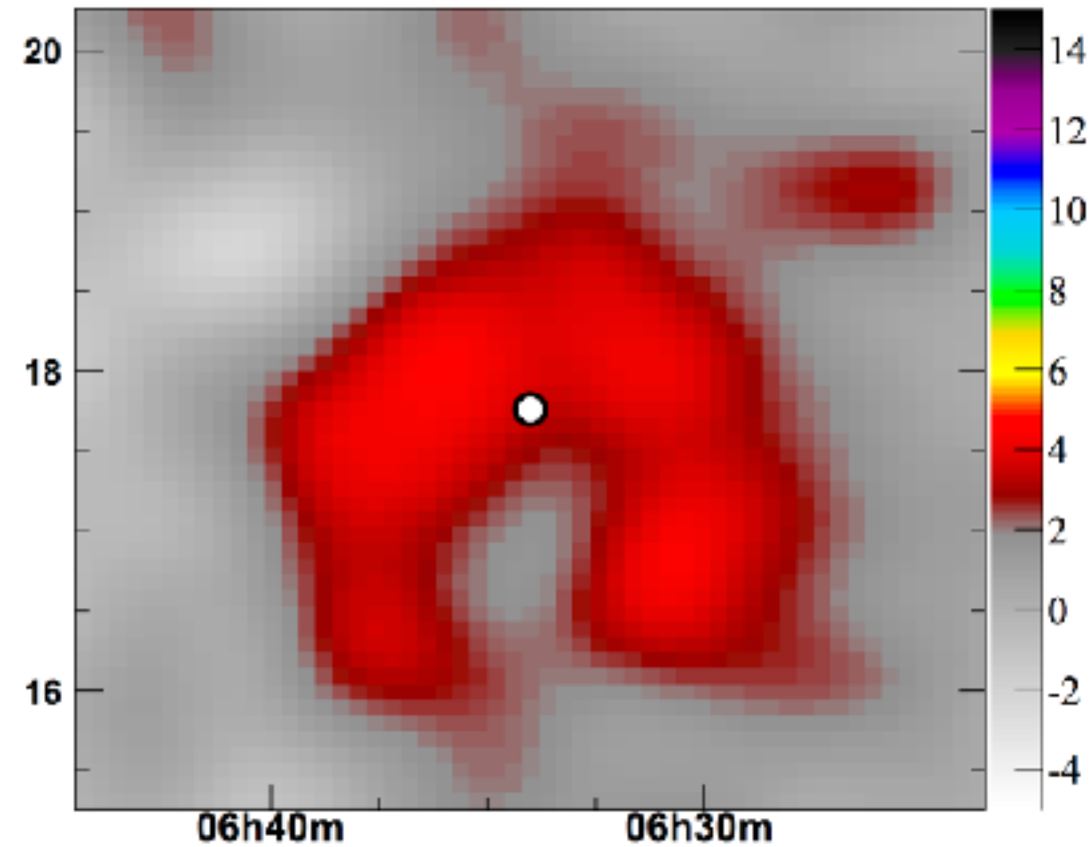

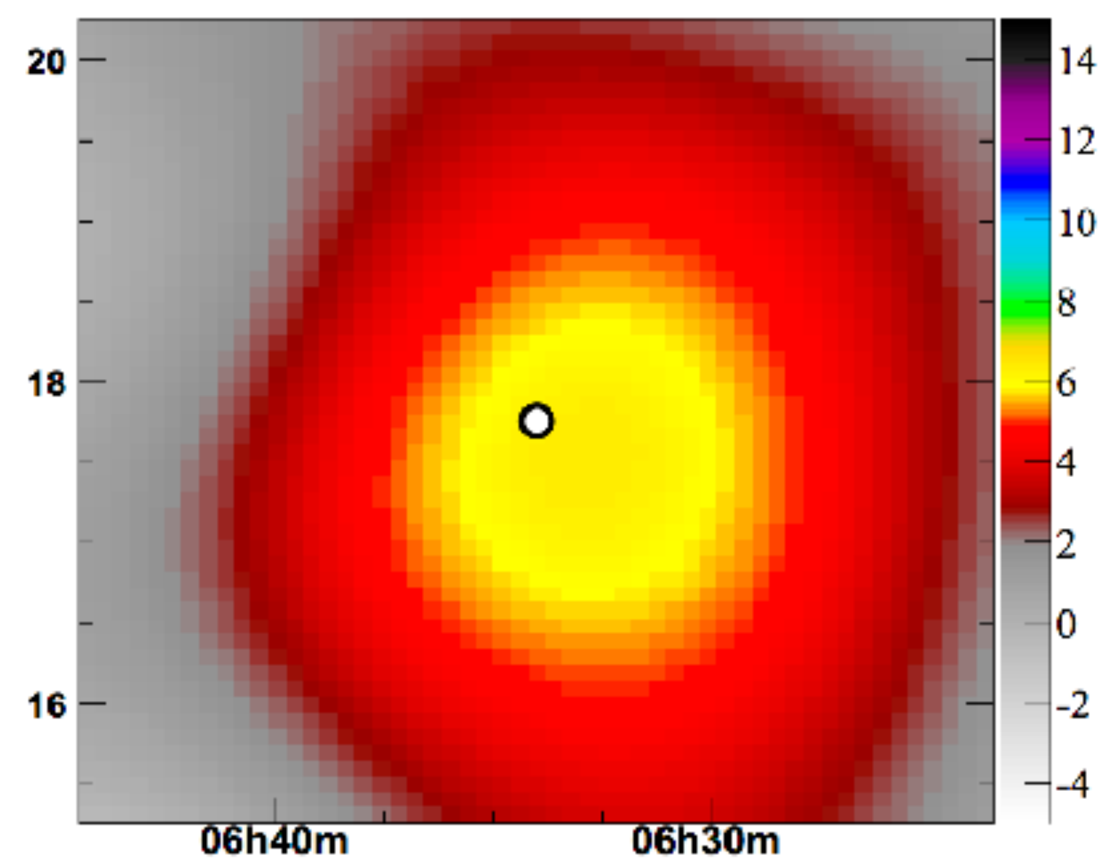

HAWC OBSERVATIONS OF GEMINGA AND MONOGEM

Name	Tested radius [°]	Index	$F_7 \times 10^{15}$ [$\mathrm{TeV}^{-1}\mathrm{cm}^{-2}\mathrm{s}^{-1}$]	TeVCat
2HWC J0534+220	-	-2.58 ± 0.01	184.7 ± 2.4	Crab
2HWC J0631+169	-	-2.57 ± 0.15	6.7 ± 1.5	Geminga
"	2.0	-2.23 ± 0.08	48.7 ± 6.9	Geminga
2HWC J0635+180	-	-2.56 ± 0.16	6.5 ± 1.5	Geminga
2HWC J0700+143	1.0	-2.17 ± 0.16	13.8 ± 4.2	-
"	2.0	-2.03 ± 0.14	23.0 ± 7.3	-

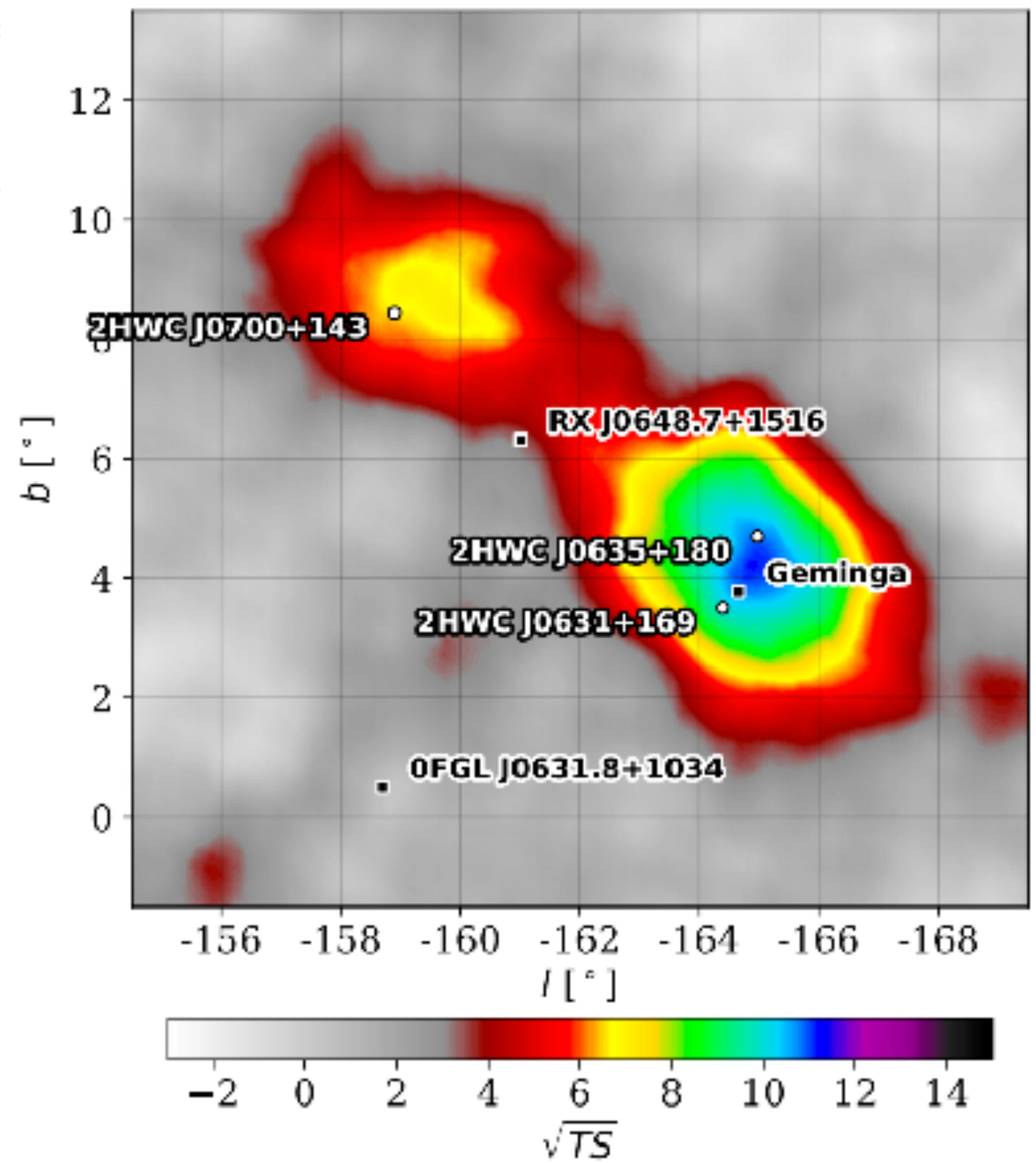

- Both Geminga and “Monogem” observed at high significance
- Both sources better fit by extended emission profiles.
- Both sources have extremely hard spectral indices.

- **TeV sources coincident with pulsars are morphologically distinct from radio and X-Ray PWN.**

- **The PWN morphology is directly connected to the physics of the termination shock.**

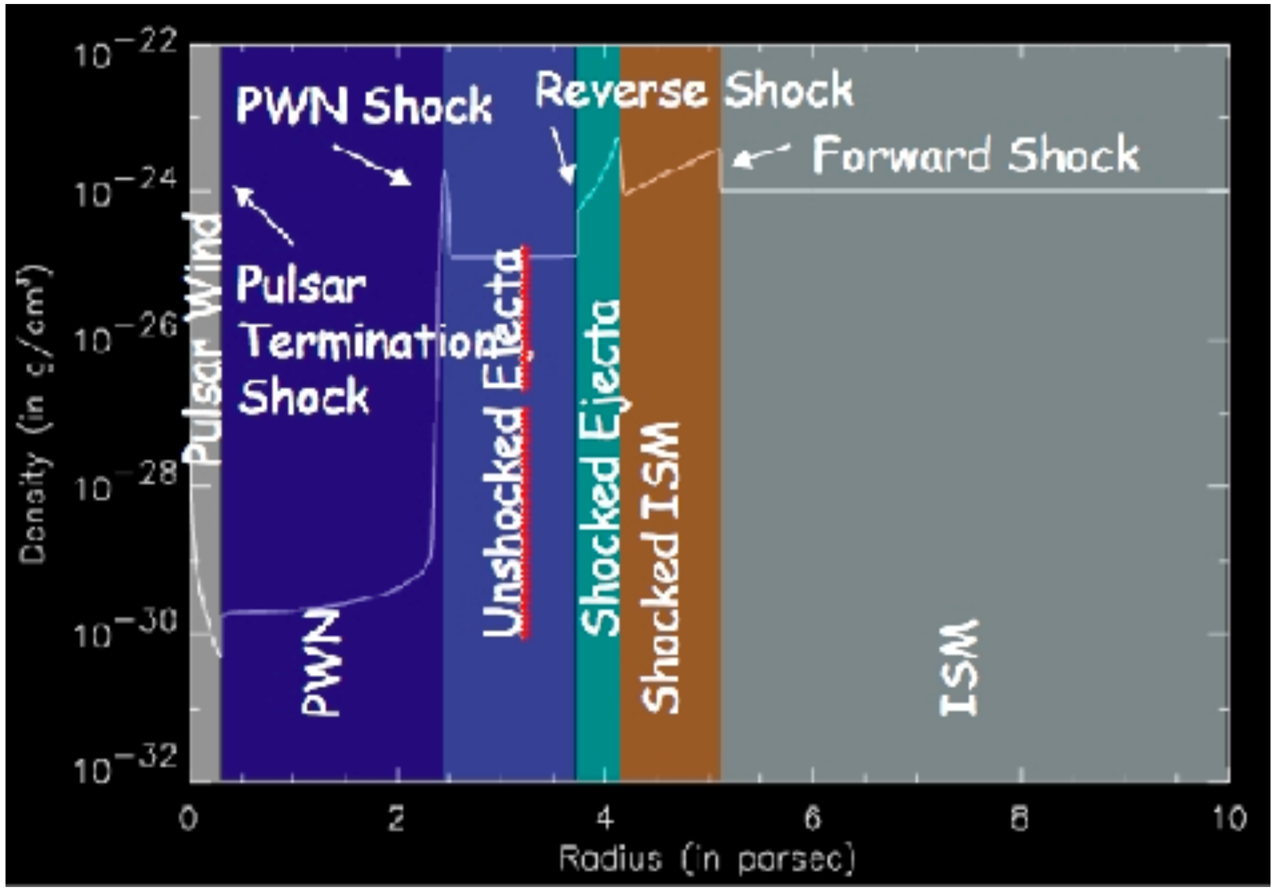

- **TeV Halos require a <u>new</u> physical mechanism to explain their morphology**

- Will temporarily focus on Geminga

- Bright
- High latitude (low background)
- Middle aged (no supernova remnant)

- Would get same results if we used Monogem (actually slightly better results).

- **The bright flux and hard spectrum of HAWC Geminga measurements indicate a significant, hard lepton component:**

Name	Tested radius [°]	Index	$F_7 \times 10^{15}$ [$\mathrm{TeV^{-1} cm^{-2} s^{-1}}$]	TeVCat
2HWC J0631+169	-	-2.57 ± 0.15	6.7 ± 1.5	Geminga
"	2.0	-2.23 ± 0.08	48.7 ± 6.9	Geminga
2HWC J0635+180	-	-2.56 ± 0.16	6.5 ± 1.5	Geminga

- **To fit this data, we use an electron spectrum $1.5 < \alpha < 1.9$ and 35 TeV < E_{cut} < 60 TeV**

- **Geminga cannot dominate the magnetic field and ISRF over the 10 pc extent of its TeV halo:**

$$U = \frac{1}{8\pi} B^2 = \frac{(10\mu G)^2}{8\pi}$$
$$= 4\times10^{-12} \frac{ergs}{cm^3}$$
$$\int_0^{10pc} U\,dV = 5\times10^{47}\ erg$$
$$\hookrightarrow \text{Magnetic Flux} \simeq 5\times10^{38} \frac{ers}{s}$$

$$ISRF = 1 \frac{eV}{cm^3}$$
$$\int ISRF\,dV = 8\times10^{47}\ erg$$
$$\hookrightarrow \text{Flux} = 8\times10^{38} \frac{ers}{s}$$

- **Using standard ISRF values, 50% of the electron power produces gamma-rays through ICS, and 50% of the electron power is converted into synchrotron.**

- **Normalizing to the Geminga luminosity:**

  2.86×10^{31} erg s^{-1} at 7 TeV (~30 TeV e^+e^-)

- **Utilizing a best-fit spectrum, we obtain a total e^+e^- injection: 3.8×10^{33} erg s^{-1}**

- **Spindown Power of Geminga: 3.4×10^{34} erg s^{-1}**

- **Conversion Efficiency: ~10% !**

- **The large luminosity of TeV halos implies that cosmic-ray leptons lose the vast majority of their energy to inverse-Compton scattering before exiting the TeV halo.**

$$\tau = 3.1 \times 10^4 \, \text{yr} \left(\frac{E_e}{10 \, \text{TeV}}\right)^{-1}$$

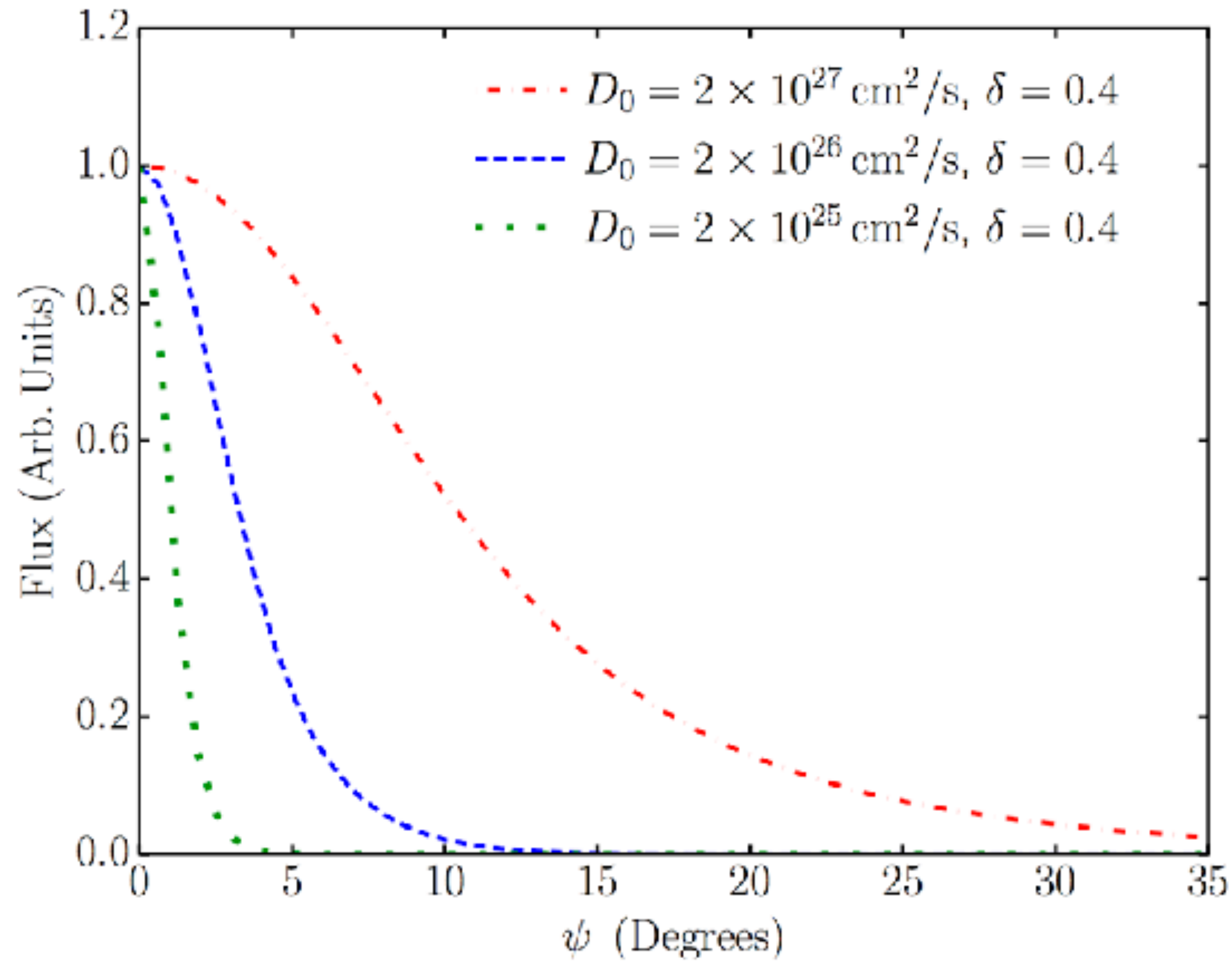

- **This constrains the efficiency of particle propagation near a pulsar.**

$$D = \frac{L^2}{6\tau} = \frac{(10\ \mathrm{pc})^2}{6(3.1\times10^4\ \mathrm{yr})} = \frac{(3.08\times10^{19}\ \mathrm{cm})^2}{5.86\times10^{12}\ \mathrm{s}}$$

$$\boxed{D = 1.6\times10^{26}\ \frac{\mathrm{cm}^2}{\mathrm{s}}}$$

- **While advective forces may also play a role, we can set an upper limit on the diffusion efficiency.**
- **Diffusion must be orders of magnitude less efficient near pulsars than typical for the interstellar medium.**

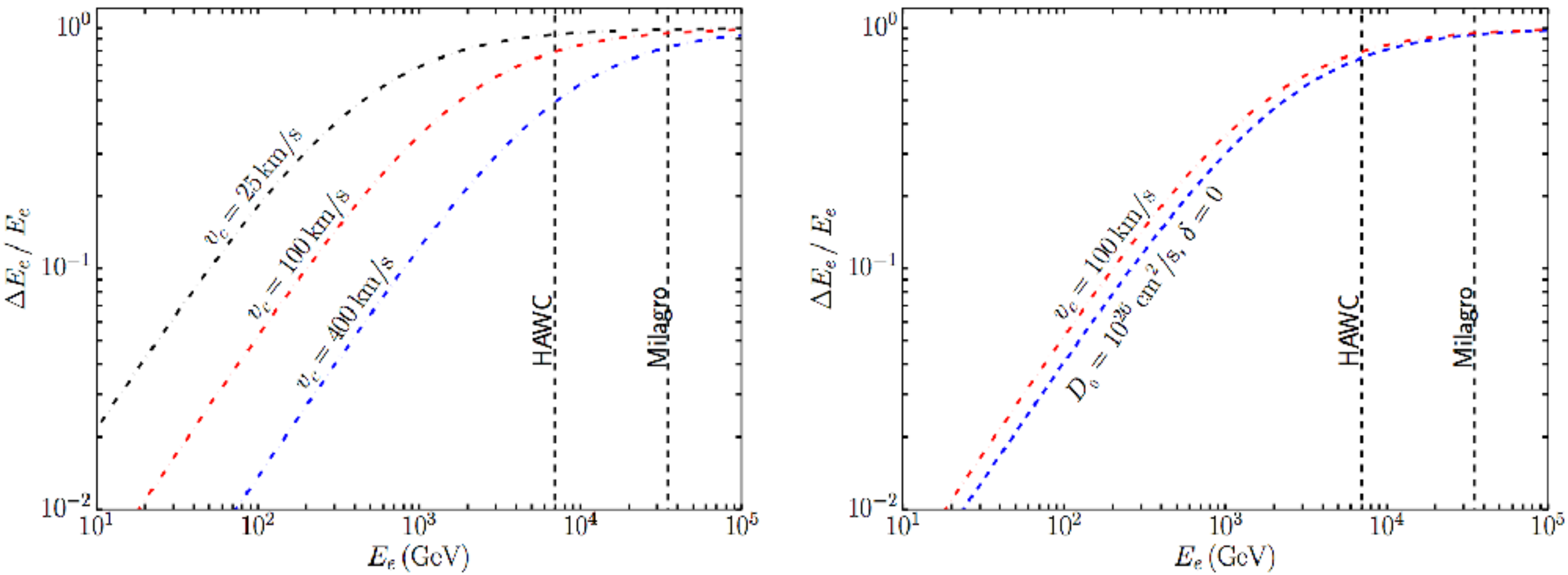

- **This scenario holds so long as δ < 1, and can be modeled as either diffusion or particle advection.**
- **A diffusion constant of 10^{26} cm^2s^{-1} or convection velocity of 100 km s^{-1} is necessary.**

COSMIC-RAY DIFFUSION IN A TEV HALO

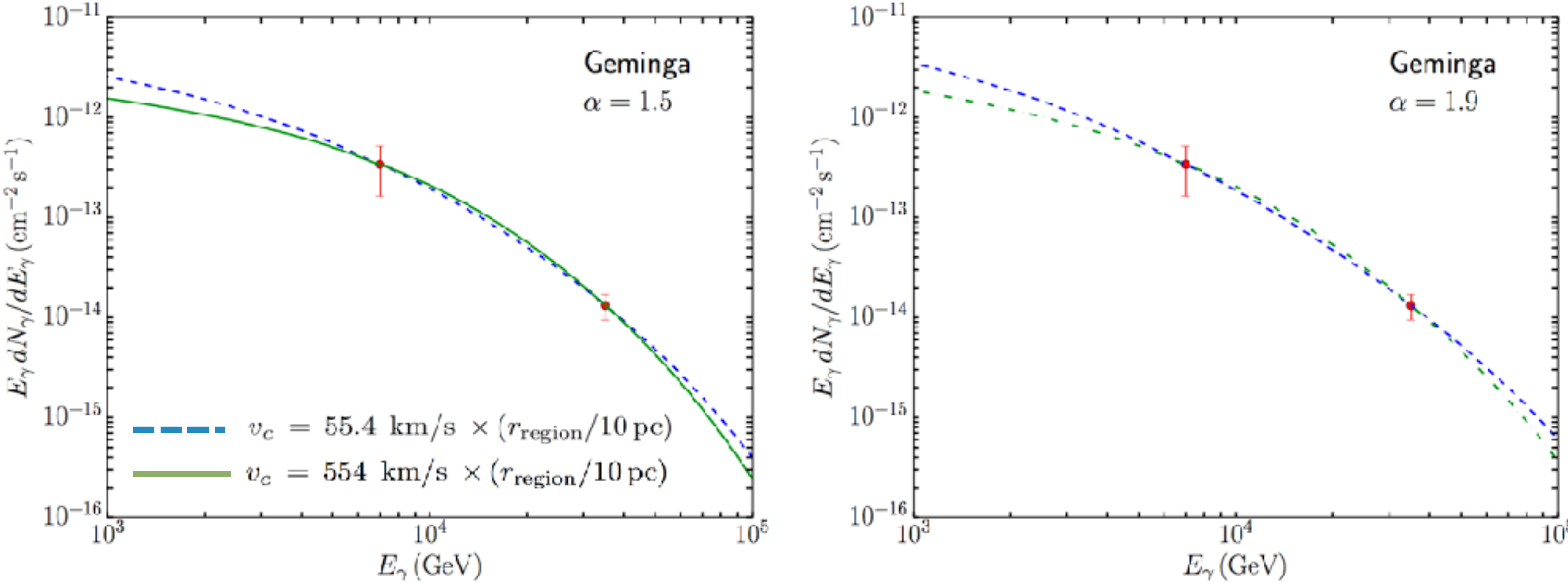

- **Combined HAWC/Milagro data can be fit with different spectra and convection velocities.**
- **The exponential cutoff of the spectrum is a free parameter, and spans 35 - 67 TeV.**

COSMIC-RAY DIFFUSION IN A TEV HALO

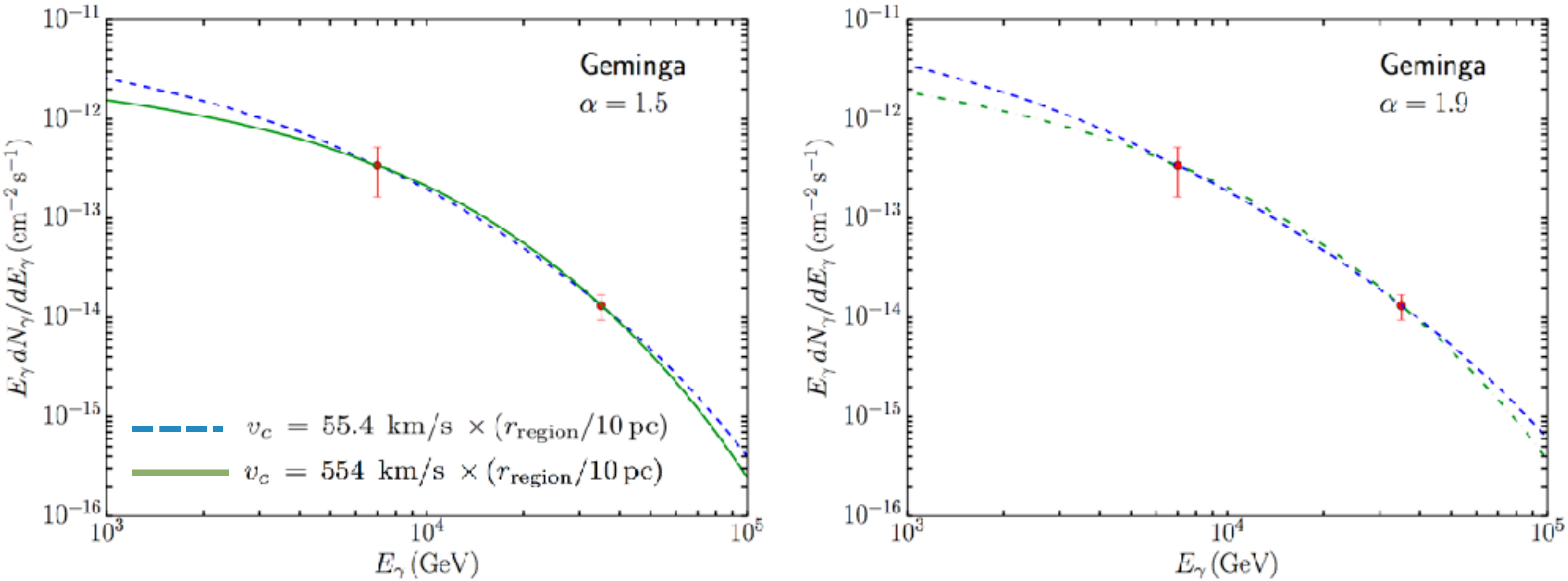

- **HAWC Spectral Constraint -2.23 +/- 0.08**
- **Strongly favors large convection velocity (-2.2 to -2.3) over small convection velocity (-2.5 to -2.6)**

BOHM DIFFUSION?

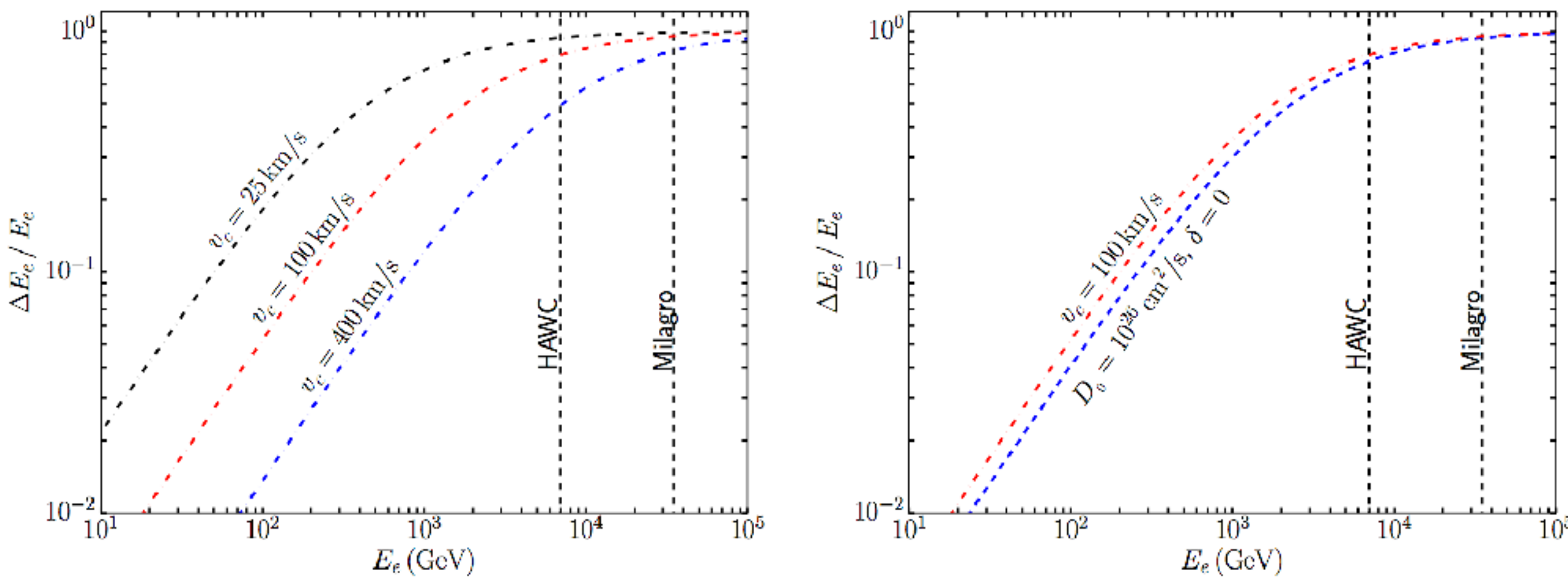

- **This energy loss rate could be tweaked, in the scenario where diffusion is Bohmian (δ < 1)**
- **In this case, low-energy electrons will also lose significant energy:** $\tau_{Diff} \propto \frac{L^2}{D_0 E^{\delta}}$ $\quad \tau_{loss} \propto E^{-1}$

$$\boxed{\left(\frac{\Delta E}{E}\right) \stackrel{\sim}{\propto} \frac{\tau_{Diff}}{\tau_{loss}} \propto E^{1-\delta}}$$

BOHM DIFFUSION?

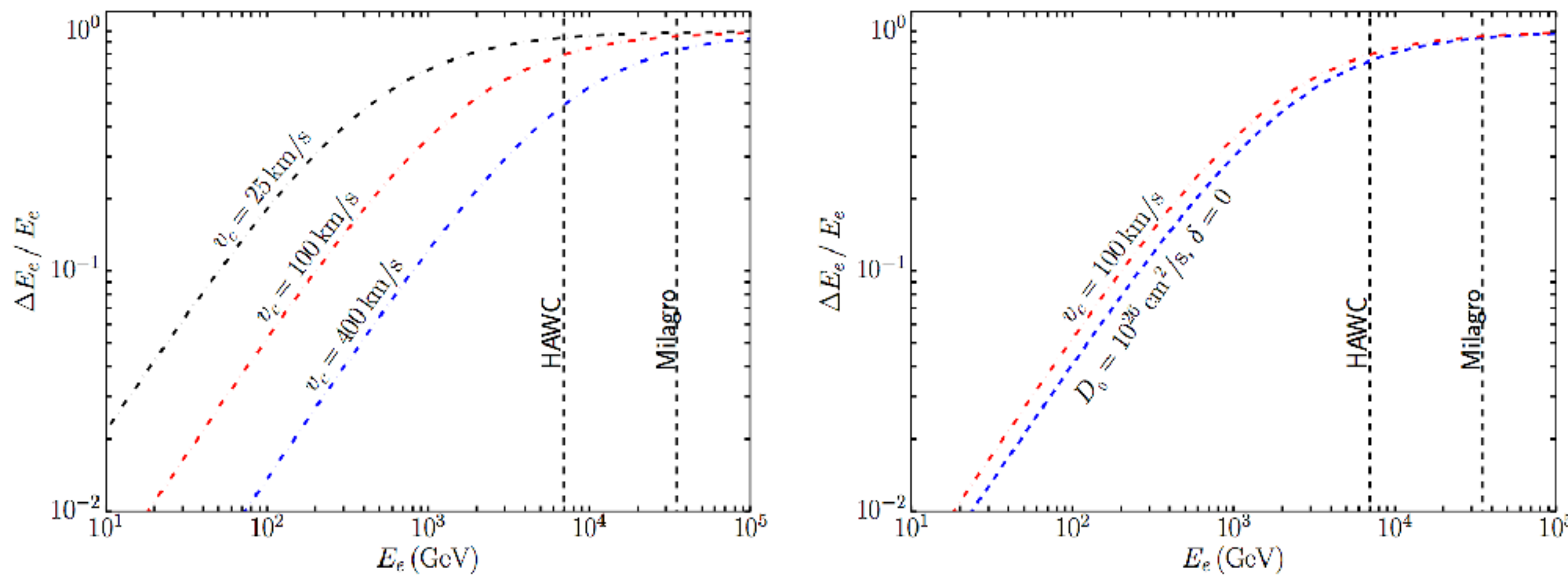

- However, the necessity for complete cooling at high-energies argues against this. Low-energy electrons would also need to be completely cooled.
- Spectrum of ICS from cooled electrons: $E^{-\alpha-1}$
- Necessary electron injection spectra: $E^{-1.23 +/- 0.08}$
- Actually much worse when Klein-Nishina effects are taken into account.

A LOWER LIMIT ON THE TEV HALO SIZE

- Thus far, we have only used HAWC observations to set a lower limit on the TeV halo size.

- The TeV halo could be much larger - and electron cooling defines the outer edge of the visible halo.

- Will now assume that observations of Geminga are typical for middle aged (100-400 kyr) pulsars.
- At least two such observed systems: Geminga, Monogem.
- Indications of many more such TeV halos.

- Cosmic-ray diffusion models indicate that the average diffusion constant in the Milky Way is ~5 x 10^{28}cm^{2}s^{-1}

- The cosmic-ray propagation parameters near Geminga must return to the average galactic value just outside the TeV halo region.

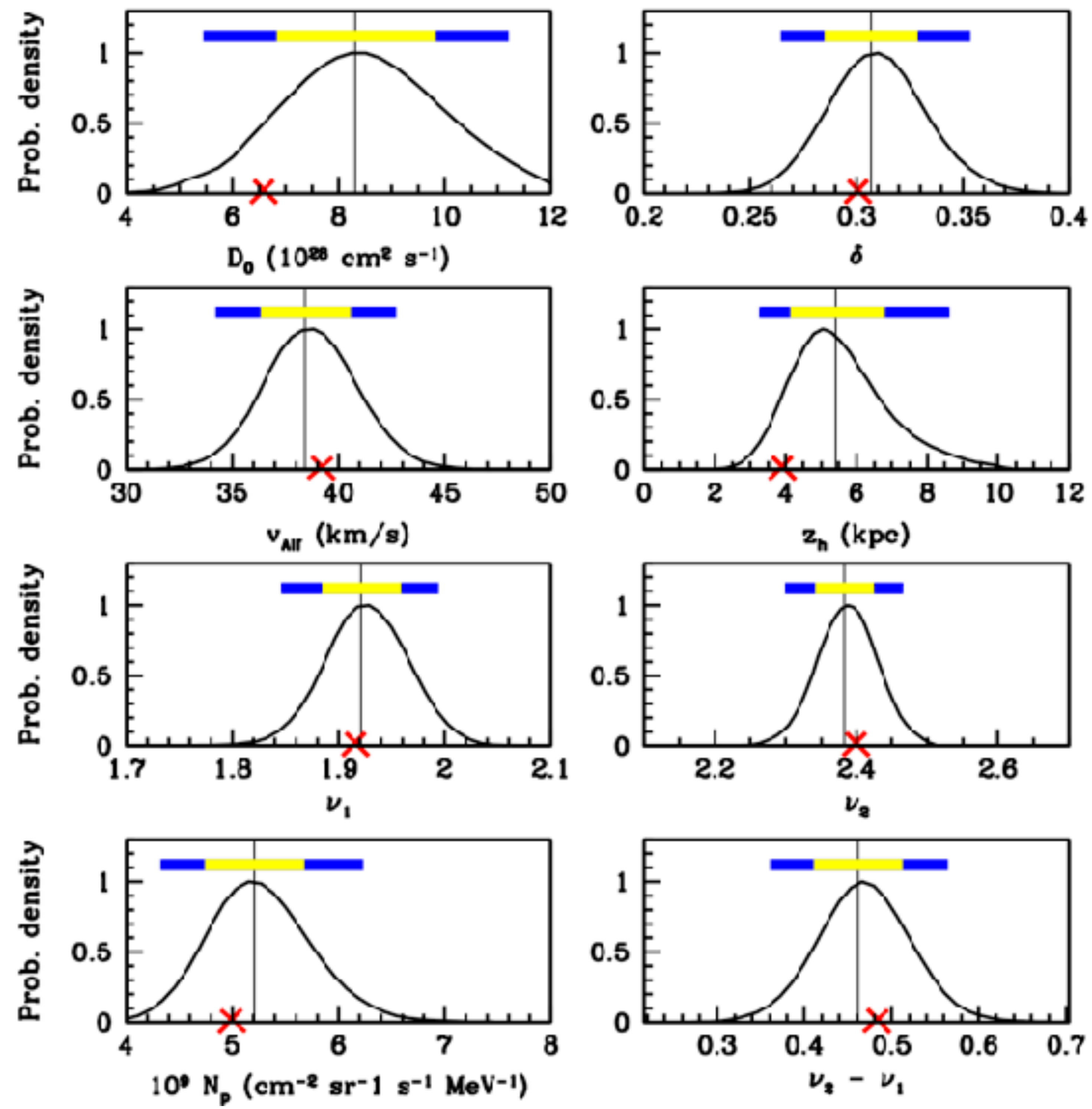

- **How large can TeV halos be without significantly altering this result?**

$$f \sim \frac{N_{\rm region} \times \frac{4\pi}{3} r^3_{\rm region}}{\pi R^2_{\rm MW} \times 2 z_{\rm MW}}$$
$$\sim 0.25 \times \left(\frac{r_{\rm region}}{100\,{\rm pc}}\right)^3 \left(\frac{\dot{N}_{\rm SN}}{0.03\,{\rm yr}^{-1}}\right) \left(\frac{\tau_{\rm region}}{10^6\,{\rm yr}}\right) \left(\frac{20\,{\rm kpc}}{R_{\rm MW}}\right)^2 \left(\frac{200\,{\rm pc}}{z_{\rm MW}}\right)$$

- **This also stands as the first indication of significant variability in the diffusion constant throughout the Milky Way.**

CAN WE BE INSIDE A TEV HALO?

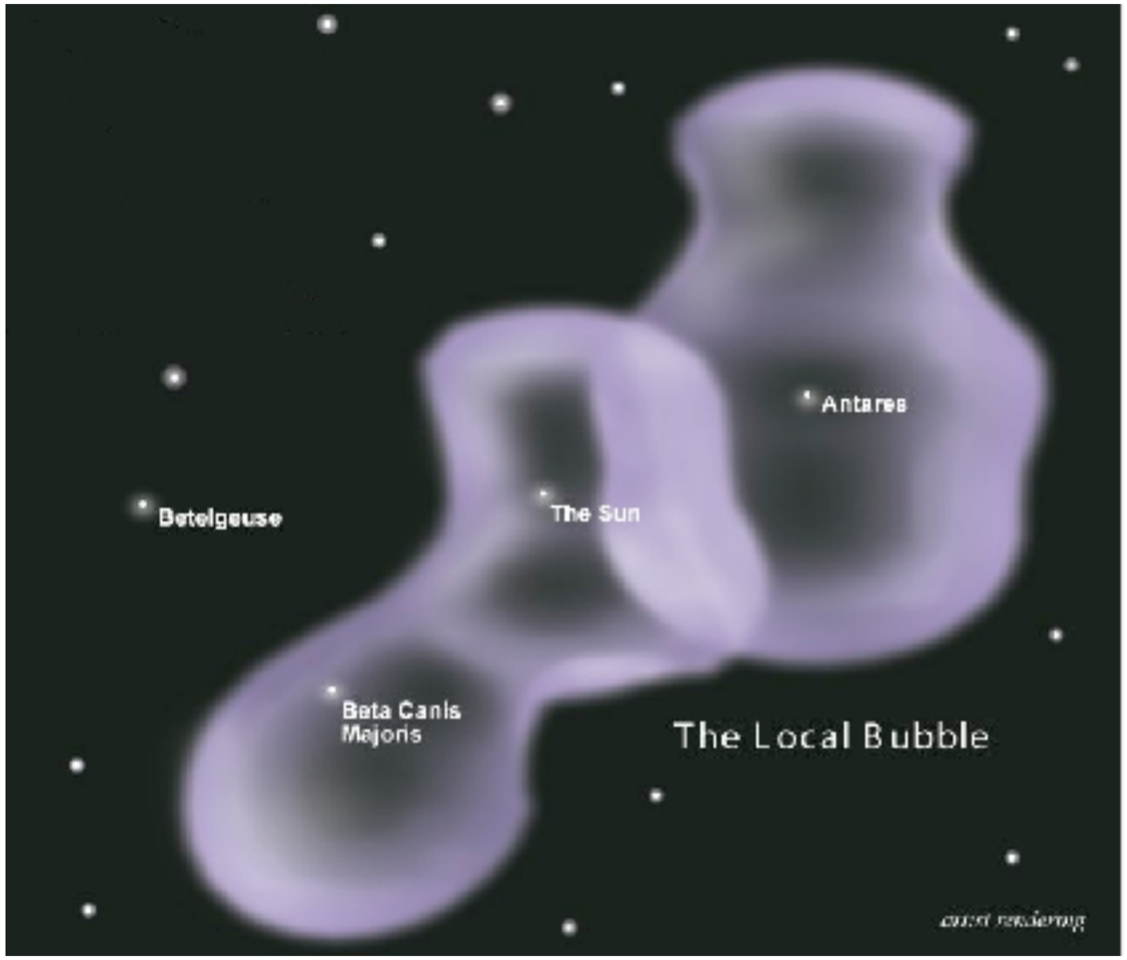

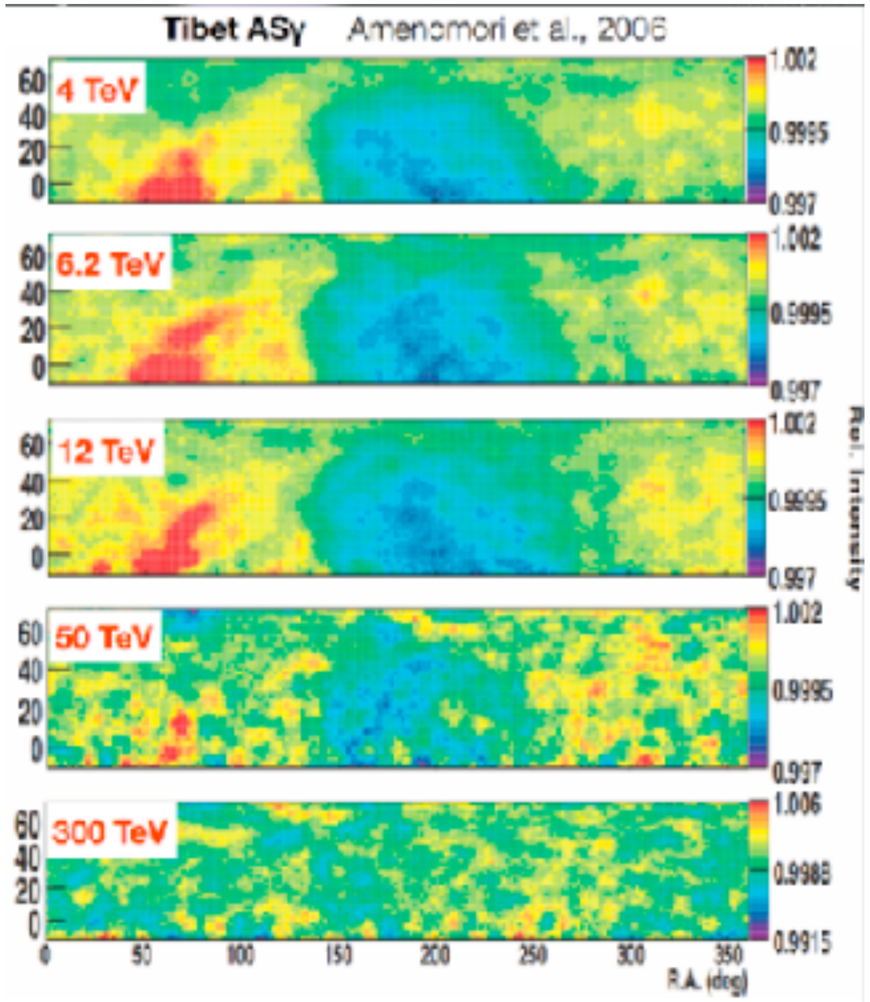

- We probably can not be inside a low-diffusion region without affecting the cosmic-ray proton anisotropy.
- If we are in a low-diffusion environment, then the source of the cosmic-ray electrons becomes significantly more confusing.

COSMIC-RAY DIFFUSION IN A TEV HALO

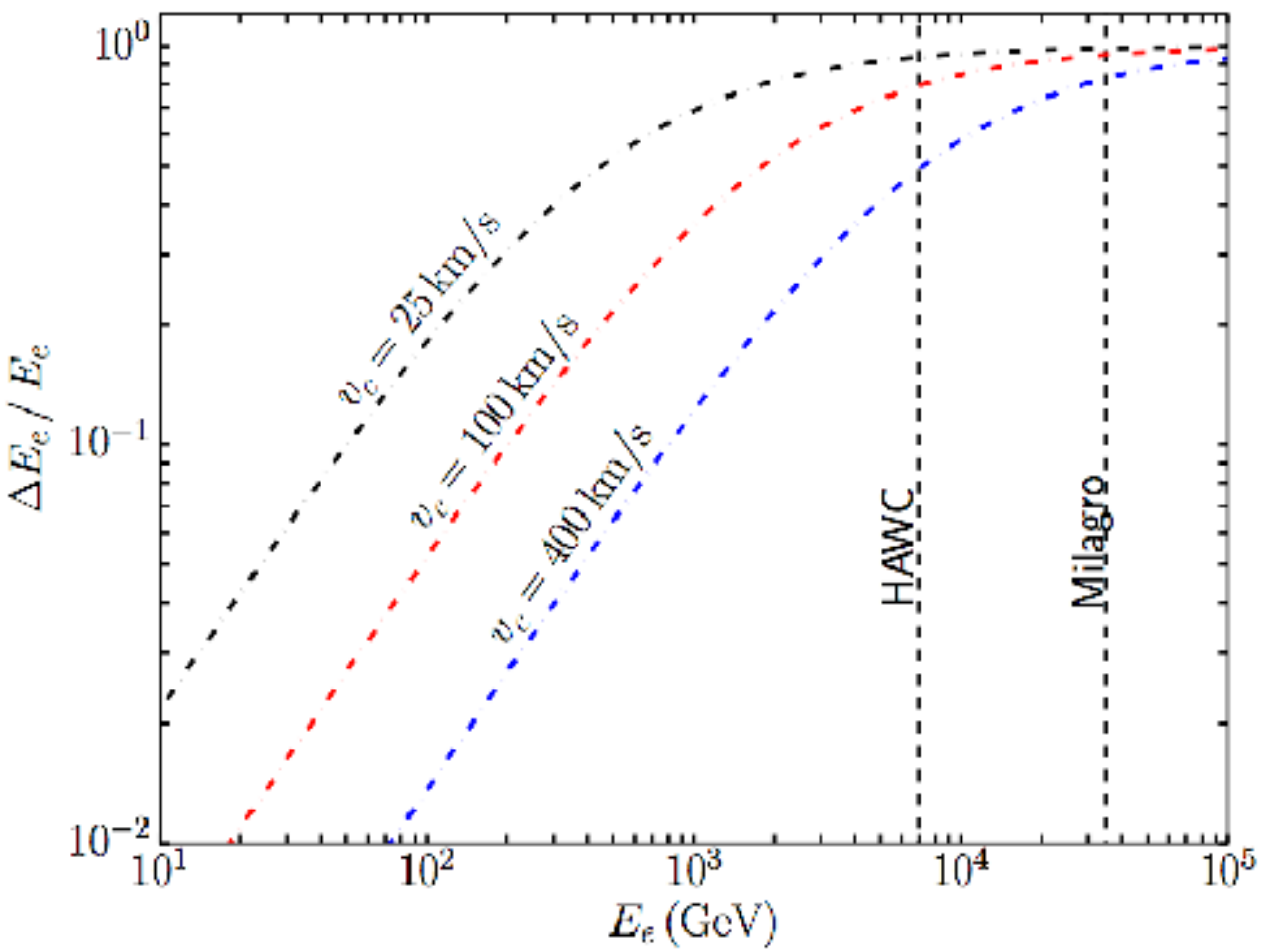

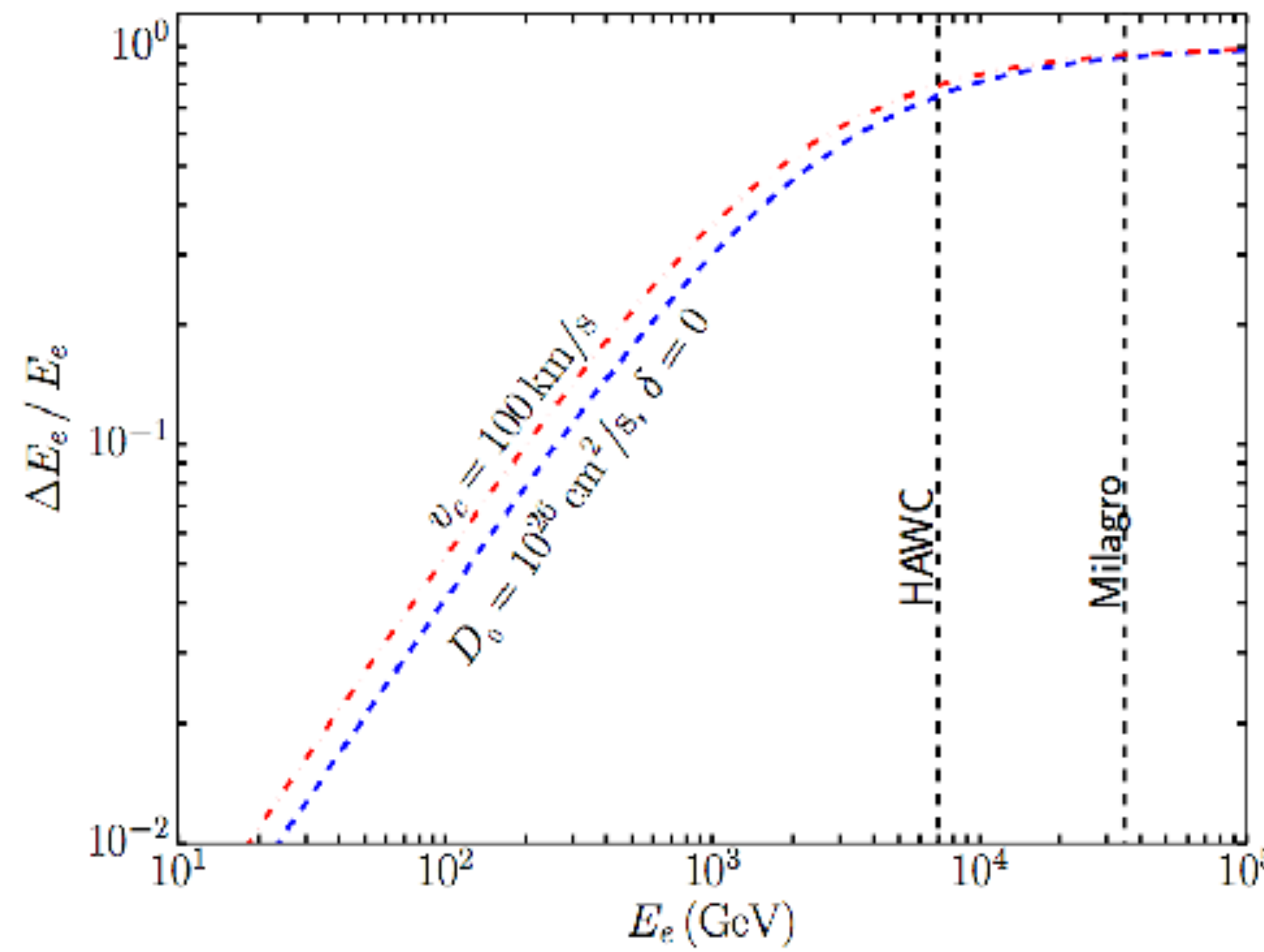

- **What about the low-energy electrons?**

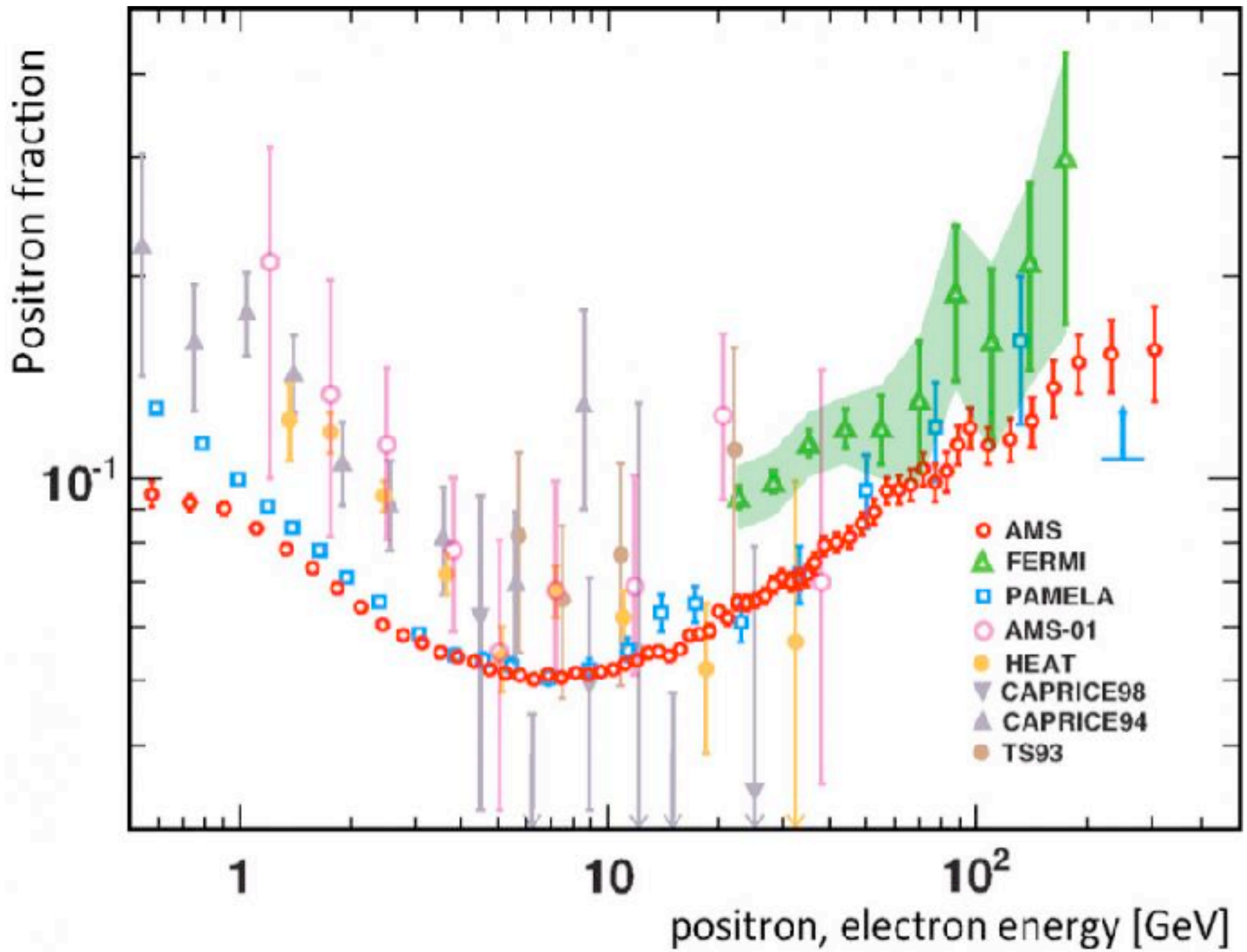

- **A significant excess in >10 GeV positrons is observed by multiple experiments.**

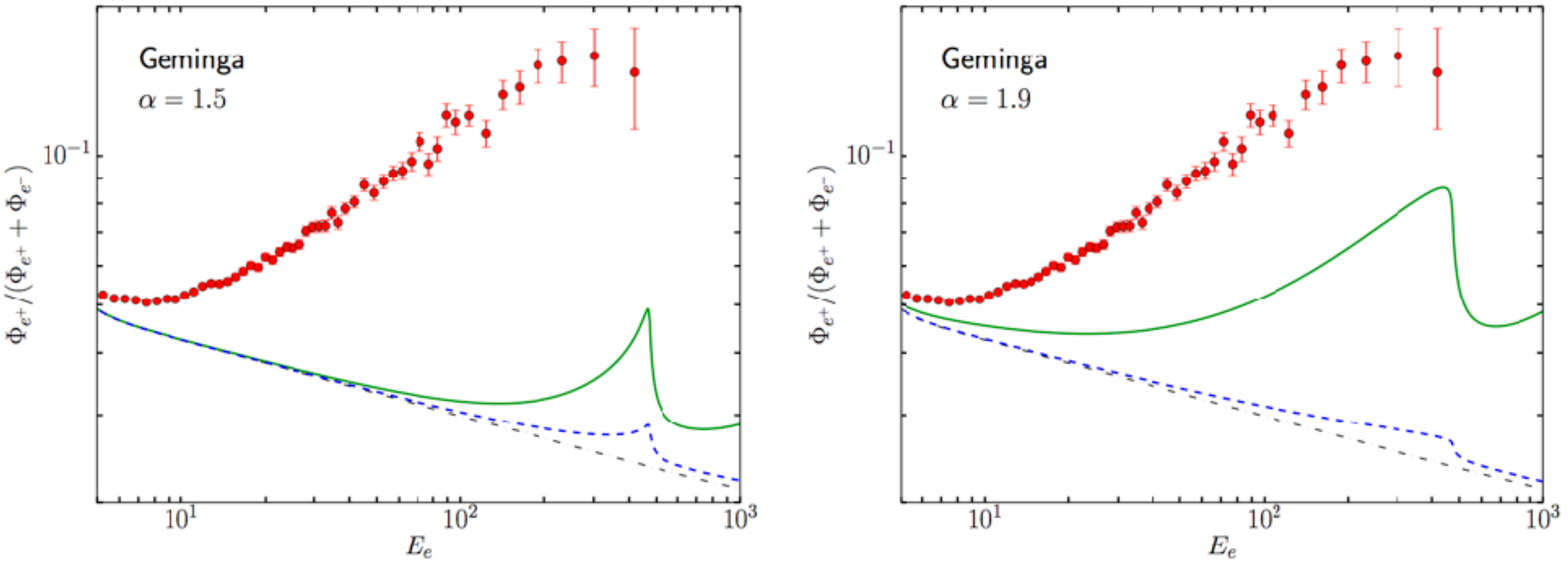

- Low energy electrons:
  - Must be produced in the pulsar wind nebula
  - Must escape the pulsar wind nebula
- Thus, they must contribute to the positron excess

- **Can extrapolate the positron contribution to all young pulsars.**

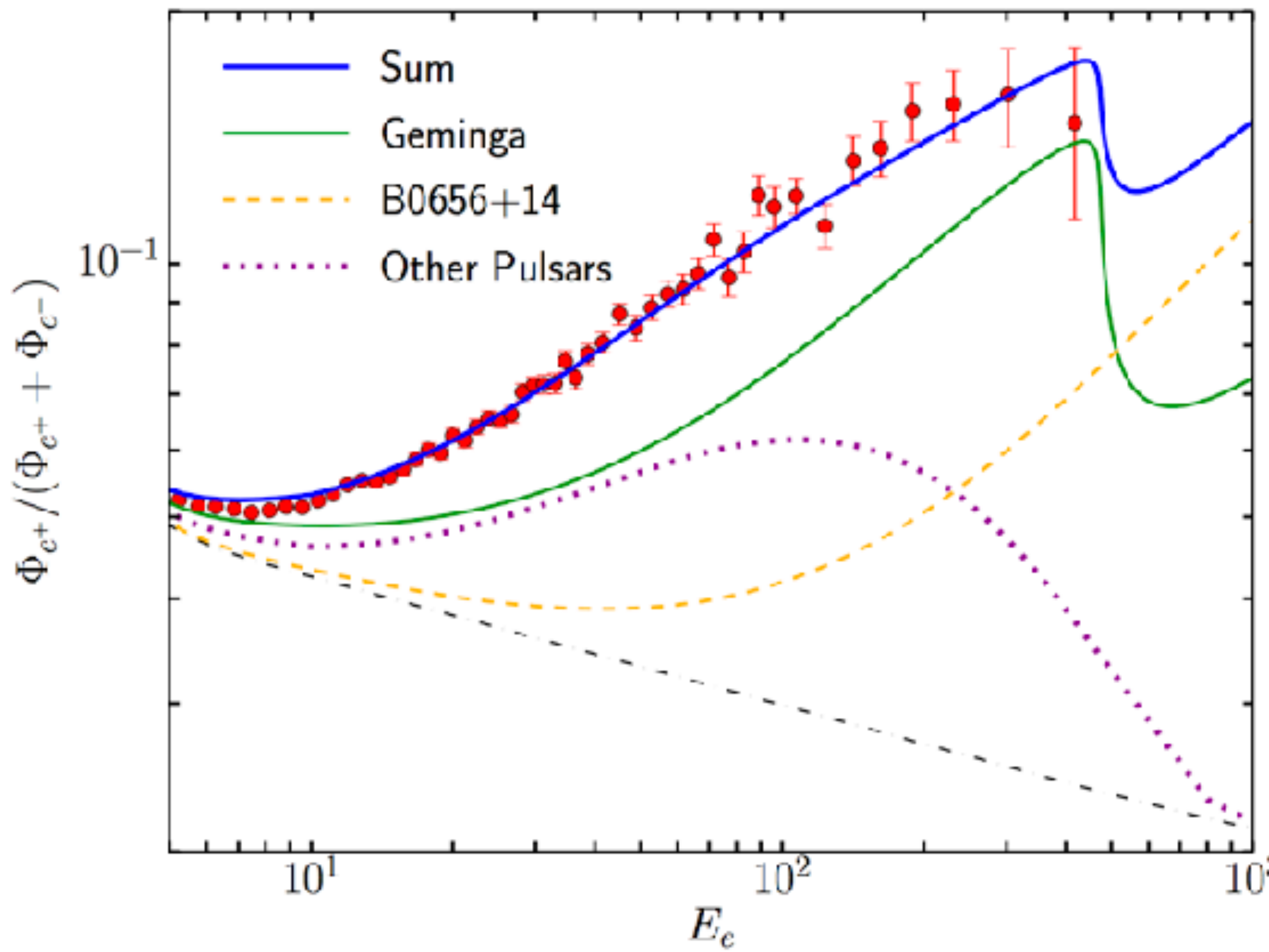

- **These systems must provide a significant contribution to the positron excess.**

- **For reasonable models of the pulsar birthrate and spindown luminosity, we can fit the full excess.**

- **Multiwavelength emission from the pulsar is highly beamed.**

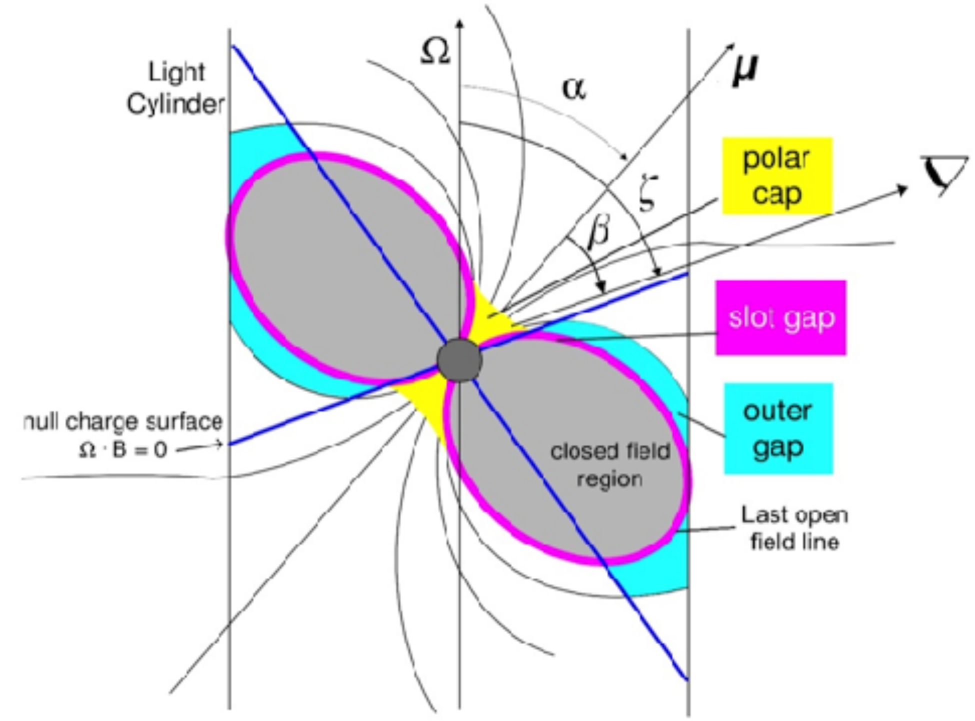

- **The energy-loss time of electrons in the TeV halo implies that their emission is isotropic.**

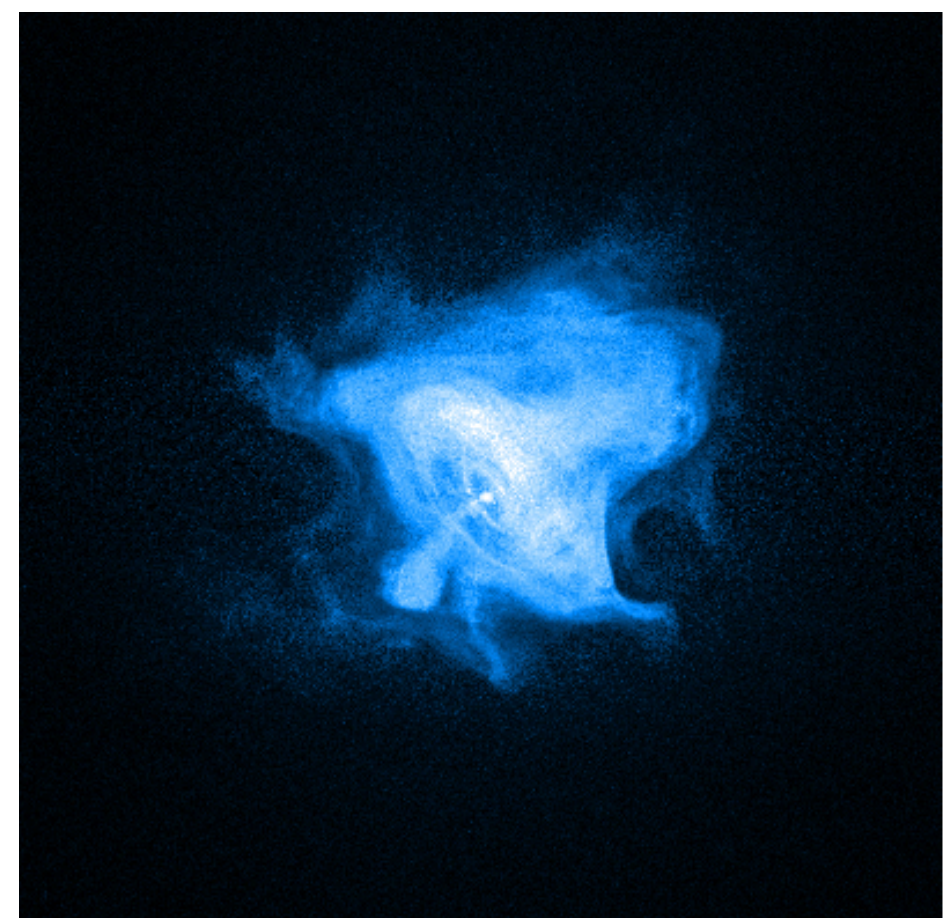

- **Can find off-beam pulsars by looking for the TeV halo signal**

ATNF CATALOG

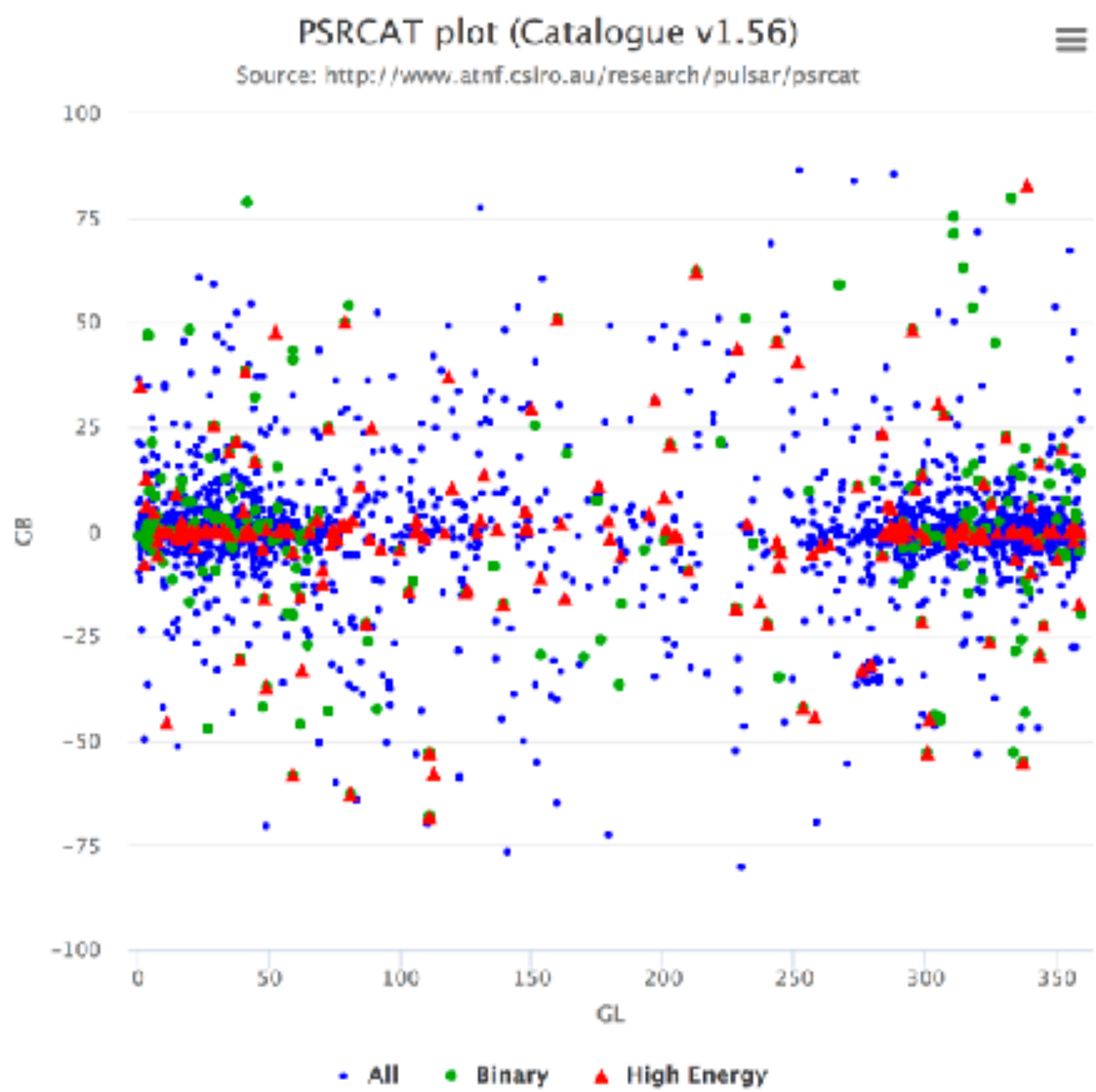

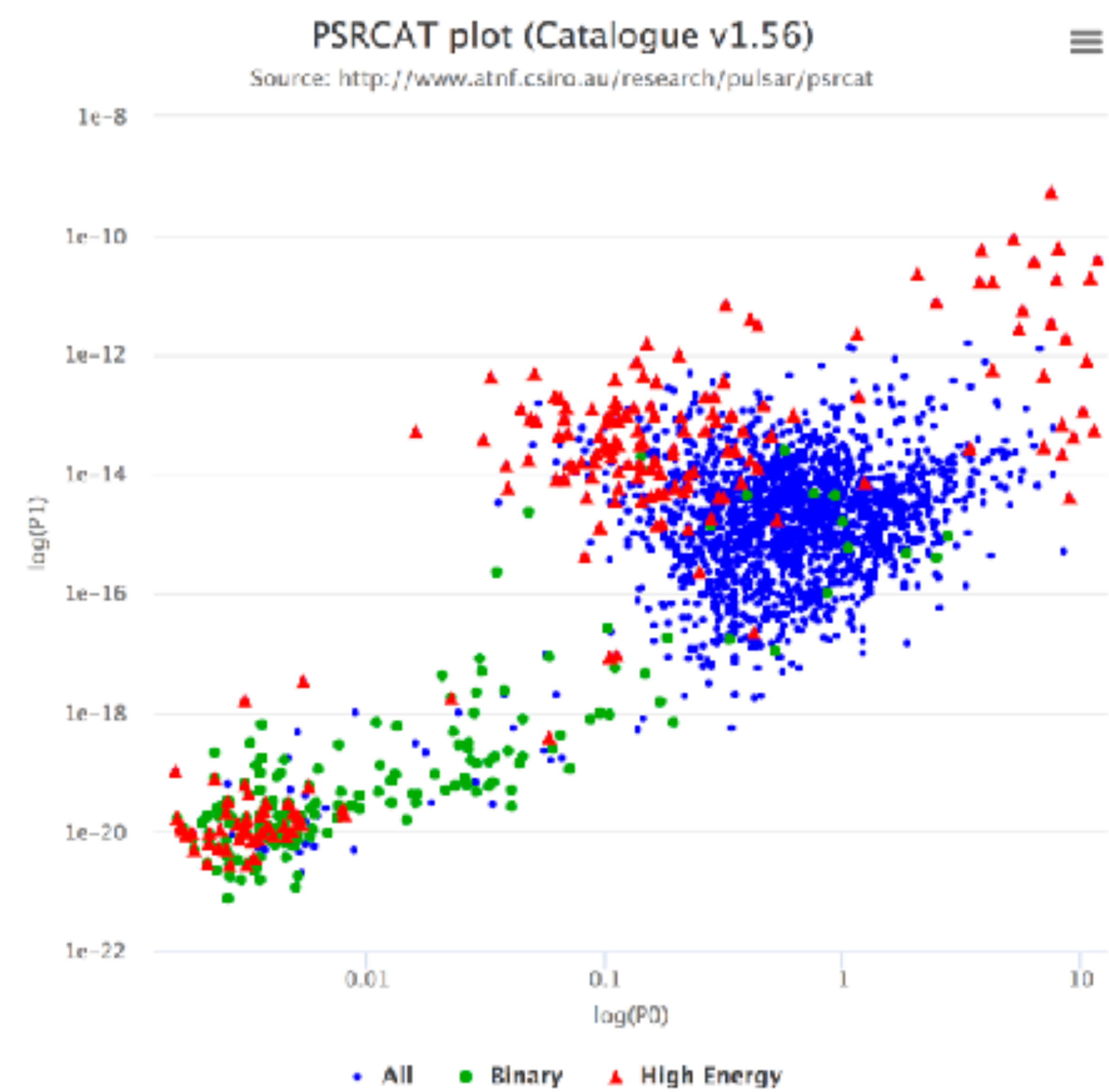

- **Current observations have detected pulsations from 2613 systems, the vast majority in radio.**

TEV HALOS AS A GENERIC FEATURE

2HWC Name	ATNF Name	Distance (kpc)	Angular Separation	Projected Separation	Expected Flux ($\times 10^{-15}$)	Actual Flux ($\times 10^{-15}$)	Flux Ratio	Expected Extension	Actual Extension	Age (kyr)	Chance Overlap
J0700+143	B0656+14	0.29	0.18°	0.91 pc	43.0	23.0	1.87	2.0°	1.73°	111	0.0
J0631+169	J0633+1746	0.25	0.89°	3.88 pc	48.7	48.7	1.0	2.0°	2.0°	342	0.0
J1912+099	J1913+1011	4.61	0.34°	27.36 pc	13.0	36.6	0.36	0.11°	0.7°	169	0.30
J2031+415	J2032+4127	1.70	0.11°	3.26 pc	5.59	61.6	0.091	0.29°	0.7°	181	0.002
J1831-098	J1831-0952	3.68	0.04°	2.57 pc	7.70	95.8	0.080	0.14°	0.9°	128	0.006

- **In addition to Geminga and Monogem, three other 2HWC sources are coincident with middle-aged ANTF pulsars.**

2HWC Name	ATNF Name	Distance (kpc)	Angular Separation	Projected Separation	Expected Flux ($\times 10^{-15}$)	Actual Flux ($\times 10^{-15}$)	Flux Ratio	Expected Extension	Actual Extension	Age (kyr)	Chance Overlap
J1930+188	J1930+1852	7.0	0.03°	3.67 pc	23.2	9.8	2.37	0.07°	0.0°	2.89	0.002
J1814-173	J1813-1749	4.7	0.54°	44.30 pc	243	152	1.60	0.11°	1.0°	5.6	0.61
J2019+367	J2021+3651	1.8	0.27°	8.48 pc	99.8	58.2	1.71	0.28°	0.7°	17.2	0.04
J1928+177	J1928+1746	4.34	0.03°	2.27 pc	8.08	10.0	0.81	0.11°	0.0°	82.6	0.002
J1908+063	J1907+0602	2.58	0.36°	16.21 pc	40.0	85.0	0.47	0.2°	0.8°	19.5	0.26
J2020+403	J2021+4026	2.15	0.18°	6.75 pc	2.48	18.5	0.134	0.23°	0.0°	77	0.01
J1857+027	J1856+0245	6.32	0.12°	13.24 pc	11.0	97.0	0.11	0.08°	0.9°	20.6	0.06
J1825-134	J1826-1334	3.61	0.20°	12.66 pc	20.5	249	0.082	0.14°	0.9°	21.4	0.14
J1837-065	J1838-0655	6.60	0.38°	43.77 pc	12.0	341	0.035	0.08°	2.0°	22.7	0.48
J1837-065	J1837-0604	4.78	0.50°	41.71 pc	8.3	341	0.024	0.10°	2.0°	33.8	0.68
J2006+341	J2004+3429	10.8	0.42°	80.07 pc	0.48	24.5	0.019	0.04°	0.9°	18.5	0.08

- **Additionally, 12 other 2HWC sources are coincident with younger ATNF pulsars.**
- **Some associations are likely to be chance-overlaps.**

ATNF Name	Dec. (°)	Distance (kpc)	Age (kyr)	Spindown Lum. (erg s^{-1})	Spindown Flux (erg s^{-1} kpc^{-2})	2HWC
J0633+1746	17.77	0.25	342	3.2e34	4.1e34	2HWC J0631+169
B0656+14	14.23	0.29	111	3.8e34	3.6e34	2HWC J0700+143
B1951+32	32.87	3.00	107	3.7e36	3.3e34	—
J1740+1000	10.00	1.23	114	2.3e35	1.2e34	—
J1913+1011	10.18	4.61	169	2.9e36	1.1e34	2HWC J1912+099
J1831-0952	-9.86	3.68	128	1.1e36	6.4e33	2HWC J1831-098
J2032+4127	41.45	1.70	181	1.7e35	4.7e33	2HWC J2031+415
B1822-09	-9.58	0.30	232	4.6e33	4.1e33	—
B1830-08	-8.45	4.50	147	5.8e35	2.3e33	—
J1913+0904	9.07	3.00	147	1.6e35	1.4e33	—
B0540+23	23.48	1.56	253	4.1e34	1.4e33	—

- **There are 57 middle-aged ATNF pulsars in the HAWC field of view.**
- **Five of the seven most luminous have been observed by HAWC.**

$$\phi_{\rm TeV\ halo} = \left(\frac{\dot{E}_{\rm psr}}{\dot{E}_{\rm Geminga}}\right)\left(\frac{d^2_{\rm Geminga}}{d^2_{\rm psr}}\right)\phi_{\rm Geminga}$$

$$\theta_{\rm TeV\ halo} = \left(\frac{d_{\rm Geminga}}{d_{\rm psr}}\right)\theta_{\rm Geminga}$$

- **Zeroeth-Order: Assume that every middle-aged TeV Halo is the same as Geminga.**
- **First-Order: Correct for the spindown luminosity and distance to each pulsar.**

- **Most radio pulsars do not have beams oriented towards Earth.**

- **Tauris & Manchester (1998) calculated the pulsar beaming fraction to be:**

$$f = \left[1.1 \left(\log_{10} \left(\frac{\tau}{100 \text{ Myr}} \right) \right)^2 + 15 \right] \%$$

- **This varies between 15-30% for middle-aged (young) pulsars. 1/f pulsars are undetected in radio.**

Tauris & Manchester (1998)

ATNF Name	Dec. (°)	Distance (kpc)	Age (kyr)	Spindown Lum. (erg s^{-1})	Spindown Flux (erg s^{-1} kpc^{-2})	2HWC
J0633+1746	17.77	0.25	342	3.2e34	4.1e34	2HWC J0631+169
B0656+14	14.23	0.29	111	3.8e34	3.6e34	2HWC J0700+143
B1951+32	32.87	3.00	107	3.7e36	3.3e34	—
J1740+1000	10.00	1.23	114	2.3e35	1.2e34	—
J1913+1011	10.18	4.61	169	2.9e36	1.1e34	2HWC J1912+099
J1831-0952	-9.86	3.68	128	1.1e36	6.4e33	2HWC J1831-098
J2032+4127	41.45	1.70	181	1.7e35	4.7e33	2HWC J2031+415
B1822-09	-9.58	0.30	232	4.6e33	4.1e33	—
B1830-08	-8.45	4.50	147	5.8e35	2.3e33	—
J1913+0904	9.07	3.00	147	1.6e35	1.4e33	—
B0540+23	23.48	1.56	253	4.1e34	1.4e33	—

$$f = \left[1.1 \left(\log_{10} \left(\frac{\tau}{100\ \mathrm{Myr}} \right) \right)^2 + 15 \right] \%$$

- **The list of detectable ATNF pulsars predicts a population of 37^{+17}_{-13} hidden pulsars that should be observed as TeV halos.**

- How many of these systems have already been detected in other ways?
  - Gamma-Ray Pulsars
  - X-Ray Pulsar Wind Nebulae
  - HESS or VERITAS TeV Sources?

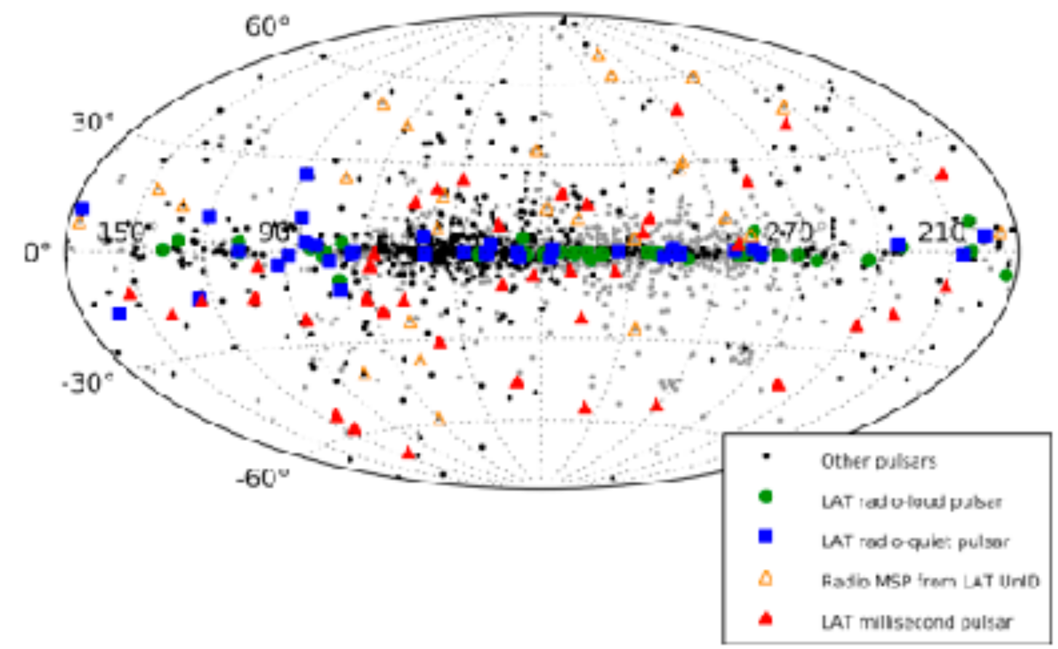

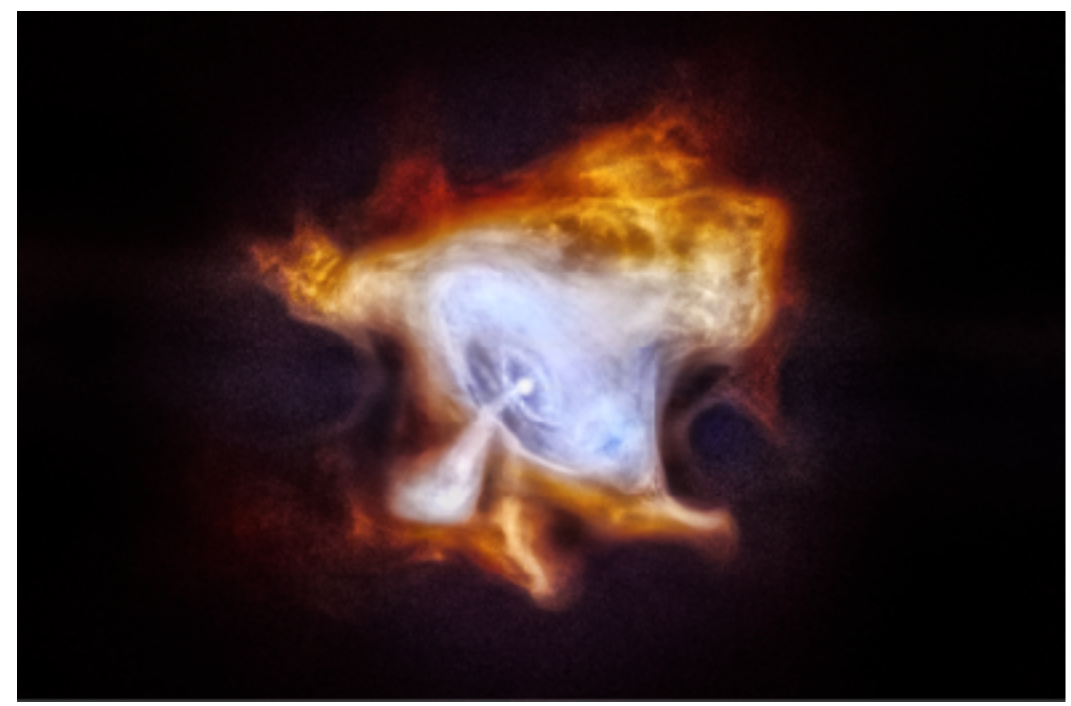

- **The Fermi-LAT has detected 54 previously unknown pulsars. However:**
  - **35 of these have ages below 100 kyr (12 have no age determination).**
  - **14 of the remaining 19 systems are not in the HAWC ROI.**

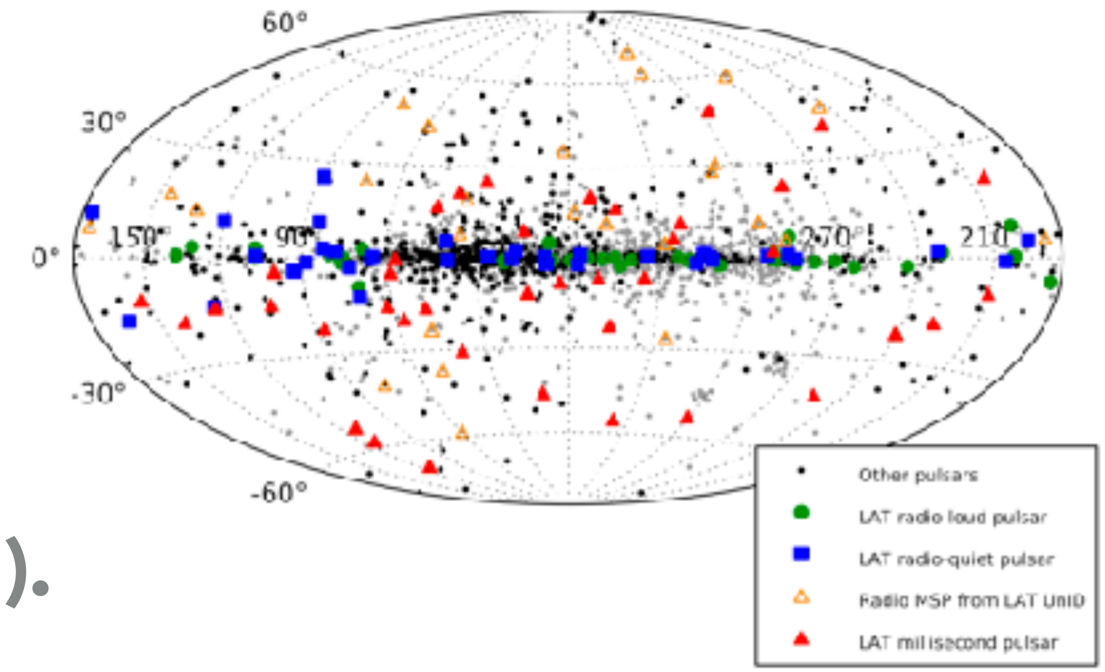

- **<u>Fermi-LAT observations account for no more than 5 of these ~40 systems.</u>**

https://confluence.slac.stanford.edu/display/GLAMCOG/Public+List+of+LAT-Detected+Gamma-Ray+Pulsars

PULSAR WIND NEBULA OBSERVATIONS

astro-ph/0402136

PWNe With No Detected Pulsar

Gname	other name(s)	R	X	O	G	
G0.13-0.11					?	notes
G0.9+0.1					N	notes
G7.4-2.0	GeV J1809-2327, Tazzie				Y	notes
G16.7+0.1					N	notes
G18.5-0.4	GeV J1825-1310, Eel				Y	notes
G20.0-0.2					N	notes
G24.7+0.6					N	notes
G27.8+0.6					N	notes
G39.2-0.3	3C 396				Y	notes
G63.7+1.1					N	notes
G74.9+1.2	CTB 87				Y	notes
G119.5+10.2	CTA 1				Y	notes
G189.1+3.0	IC 443				?	notes
G279.8-35.8	B0453-685				N	notes
G291.0-0.1	MSH 11-62				Y	notes
G293.8+0.6					N	notes
G313.3+0.1	Rabbit				Y	notes
G318.9+0.4					N	notes
G322.5-0.1					N	notes
G326.3-1.8	MSH 15-56				N	notes
G327.1-1.1					N	notes
G328.4+0.2	MSH 15-57				N	notes
G358.6-17.2	RX J1856.5-3754	N	N		N	notes
G359.89-0.08					Y	notes

- No more than 6 systems have been previously detected as X-Ray PWN.

- **Atmospheric Cherenkov Telescopes could also detect TeV halos.**

- **However, ACTs are not sensitive to highly extended sources (>0.5°)**

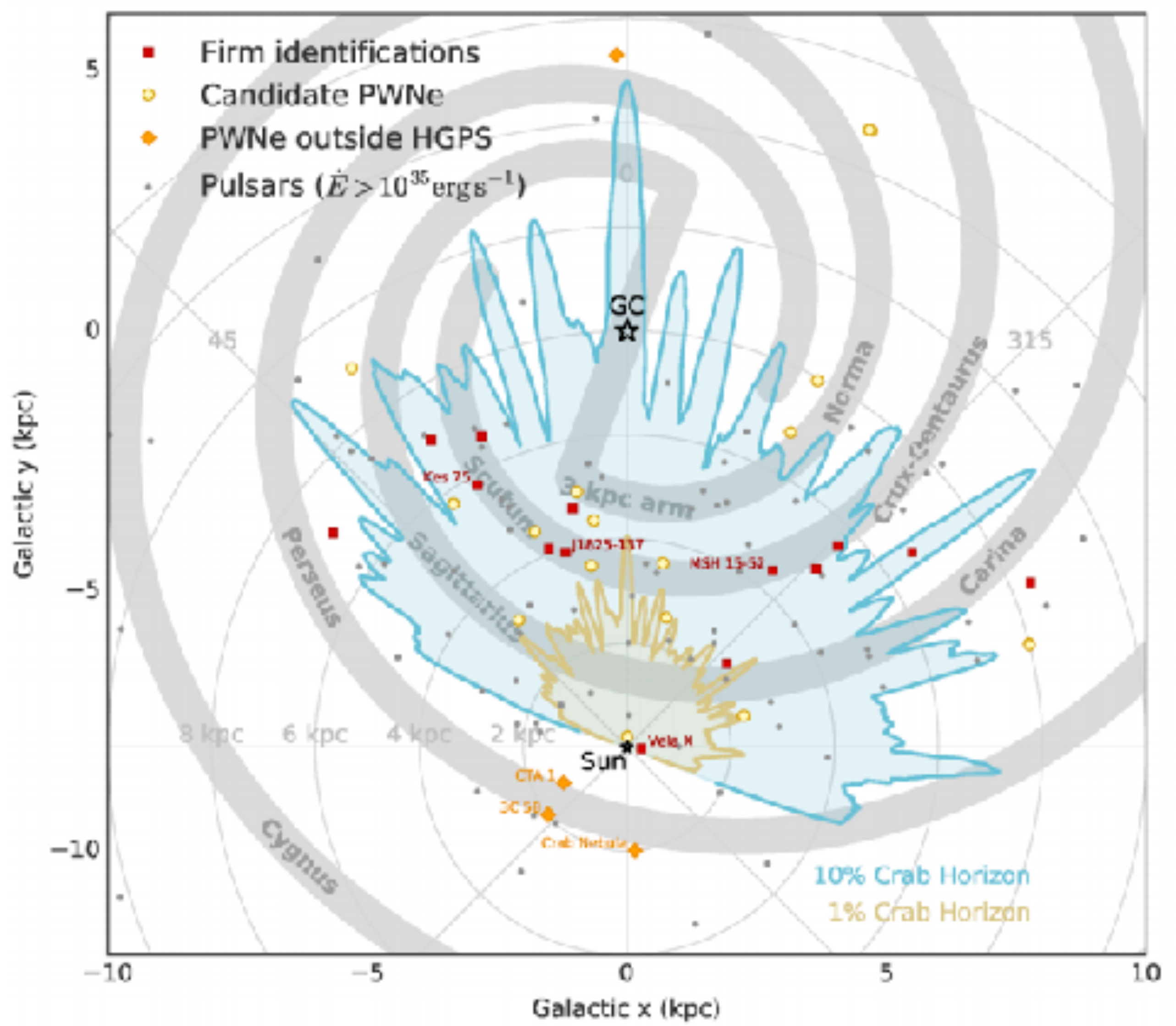

- **<u>There is a large parameter space for HAWC detections that is untouched by all previous observations.</u>**

HAWC OPENS A NEW PARAMETER SPACE FOR TEV HALO DETECTION

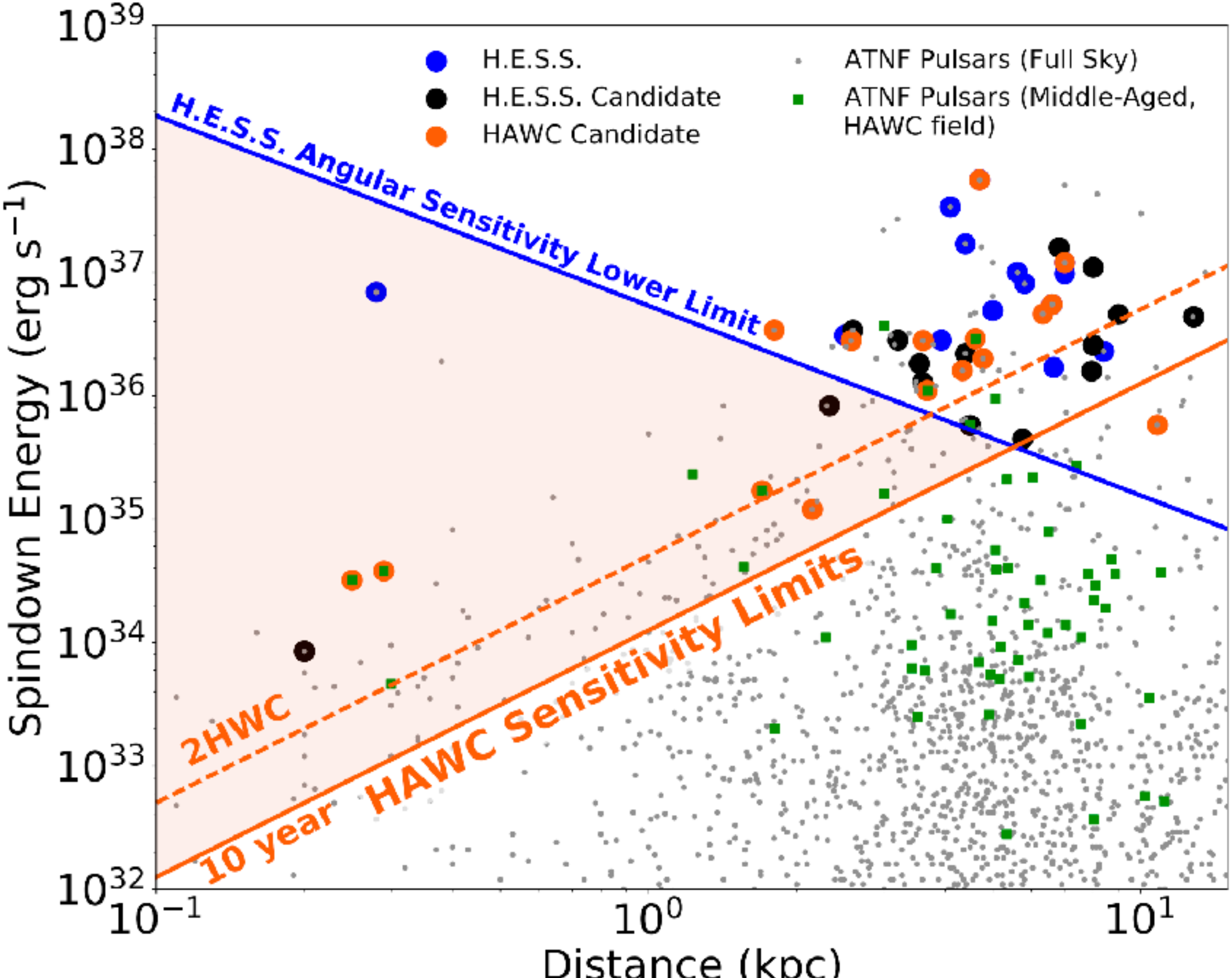

- **HAWC observations of TeV halos have significant implications for many open questions of pulsar evolution:**
  - **Pulsar Contributions to the positron excess.**
  - **Pulsar Braking Index**
  - **Cosmic-Ray Diffusion near compact objects**

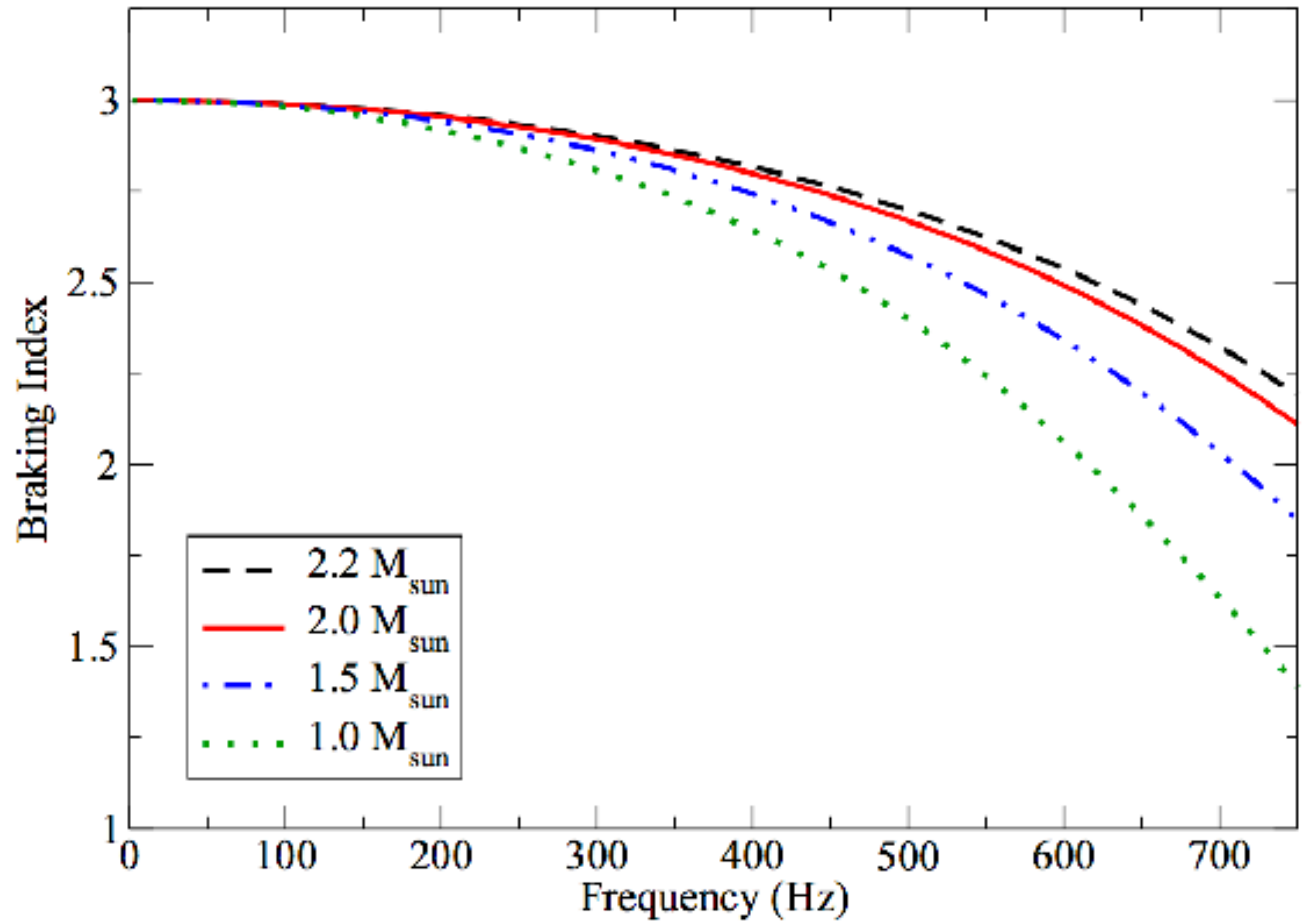

- **Several ways to confirm TeV halos:**
  - **X-Ray Halos**
  - **X-Ray PWN**
  - **Thermal Pulsar Emission**

- **If TeV Halos are powered by inverse-Compton scattering, an X-ray flux from synchrotron <u>must</u> be present.**
- **Hard to observe because:**
  - **1.) Diffuse**
  - **2.) Low-energy cutoff**

$$E_{\mathrm{sync,critical}} = 22\ \mathrm{eV} \left(\frac{B}{5\ \mu G}\right) \left(\frac{E_e}{10\ \mathrm{TeV}}\right)^2$$

- Some evidence in G327-1.1 !?
  - Young pulsar (17.4 kyr)
  - Two “PWN” observed
    - Diffuse PWN is much larger with softer spectrum

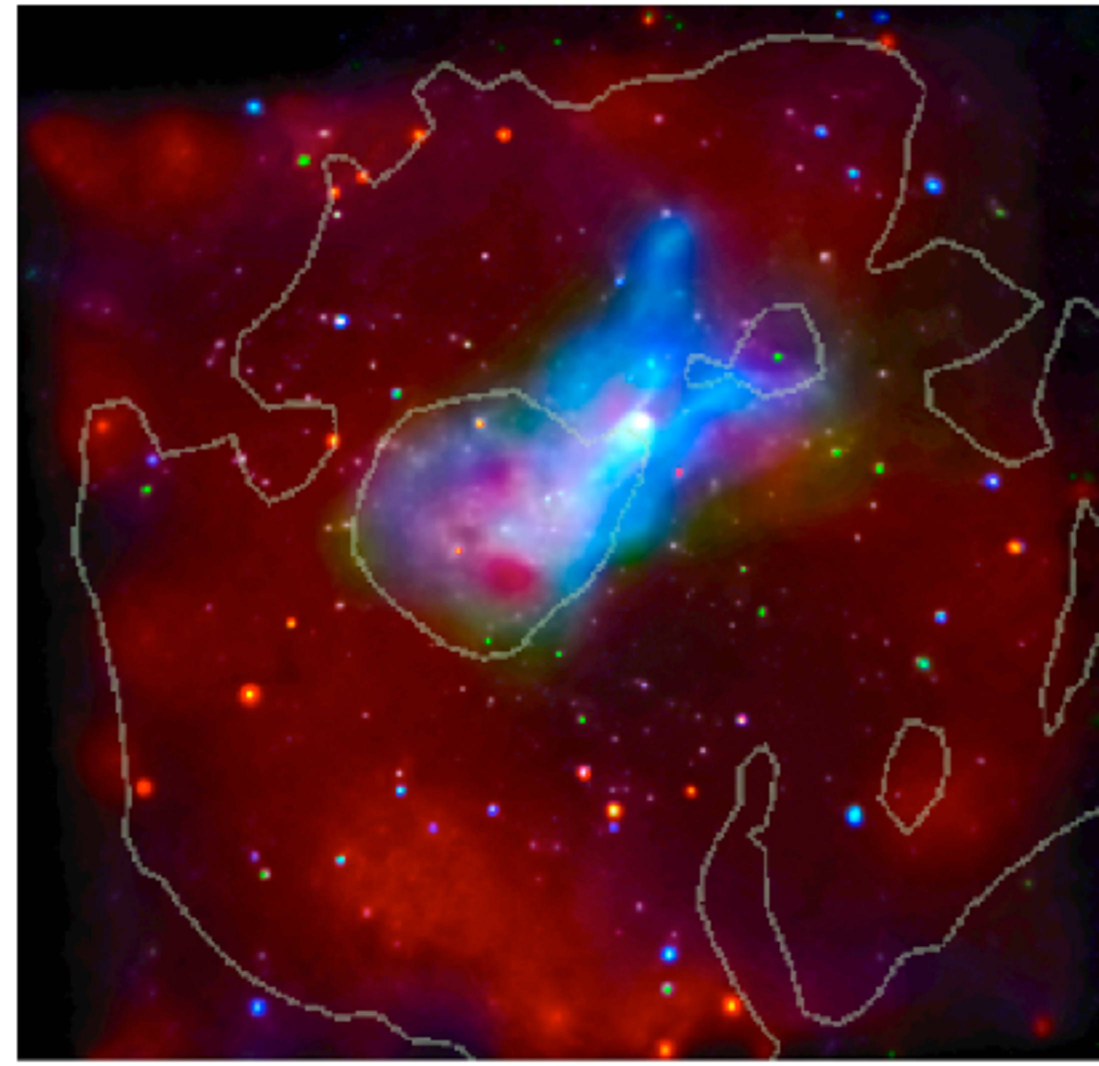

	Region	Area (arcsec^2)	Cts (1000)	N_H (10^{22} cm^{-2})	Photon Index	Amplitude (10^{-4})	kT (keV)	τ (10^{12} s cm^{-3})	Norm. (10^{-3})	F_1 (10^{-12})	F_2 (10^{-12})	Red. χ^2
1	Compact Source	84.657	6.34	$1.93^{+0.08}_{-0.08}$	$1.61^{+0.08}_{-0.07}$	$1.05^{+0.11}_{-0.10}$	...	...	...	0.45	...	0.80
2	Cometary PWN	971.22	7.75	1.93	$1.62^{+0.08}_{-0.07}$	$1.47^{+0.16}_{-0.14}$	...	...	...	1.09	...	...
3	Trail East	537.42	2.13	1.93	$1.84^{+0.12}_{-0.12}$	$0.44^{+0.07}_{-0.06}$	...	...	...	0.27	...	...
4	Trail West	766.56	3.12	1.93	$1.80^{+0.11}_{-0.11}$	$0.61^{+0.09}_{-0.08}$	...	...	...	0.39	...	...
5	Trail 1	424.45	1.98	1.93	$1.76^{+0.12}_{-0.12}$	$0.39^{+0.05}_{-0.05}$	...	...	...	0.26	...	...
6	Trail 2	588.19	2.13	1.93	$1.95^{+0.11}_{-0.11}$	$0.49^{+0.07}_{-0.06}$	...	...	...	0.28	...	...
7	Trail 3	994.92	2.99	1.93	$2.09^{+0.10}_{-0.10}$	$0.78^{+0.09}_{-0.08}$	...	...	...	0.42	...	...
8	Trail 4	839.48	2.38	1.93	$2.28^{+0.12}_{-0.12}$	$0.74^{+0.09}_{-0.09}$	...	...	...	0.37	...	...
9	Prong East	828.58	1.66	1.93	$1.72^{+0.14}_{-0.14}$	$0.30^{+0.06}_{-0.05}$	...	...	...	0.27	...	...
10	Prong West	971.22	2.06	1.93	$1.85^{+0.14}_{-0.14}$	$0.44^{+0.08}_{-0.07}$	...	...	...	1.09	...	...
11	Diffuse PWN*	20007	27.7	1.93	$2.11^{+0.04}_{-0.05}$	$6.91^{+0.37}_{-0.74}$	$0.23^{+0.14}_{-0.05}$	$0.21^{+0.88}_{-0.16}$	$6.0^{+16}_{-4.0}$	3.68	17.7	0.82
12	Relic PWN*	26787	17.2	1.93	$2.58^{+0.07}_{-0.10}$	$6.51^{+0.53}_{-0.71}$	0.23	0.21	$6.9^{+18}_{-5.5}$	3.14	20.3	...

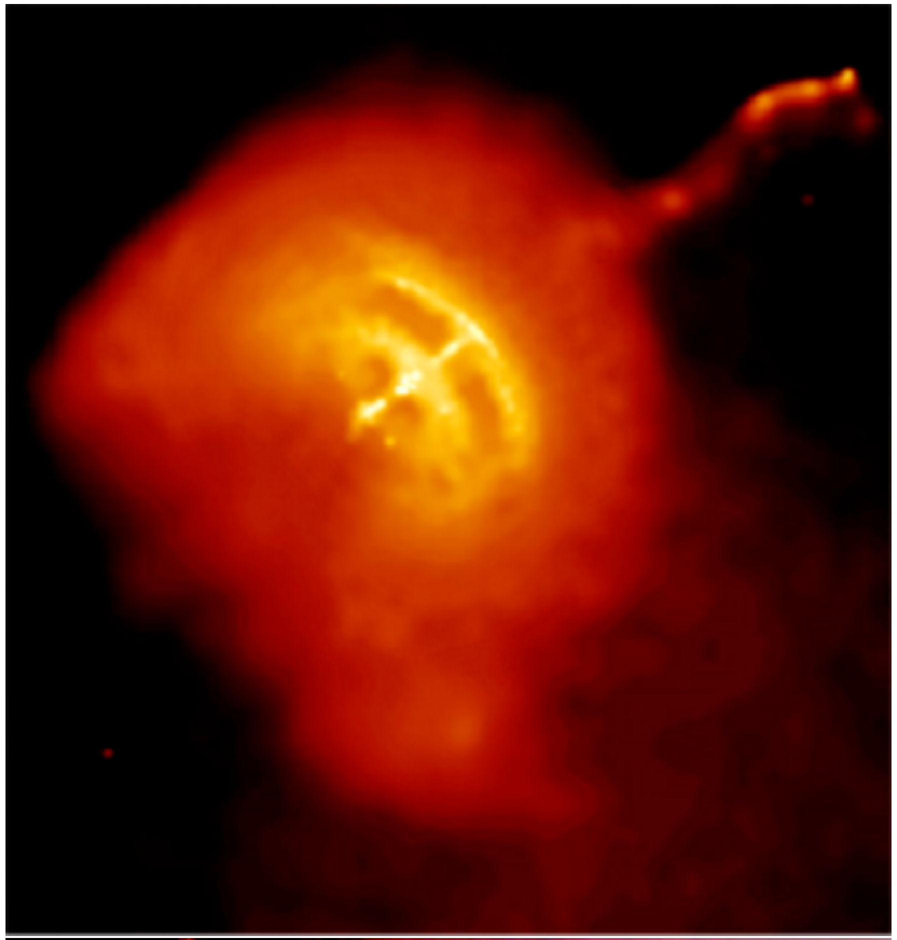

- Larger magnetic field may make compact PWN easier to see.
  - Increases spectral peak
  - Increases synchrotron to ICS ratio.
- More distant sources may be easier to see.
- Significant observation time requires careful HAWC analysis.

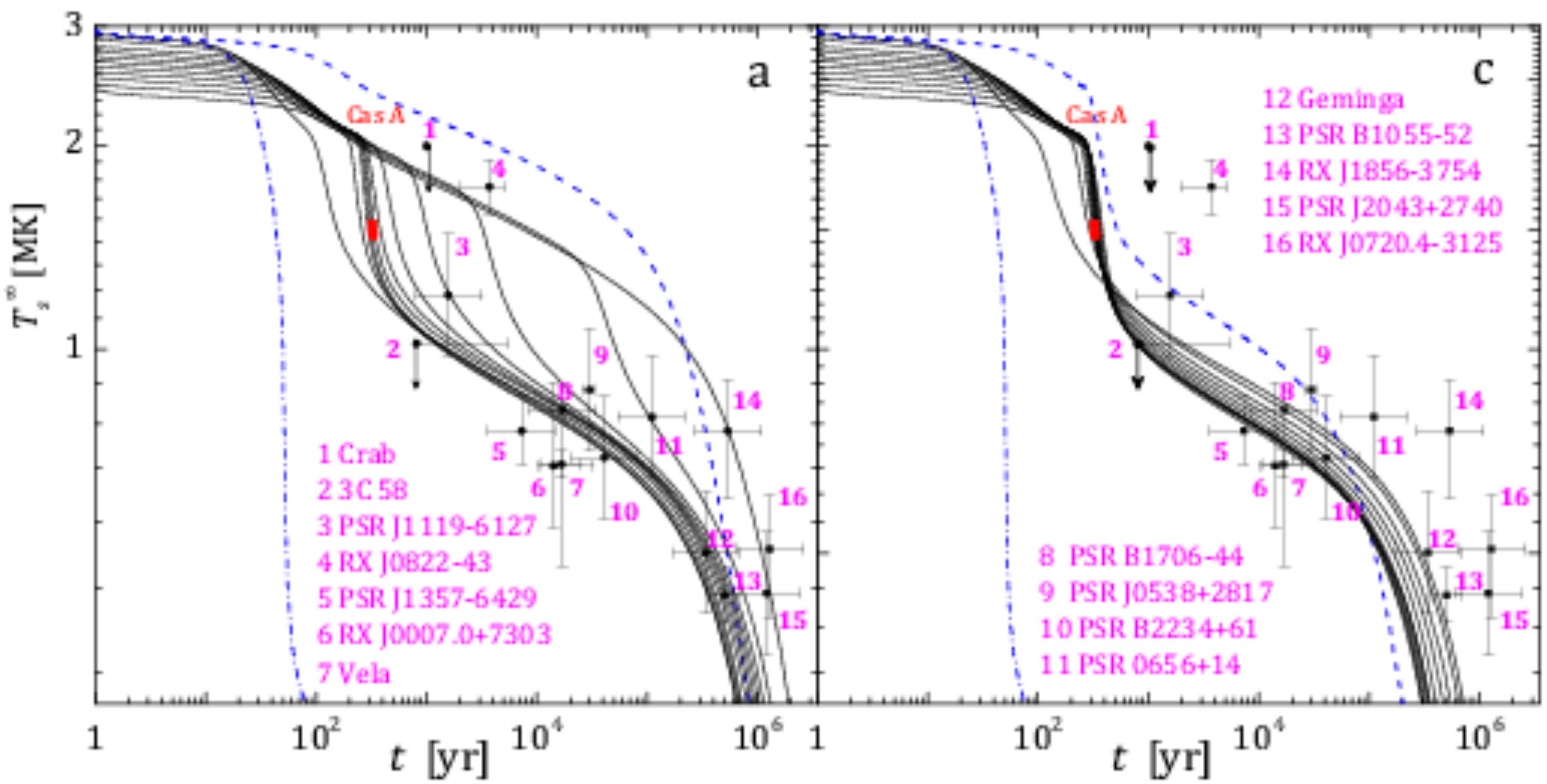

- Hot neutron stars can also be observed via their isotropic thermal emission.
- X-Ray observations can be sensitive to ~2 kpc for 10^6 K NS.
- Cooler NS extremely hard to see.
- Could potentially detect a system which has recently ceased producing TeV particles.

Hooper, TL, Cholis (To Be Submitted)

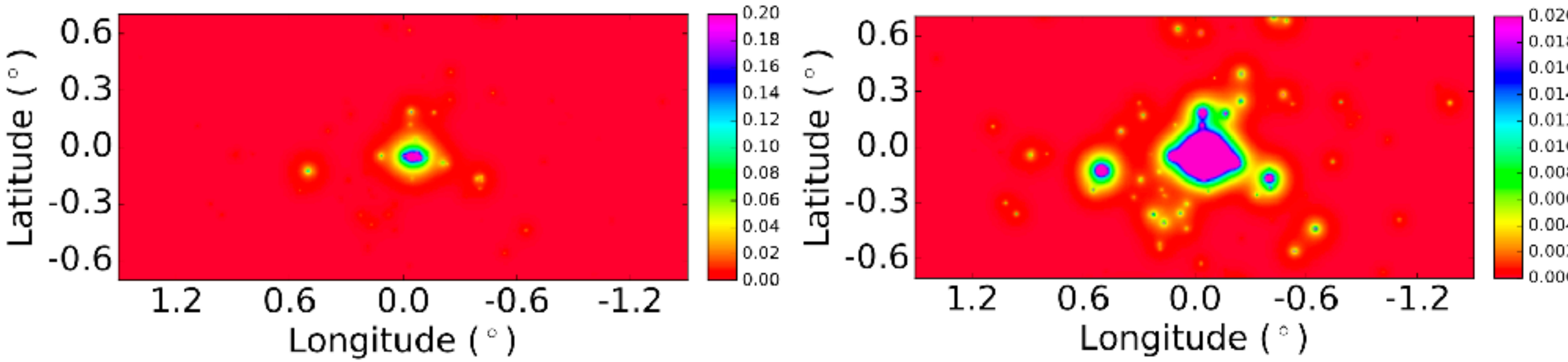

- **Significant star formation is observed in the central parsec of the Milky Way (Do et al. 1301.0539, 1301, 0540)**
- **Pulsars will produce TeV halos in this region, and be kicked out into the surrounding interstellar medium.**
- **This is a potential source of significant diffuse TeV gamma-ray emission in the Galactic center.**

- **Recent HESS observations indicate diffuse 100 TeV emission surrounding Sgr A***
- **If gamma-ray emission is Hadronic in nature, would be an indication of PeV proton acceleration in GC.**
- **Some correlation with molecular cloud density (not strong).**

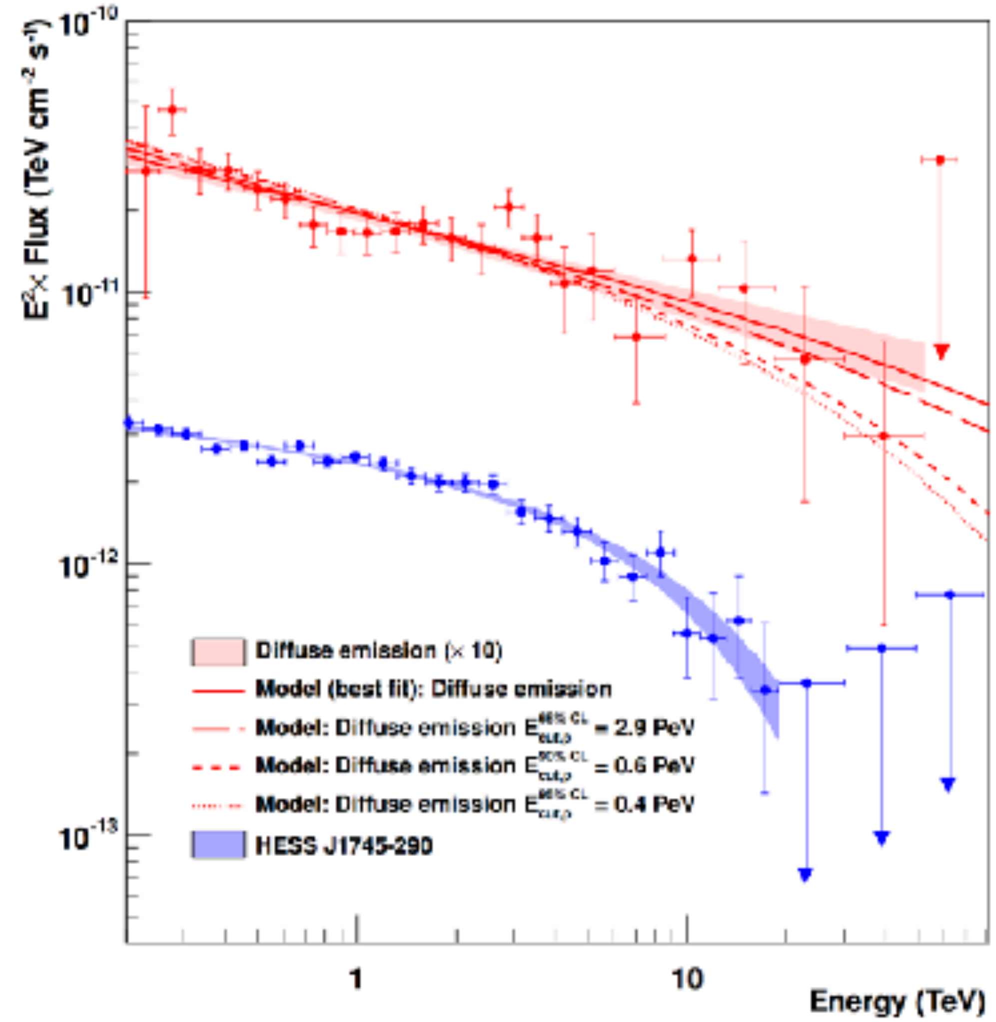

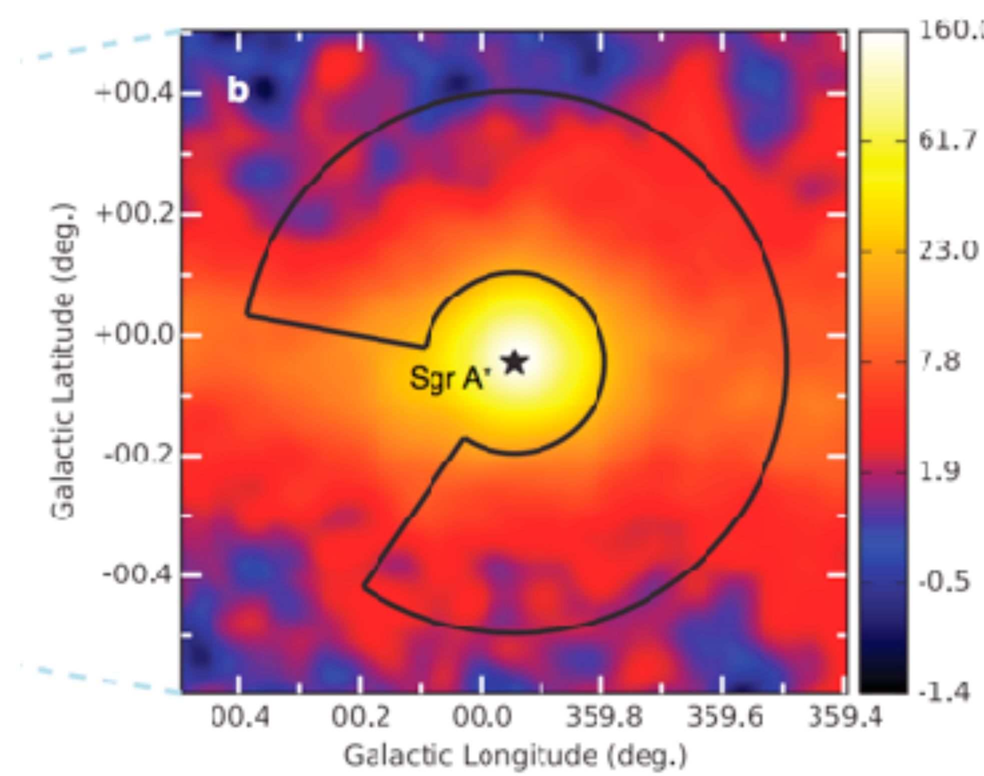

Hooper, TL, Cholis (To Be Submitted)

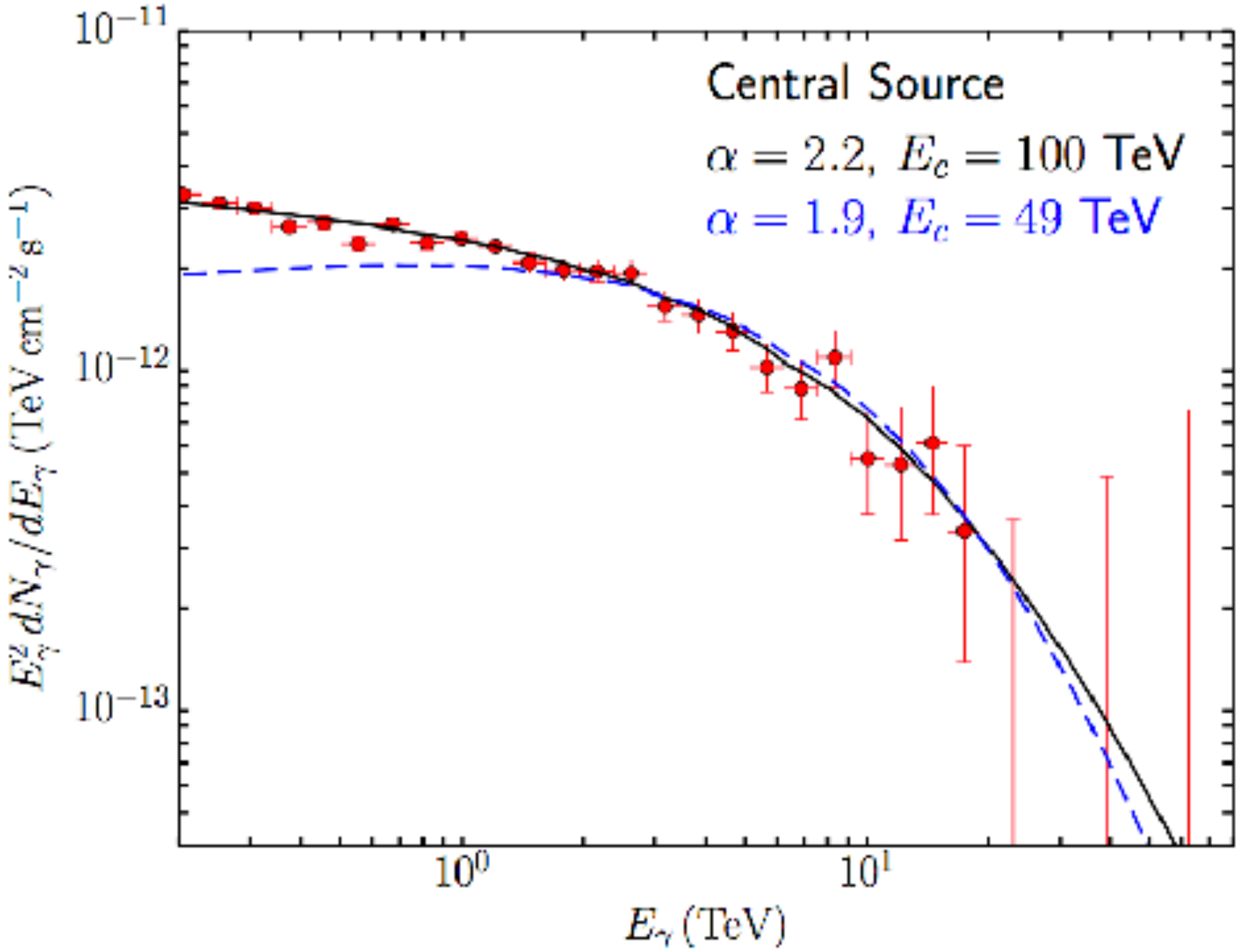

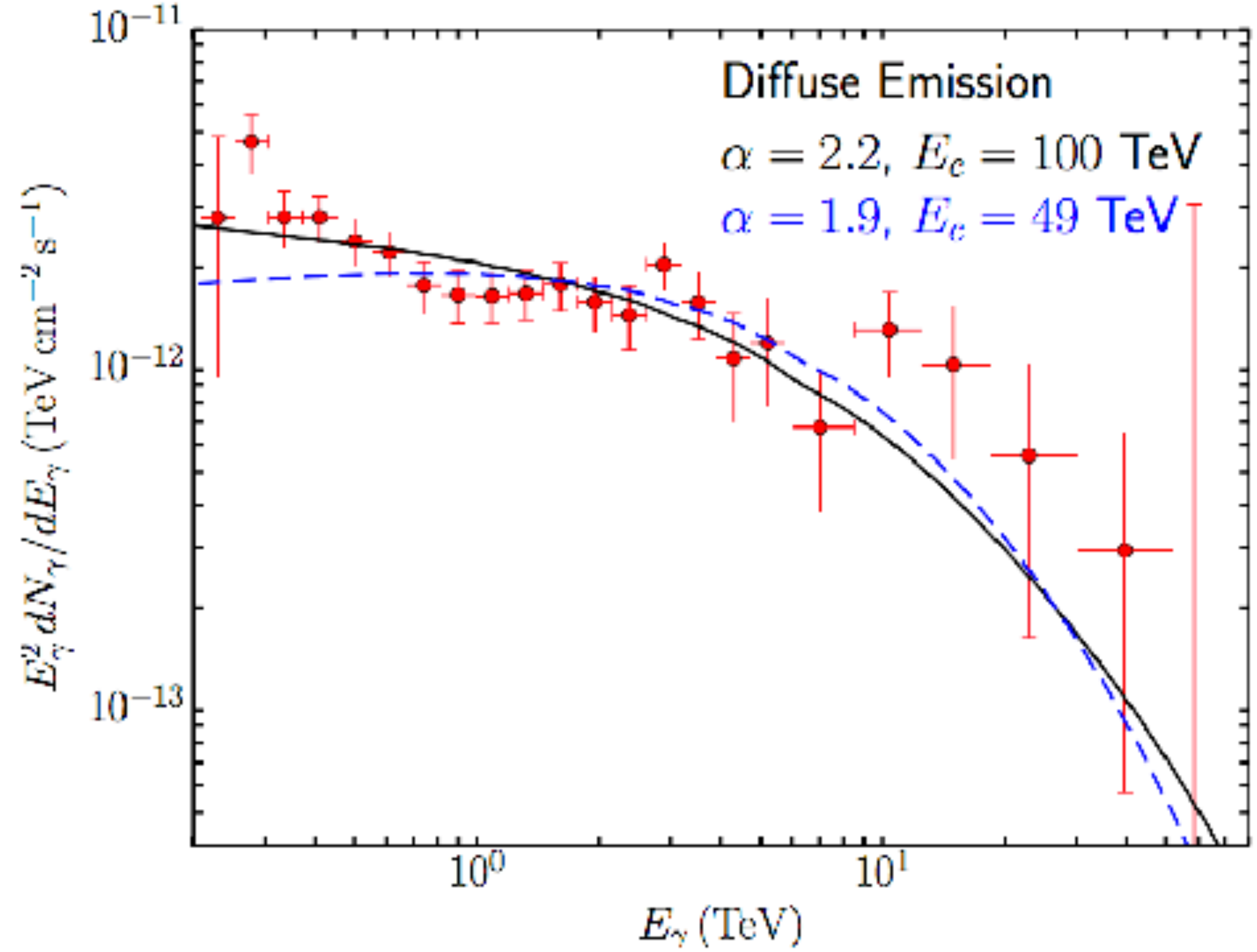

- **TeV halos naturally fit the gamma-ray spectrum of both the point source and diffuse HESS emission.**
- **If pulsars produce TeV halos, this level of TeV emission is required in the Galactic center.**

Hooper, TL, Cholis (To Be Submitted)

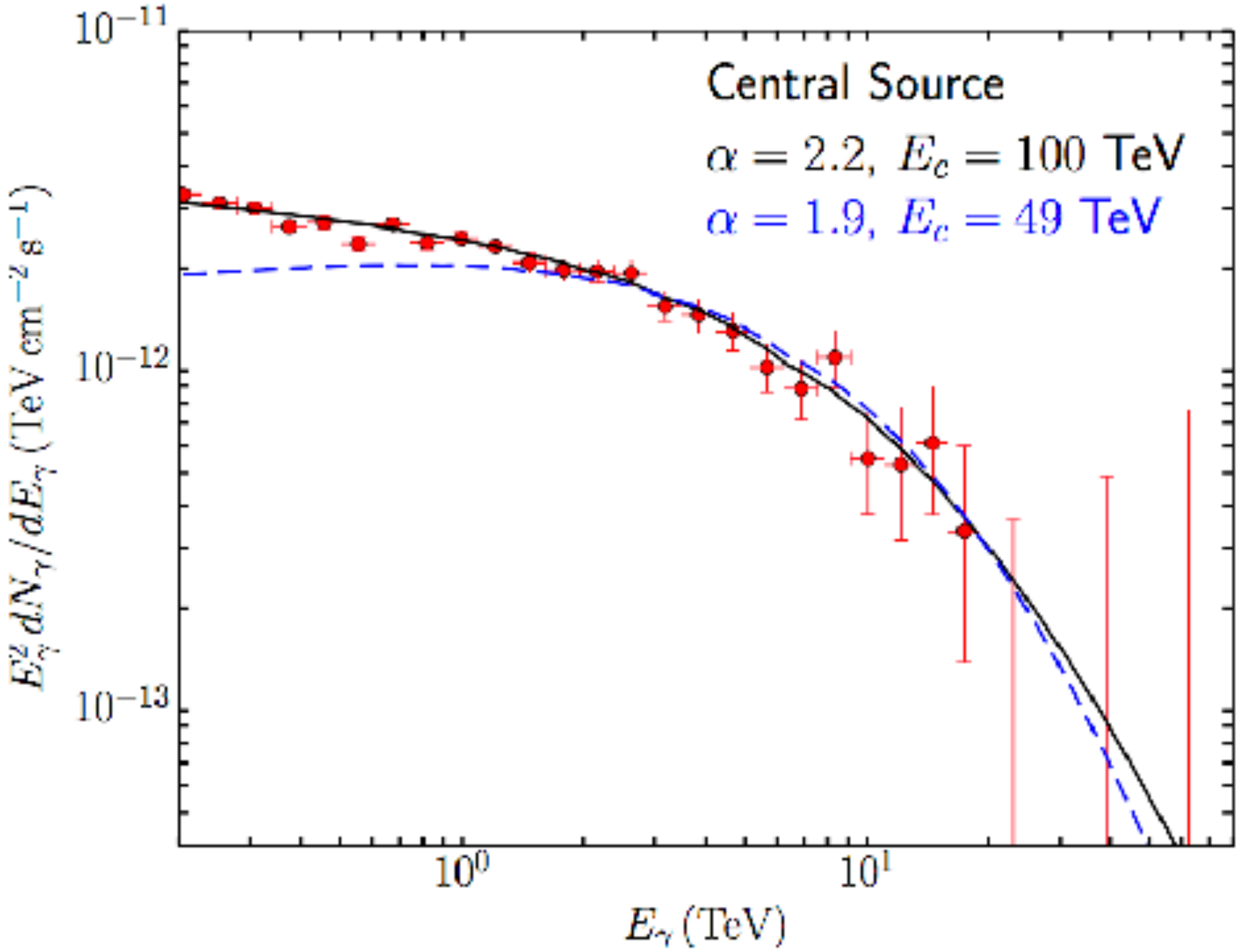

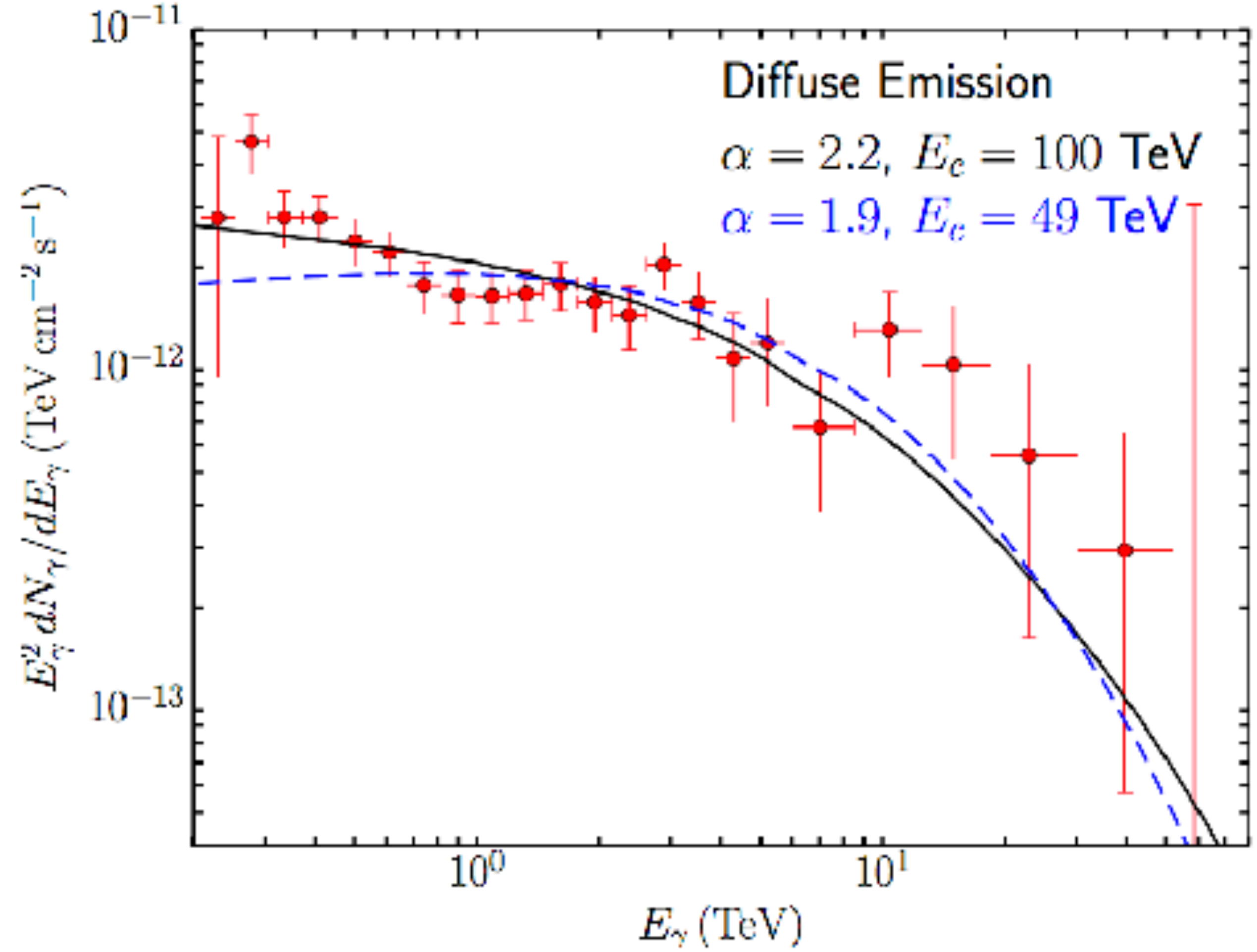

- This requires a birth rate of 100-750 pulsars/Myr, in line with expectations.
- This would indicate a population of 30-200 pulsars with beamed emission towards Earth - providing insight into the missing pulsar problem (1310.7022, 1311.4846)

- **Evidence for a diffuse TeV excess along the Galactic plane from Milagro**

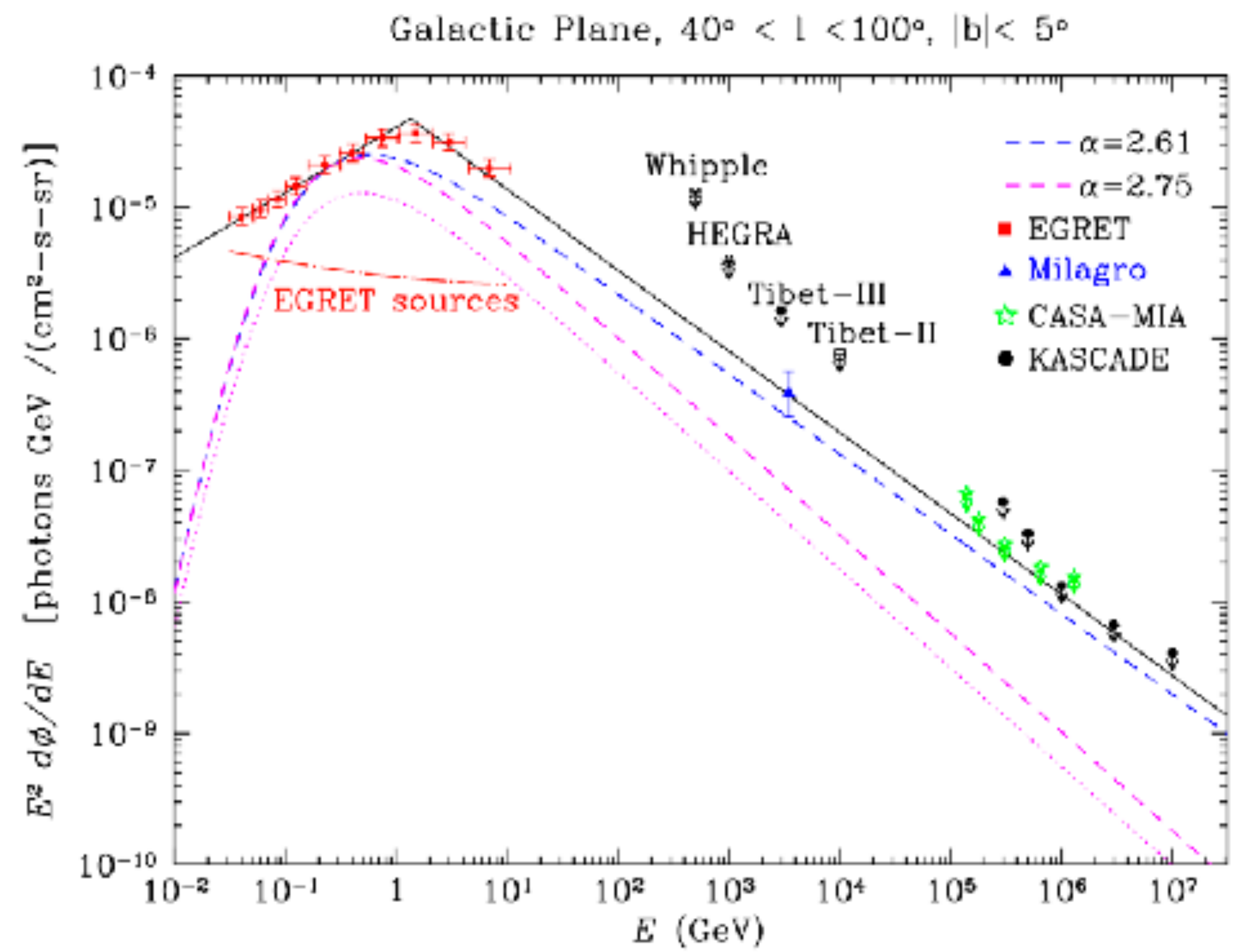

- **Hard to fit with diffuse emission models ($\phi_{\pi 0} \propto E^{-2.7}$)**

- **Diffuse ICS is <u>too</u> diffuse to describe planar emission.**

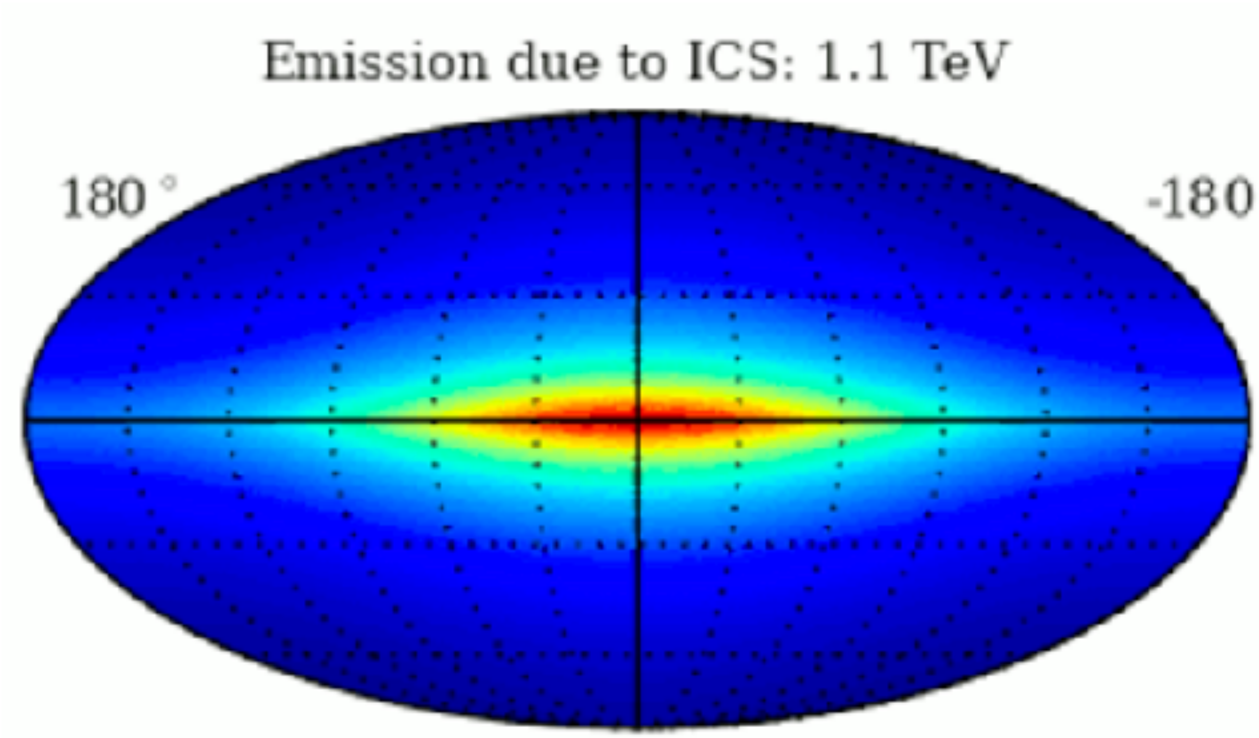

 Linden et al. (in prep)

- What about TeV halos?

- The hard spectrum of TeV halos indicates that they may dominate the >1 TeV emission from the Milky Way.

- Many sources mean that these look diffuse.

Linden et al. (in prep)

- What about TeV halos?
- TeV Halos have hard spectrum -> May dominate high energy emission.
- Many sources

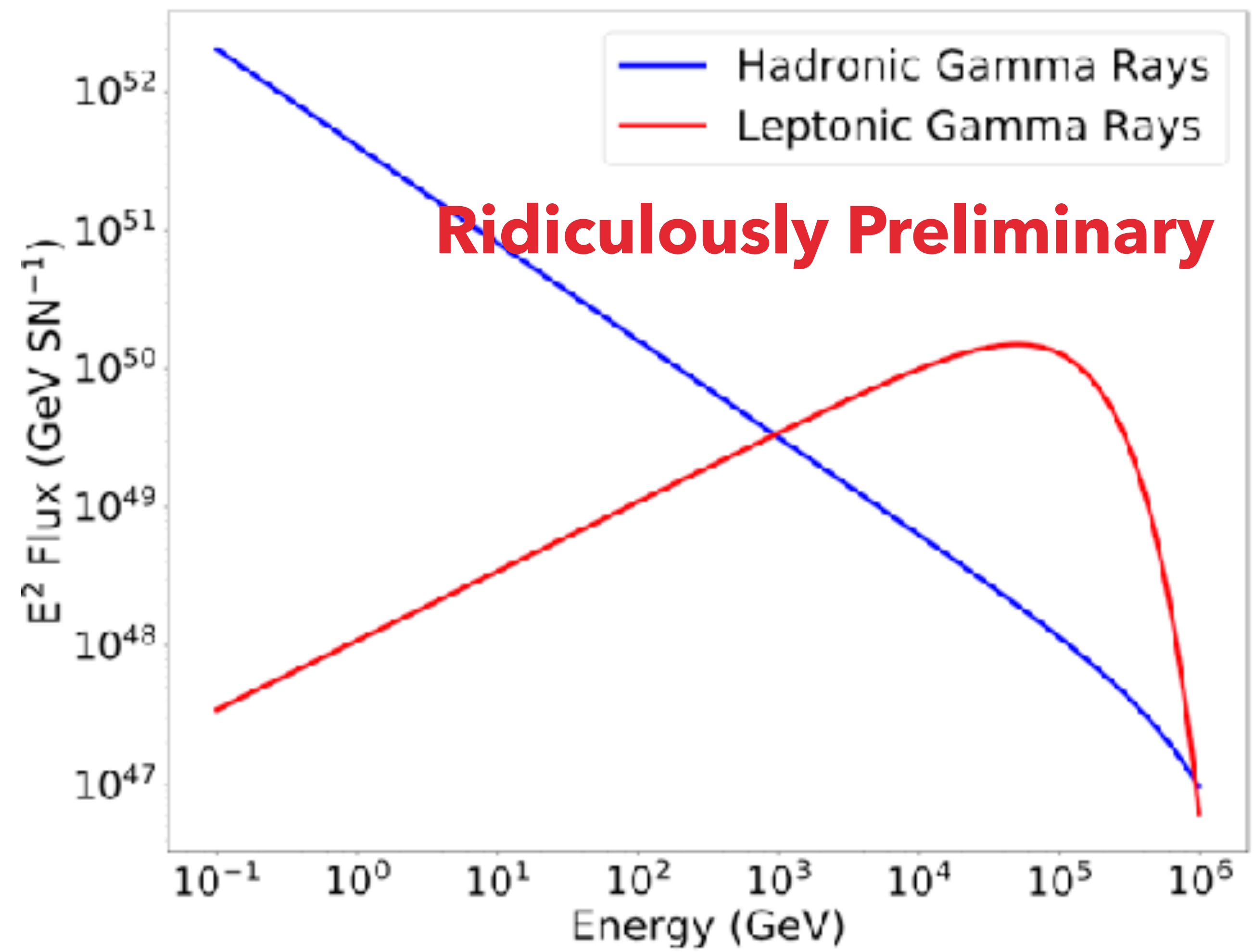

$$E_{p,SN} = 10^{50}\ \mathrm{erg}$$

$$\frac{dN_{p,SN}}{dE} = 4\times 10^{51}\, E^{-2}\, e^{-E/1\,\mathrm{PeV}}\ \mathrm{GeV}^{-1}$$

$$\boxed{\phi_{\gamma,\pi_0} \propto E^{-2.7} \rightarrow 4\times 10^{51}\, E^{-2.7}\, e^{-E/1\,\mathrm{PeV}}}$$

Linden et al. (in prep)

- **What about TeV halos?**
- **TeV Halos have hard spectrum -> May dominate high energy emission.**
- **Many sources**

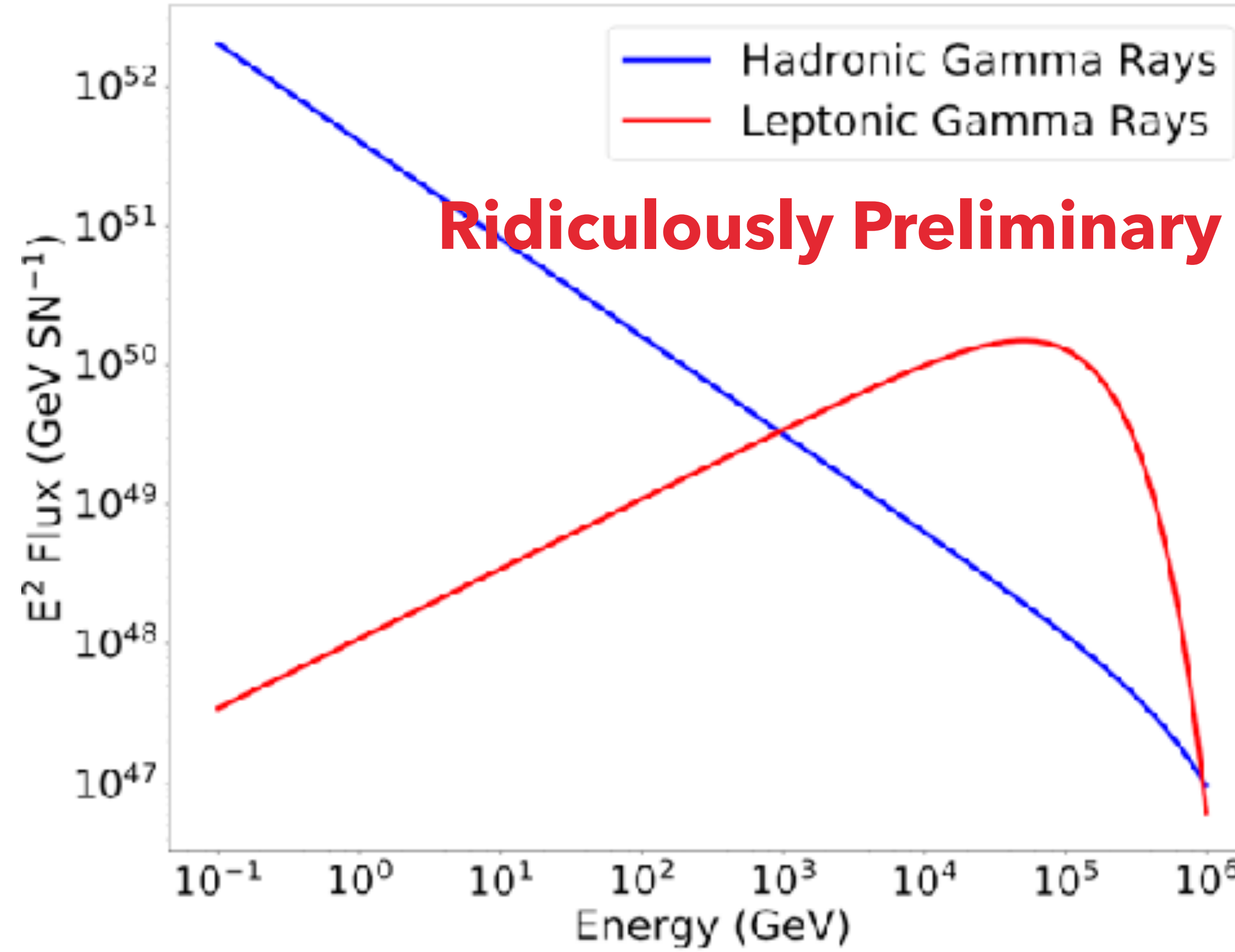

$$KE_{pulsar} = 10^{49} \text{ erg}$$

$$e^+e^-_{pulsar} \simeq 10^{48} \text{ erg}$$

$$\frac{dN_{e^+e^-,P}}{dE} = 1.1 \times 10^{48} E^{-1.5} e^{-E/100\,\text{TeV}}$$

$$\boxed{\phi_{\gamma,ICS} = 1.1 \times 10^{48} E^{-1.5} e^{-E/100\,\text{TeV}}}$$

- HAWC sources are potential IceCube neutrino sources.
- Spectral measurements of HAWC sources are imperative to calculating the expected neutrino flux.

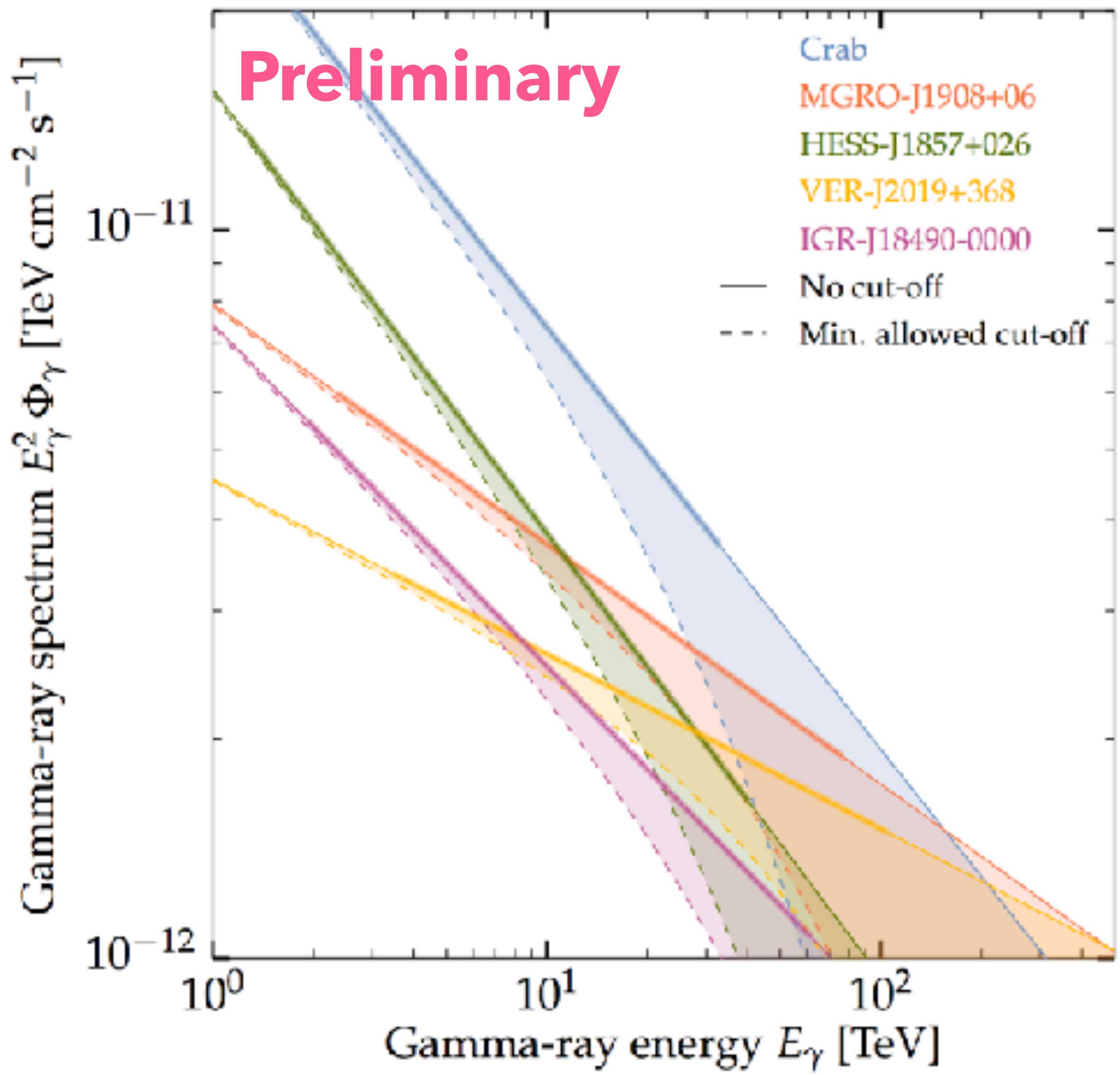

- Here we produce an analysis taking into account a 20% uncertainty in total flux, as well as spectral uncertainty due to an exponential cutoff.

ICECUBE NEUTRINOS FROM 2HWC SOURCES

Bustamante, Li, TL, Beacom (TBS)

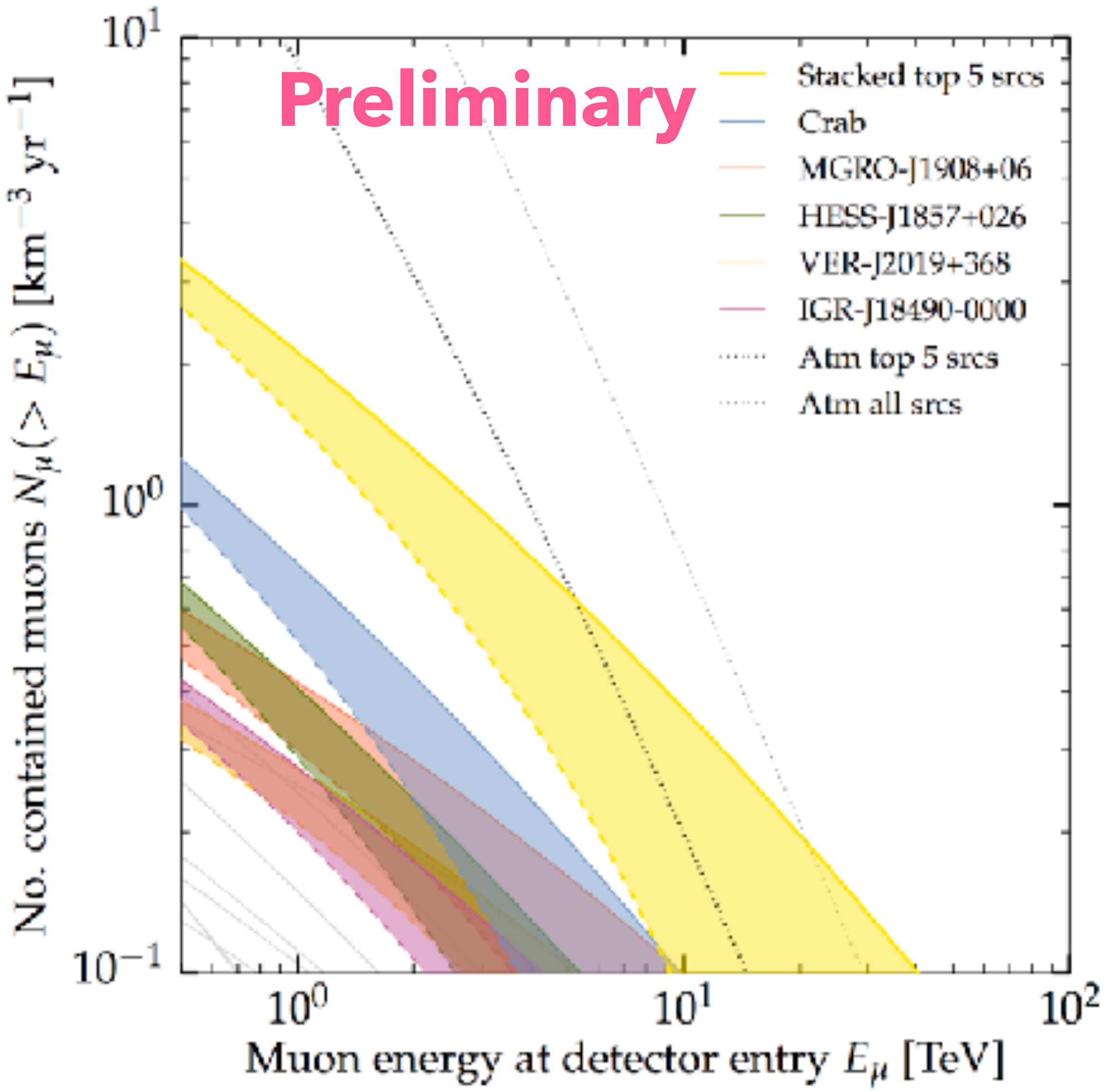

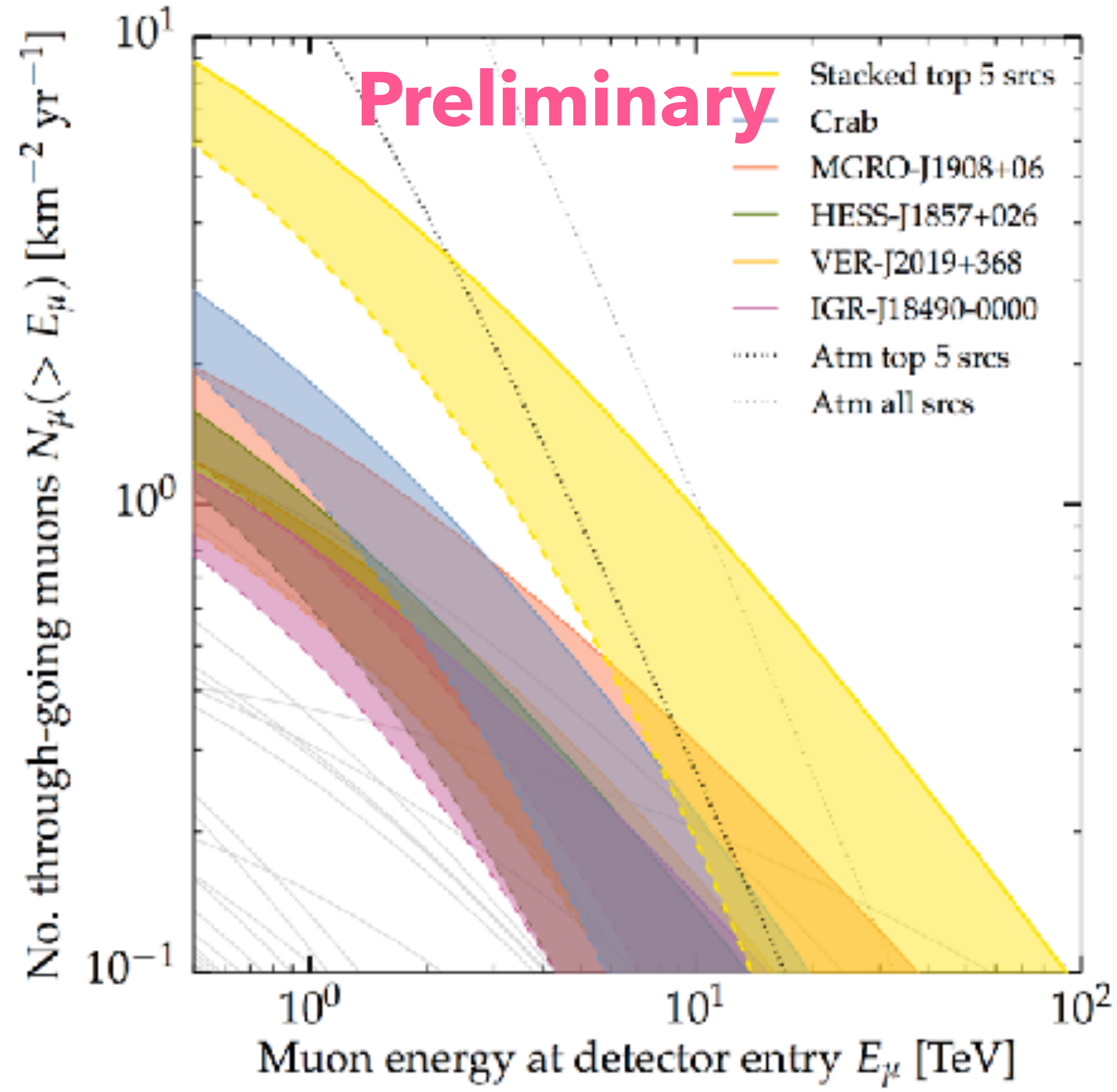

- If these sources are hadronic, their stacked neutrino flux is detectable in current IceCube data.
- Alternatively, can place a strong constraint on the hadronic fraction of the brightest HAWC sources.

TeVPA 2017

tevpa2017.osu.edu

- August 7–11, Columbus, OH
- Registration and abstract submission are open
- Pre-meeting mini-workshops on Sunday, August 7

Pre-Conference Mini-Workshops

We want to make TeVPA an opportunity for the community to get together to tackle open problems that require the combined input from different experimental collaborations and theorists.

To help achieve this, we are planning to host a number of optional informal pre-conference mini-workshop sessions on Sunday, August 6th, at OSU, provided there is sufficient expression of interest from participants. Each session would address a particular open problem. Most of the time should be dedicated to discussion within and between different experiments, with perhaps one or two short presentations.

When you register as participant in TeVPA, you may express your interest in participating in one of the following mini-workshops: anisotropy and propagation in the Galaxy, Galactic Center excess, multi-messenger sources, radio detection of ultra-high-energy neutrinos and cosmic rays, or dark matter complementarity. You may also propose a different topic.

Mini-workshops should be primarily self-run by participants. We would help set them up and provide facilities and coffee.

If you are interested in proposing, attending, or planning a mini-workshop broadly centered on TeV Particle Astrophysics, please indicate so at registration time or contact us at tevpa2017@osu.edu.

- HAWC observations open up an exciting new window into TeV emission from the inverse-Compton scattering of pulsars.

- Early indications:
  - Positron Excess is due to pulsar activity
  - A new method for finding hidden pulsars
  - An explanation for the Galactic center and diffuse TeV fluxes
  - A constraint on IceCube neutrino sources